INSURGE PRESSURE RESPONSE AND HEAT TRANSFER FOR PWR PRESSURIZER

by

HAMID REZA SAEDI

B.S. Mechanical Engineering
University of Miami
(1981)

Submitted in Partial Fullfillment
of the Requirements for the
Degree of

MASTER OF SCIENCE IN

MECHANICAL ENGINEERING

at the

MASSACHUSETTS INSTITUTE OF TECHNOLOGY

November 1982

Signature of Author: Hamid Reza Saedi
Department of Mechanical Engineering
November 30,1982

Certified by: _____
Thesis Supervisor

Accepted by: _____
Chairman, Mechanical Engineering Department Committee

ENCLOSURE 1

ACKNOWLEDGEMENTS

I owe a debt of gratitude to Professor Peter Griffith for taking me as one of his students and his guidance throughout the research.

I thank Mr. Joseph Caloggero, Mr. Bill Finley, Mr. Fred Johnson, and Mr. Dan Wassmouth for their continuous help in keeping the test facility intact; and Ms. Sandy William Tepper for her kindness and administrative advice, and Ms. Karla Stryker for typing this thesis.

Cooperation of Dr. Sang-Nyung Kim is acknowledged. I would also like to thank my friends, Warren Davis, Robin Baines, Chan-Young Paik, Doug Reitz, and others in the heat transfer lab, for making the last year so enjoyable for me.

Finally, I wish to thank Northeast Utilities and the Yankee Atomic who sponsored the research.

TABLE OF CONTENTS

LIST OF FIGURES

LIST OF TABLES

LIST OF SYMBOLS

a_o	Constant used in equation (22)
a_1	Constant used in equation (22)
a_2	Constant used in equation (22)
A	Area
C	Concentration (used in Section 4.3)
C	Heat capacitance
C_2	Dimensionless coefficient used in equation (11)
D	Diameter
e	Specific energy
Fr	Froude Number (modified)
g	Gravitational constant
h	Enthalpy
h_{cond}	Condensation coefficient of heat transfer
h_z	Coefficient of heat transfer
h_{avg}	Averaged coefficient of heat transfer
K	Conductivity
K	Constant of Gaussian distribution used in equation (12)
L	Length
m	Mass
$\dot{m}$	Rate of change of mass
M	Momentum
P	Pressure
q''	Heat flux
$\dot{Q}$	Heat transfer rate
Q''	Total heat flux

r	Coordinate in transverse direction (used in §4.3)
Re	Reynolds number
t	Time
T	Temperature
u	Specific internal energy
v	Velocity
V	Volume
υ	Specific volume
z	Vertical distance from nozzle of jet
α	Diffusivity
ρ	Density
μ	Viscosity
μ	Constant of Gaussian distribution used in Equation (12-ii)
δ	Depth of penetration of heat

Subscipts

cond	Condensation
e	Zone of establishment of jet
f	Saturated liquid
g	Saturated vapor
int	Interface
n	Spatial coordinate
m	Evaluated at the axis of jet
o	Insurged fluid
s	Ambient fluid
t	Transition zone of jet

v Vapor

w Wall

Superscript

i Time coordinate

CHAPTER 1

INTRODUCTION

1.1 Issues and Recent Events

During the past few years, prediction of the pressurizer transient response has become an important factor in the licensing of pressurized water reactors (PWR's). A transient can be caused from a simple loss of secondary steam flow [1] to more complicated accidents such as pressurized thermal shock (PTS), steam generator tube rupture (SGTR), or small break loss-of-coolent accident (SBLOCA) [2]. In the next section the processes taking place during the above transients will be briefly discussed.

Experiments run on Loss of Fluid Test (LOFT), series L6-3 and L6-5 [3], have shown substantial deviations between calculated and measured pressurizer level and system pressures. These calculations were based on the RETRAN computer code [5]. Recently, an attempt was made to make prediction of transient response to the reactor trip of Millstone Point Unit 2 and Connecticut Yankee power plants [4]. Predictions for the system pressure response were made using RETRAN 2 and RELAP-MOD 6 [16] computer codes. Both codes overestimated the pressure by a significant amount. The primary conclusion in both cases was that the pressurizer model used in the above codes, and most possibly others, needs improvement.

1.2 Some Important Transient Processes

In order to understand and model an accident, one should recognize the processes that take place during a transient. In general, these processes are insurge, outsurge, and empty pressurizer refill. This thesis will address the two possible insurge processes; i.e. insurge to partially

filled and refilling of empty pressurizer. In the next few paragraphs, the processes involved in particular accidents will be discussed.

1.2.1 Loss of Secondary Steam Load

In a typical accident of this kind, a series of insurge/outsurge maneuver are made. This is due to a variation in the steam load which causes expansion of primary coolant. Therefore, the only processes involved are insurge and a partial outsurge of a partially filled tank.

1.2.2 Pressurized Thermal Shock

This accident involves a combination of all processes. In a typical PTS, the secondary pressure drops very rapidly causing the primary to overcool. At this point the pressurizer can be emptied at which the Emergency Core Cooling System (ECCS) comes on, and refills the pressurizer. The system is then overpressured.

1.2.3 Small Break Loss-of-Coolant Accident

This accident involves system refill and repressurization, since the primary refills with subcooled liquid from the High Pressure Injection System (HPIS).

1.3 Summary

As the recent events have shown, the ability of the present codes to accurately calculate transient responses in which multiple failure occurs is questionable. In order to find the range of the pressure response, one may solve the upper and the lower limit cases; i.e. adiabatic and equilibrium models. But, there is a substantial difference in magnitude between these two limits; therefore a realiable operational limit cannot be

estimated from this method. Until a justifiable model is introduced NRC recommends calculations based on adiabatic assumption for all kinds of transients including PTS.

The proper calculation of primary system pressure response depends on accurate modeling of phenomena such as heat transfer and condensation on the wall, spray operation and effectiveness, and nonequilibrium between the vapor and liquid in the pressurizer. Though models do exist for calculating pressurizer transient performance, they do not all consider all of the important processes and even if they do, the adequacy of the elements constituting the models has not been tested. Therefore, a systematic, analytical study accompanied by experimental work is needed to investigate the true behavior of important processes occuring in the pressurizer. This thesis is intended to fulfill the above objective for some cases of insurge transients.

CHAPTER 2

EXPERIMENTAL INVESTIGATION

2.1 Experimental Apparatus

The apparatus is shown schematically in Fig. 1. It consists of two cylindrical stainless steel tanks: the primary tank, 45 inches high and 8 inches ID, and the storage tank, 57 inches high and 8 inches ID. The main tank has six windows and is equipped with six immersion heaters totalling 9 KW, Fig. 2. The baffle at the inlet pipe of the primary tank was made of a 3 inch diameter stainless steel, 1/4 inch plate and was welded to the bottom flange by four legs, 1-1/4" x 1/8" x 1/8", Fig. 3. As shown in the Fig. 1, the line connecting two tanks consists of two quick-opening valves for rapid inputs, an orifice to measure mass flow rate and a control valve. The storage tank was pressurized with bottled nitrogen.

For the first set of experiments, three 5/16" brass rods were welded to the top flange of the primary tank, Fig. 4. A 3/32" hole was drilled every one inch in each of the rods in order to hold the thermocouples inside the tank. The rods were placed at 120° from each other and at different radial positions. A cap made of cast iron was welded around each rod, each having six drilled holes, Fig. 5. In order to accomodate each thermocouple, compression fittings were welded in the drilled holes and Buna-N o'rings were used to prevent any leakage.

For the second type of experimental runs, a new type of flange was built. In this case one 5/16" x 42" heavy walled stainless steel tube was used as the thermocouple housing. The flange was drilled and tapped to accomodate one 1/2" NPT compression fitting (for the tube) and sixteen

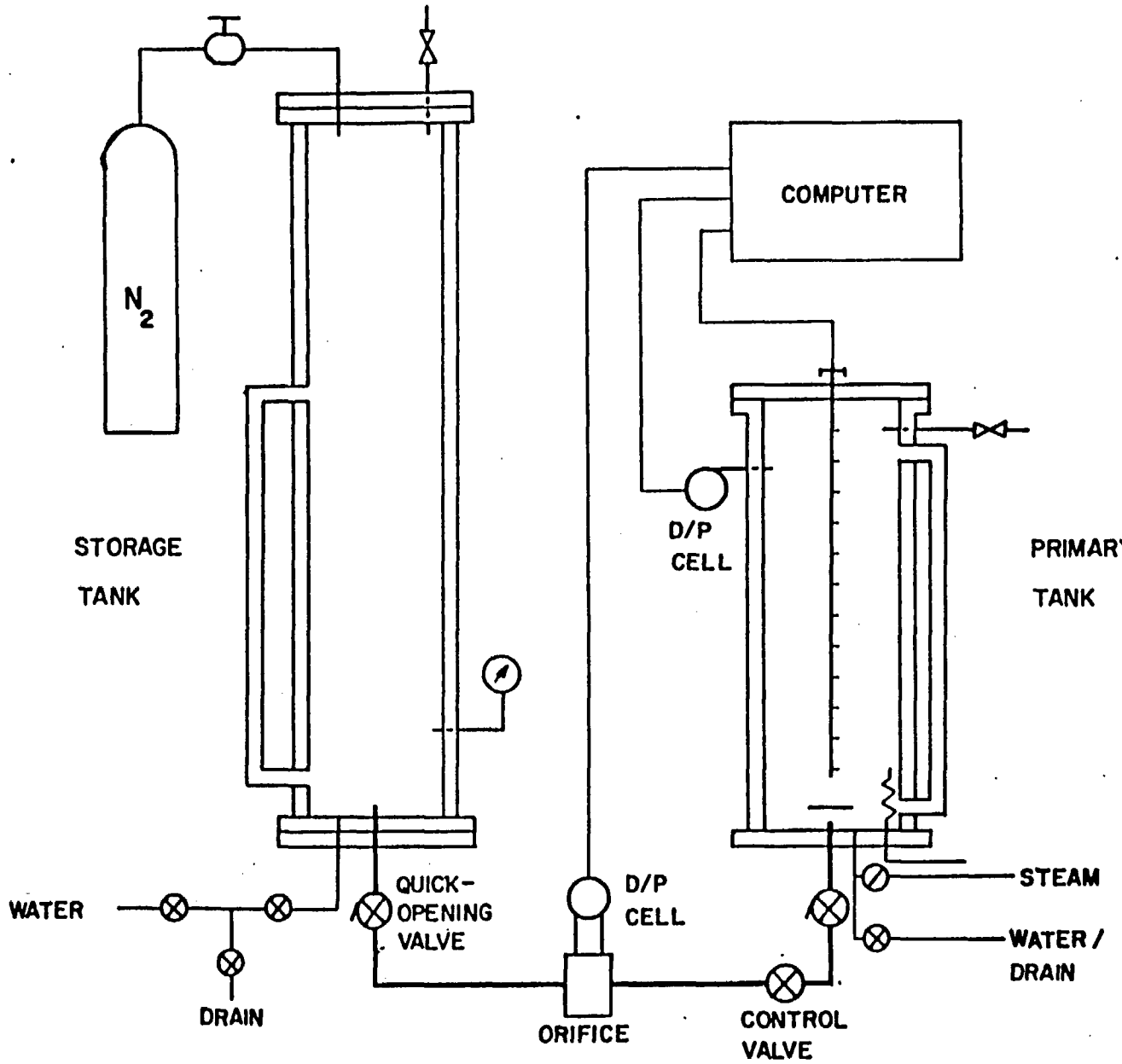

SCHEMATIC DIAGRAM OF APPARATUS

FIG. 1

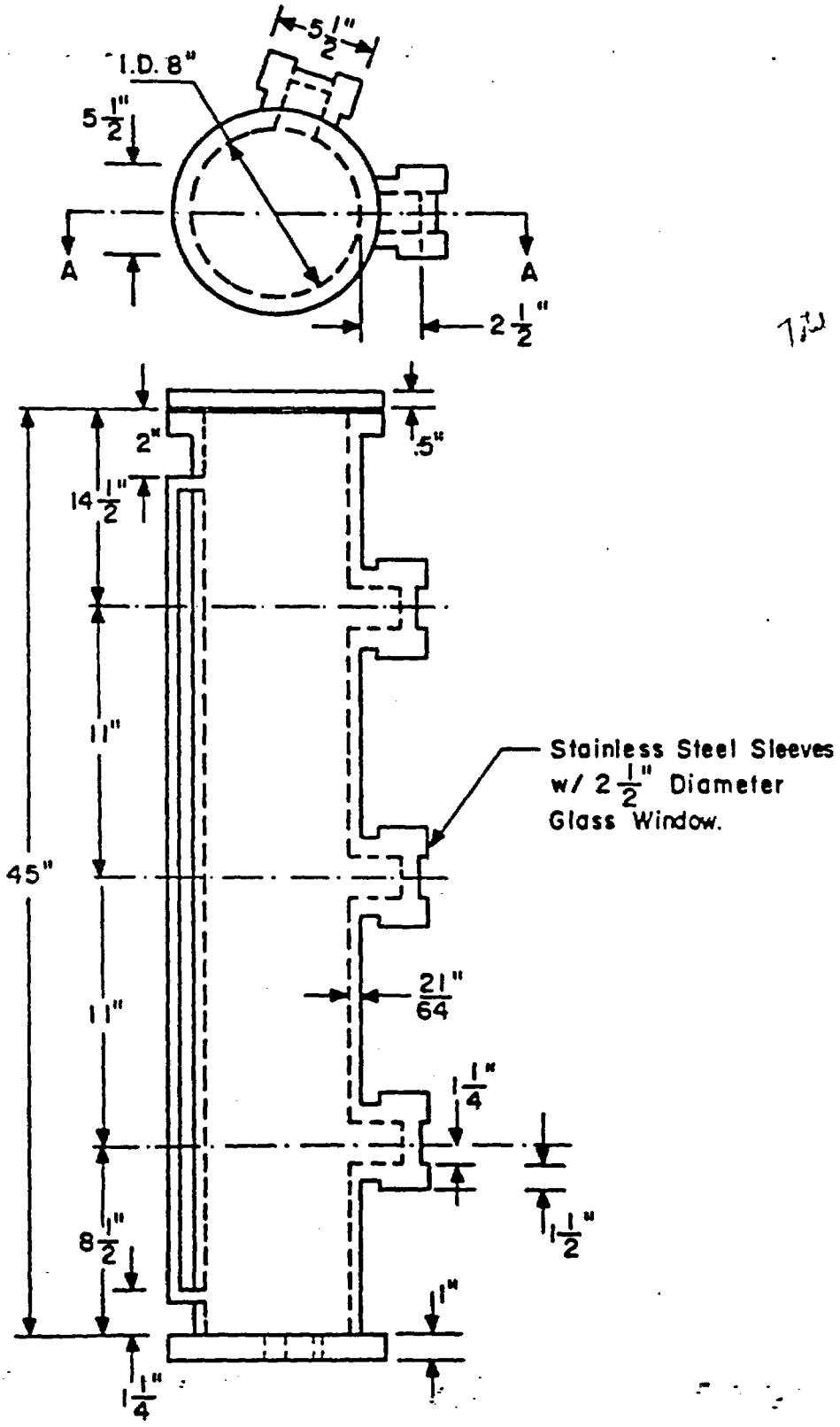

Schematic Diagram of Main Tank

FIG. 2

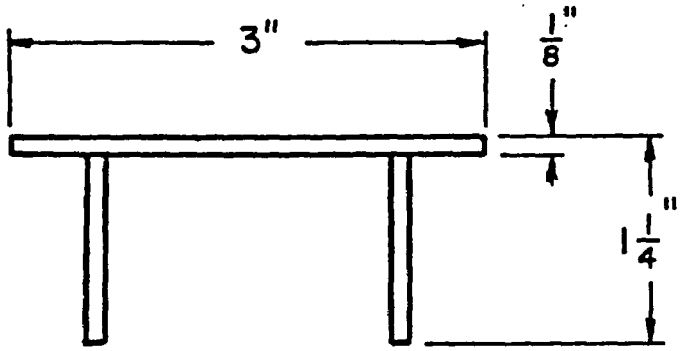

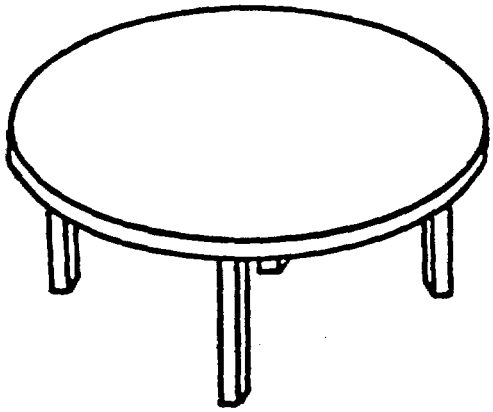

BAFFLE ASSEMBLY

FIG. 3

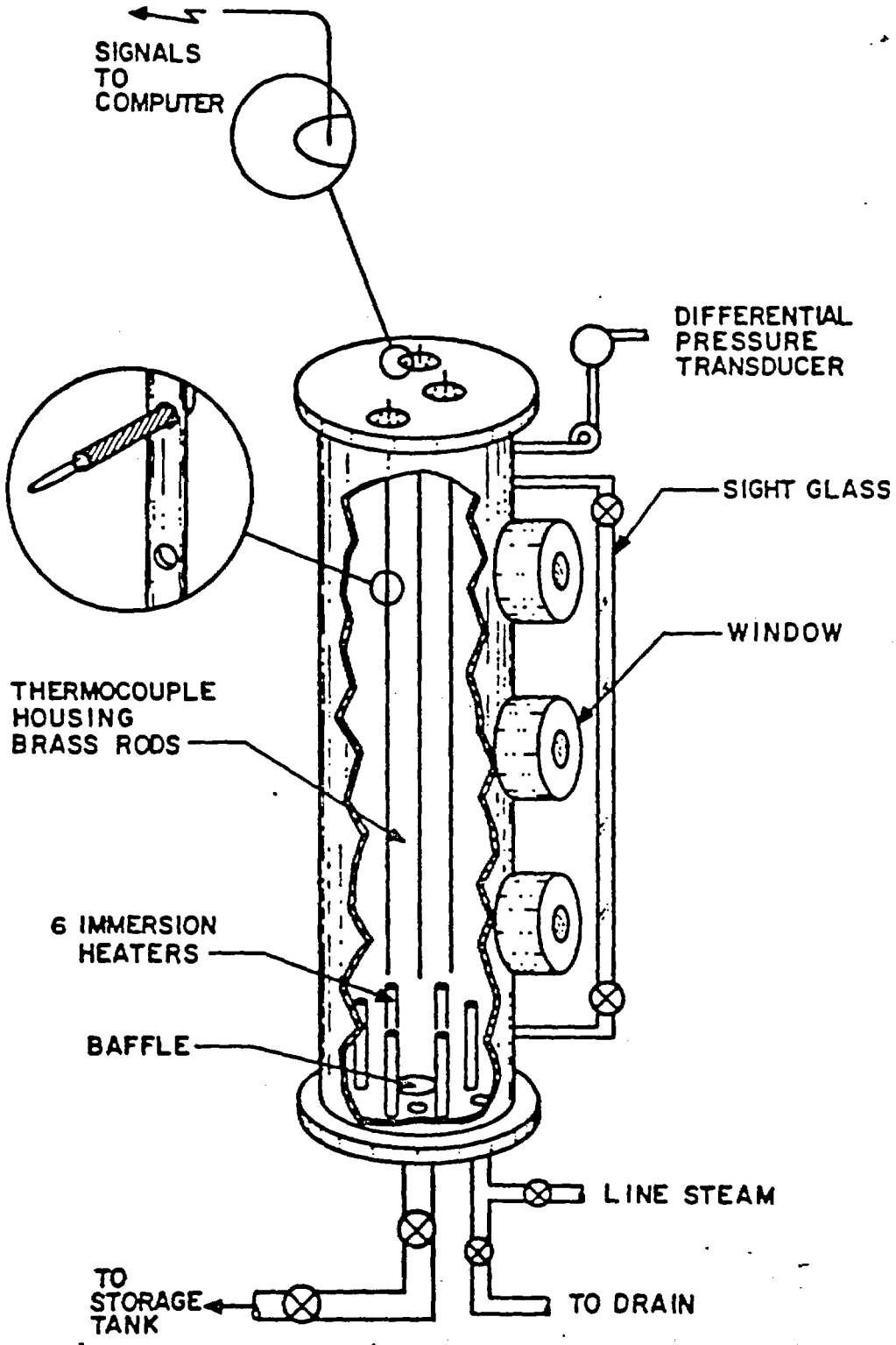

SCHEMATIC DIAGRAM OF PRIMARY TANK

FIG. 4

1/16" NPT compression fittings, for the thermocouples. As before, the rod was drilled every one inch along its length.

2.2 Instrumentation

Steam pressure and pressure drop across the orifice were measured by using variable reluctance type transducers. The transducers were calibrated before the run by a dead-weight gage tester.

Temperature measurements were made by using copper-constantan thermocouples. The thermocouples that measured temperature inside the tanks were insulated with magnesium oxide and shilded by a stainless steel metal sheath. Steam and water temperatures were measured by the two different sets of thermocouple arrangements mentioned earlier. Originally, eighteen thermocouples were arranged radially. They were intended to measure temperature at centre line, half way to the wall and 1/4 inch close to the wall, Fig. 5. For the second type of runs, 13 thermocouples were arranged axially inside the tank while 8 thermocouples were used to measure temperature on the outside wall. The thermocouples on the outside were attached to the tank by means of thin layers of mica and were strapped with wire to assure their position.

The signals from the pressure transducers and the thermocouples were recorded on floppy disks using a Perkin-Elmer mini-computer. The computer was furnished with an interface, hence making it a Real Time Data Acquisition System (RTDAS). The DAS was able to record up to 8000 data points per second using 24 channels.

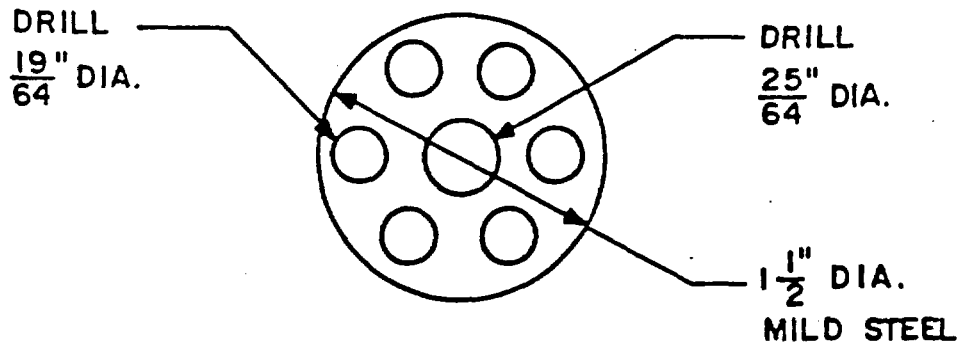

Thermocouple supporting cap

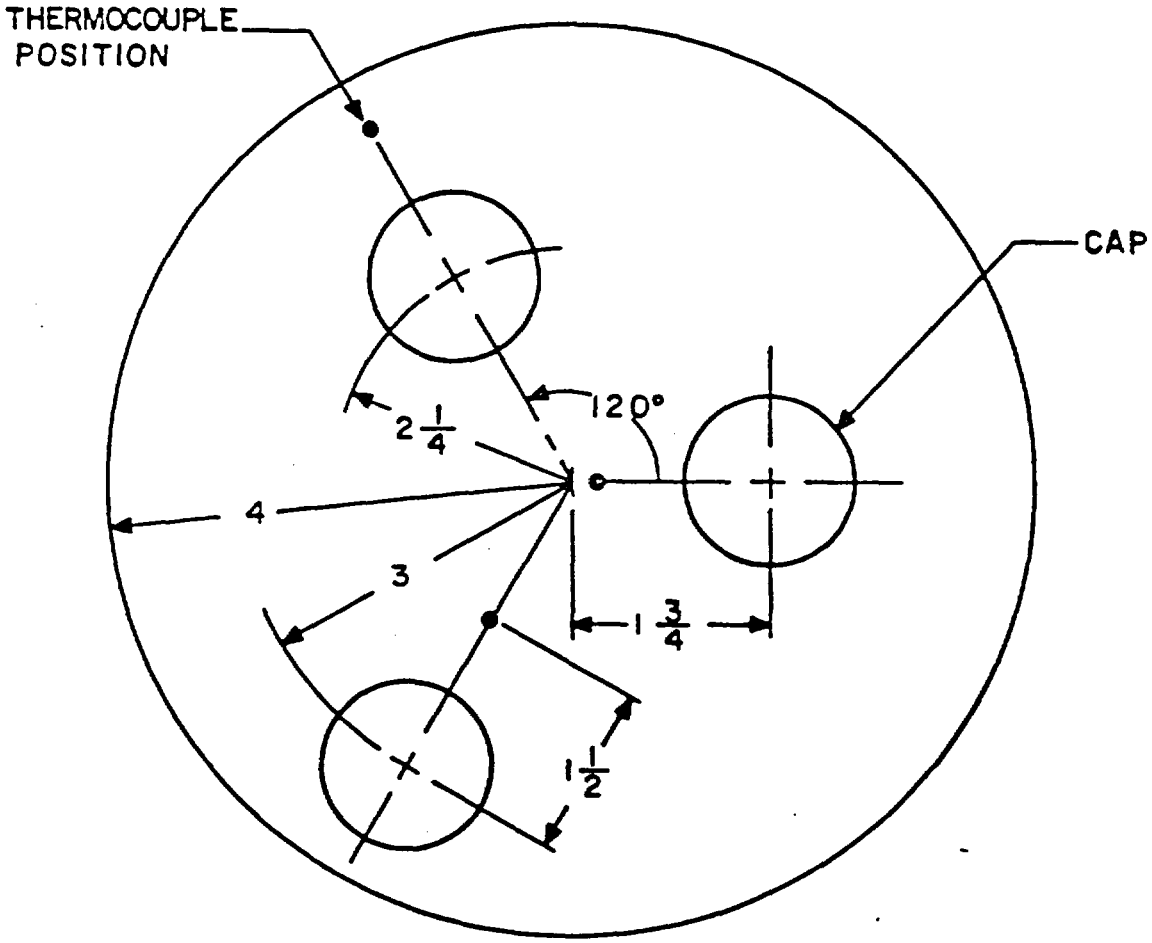

Top Flange of Primary Tank

FIG. 5

2.3 Experimental Procedure

2.3.1 Insurge Experiments

The primary tank was filled partially with water. In order to heat up the water quickly, live steam was bubbled into the water. This caused the tank pressure to raise up to 75 psia and a temperature increase to 303°F. After the water began to boil, the tank was deaerated by opening the relief valve. This was done until most of the non-condensible gas was driven out. The pressure and temperature were maintained at a constant value so that equilibrium would establish.

Meanwhile, the storage tank was filled with water and pressurized with nitrogen. After steady state was reached in all components, the two quick-opening valves were thrown open. The rate that water was charged to the primary tank was adjusted for different runs by controlling nitrogen pressure, which was around 300 psi, and the control valve.

2.3.2 Loss of Heat Experiments

Each time the insulation was changed, a set of heat loss experiments were run.

After the tank was deaerated, it was brought to steady state condition leaving only vapor at approximately 75 psia. The steam supply was then closed and pressure and temperature signals were recorded.

CHAPTER 3

EXPERIMENTAL RESULTS

3.1 Insurge Into Partially Filled Tank

Two types of experiments were run, using the two different arrays of thermocouples. Tests were run using wide range of insurge rates for both cases. Typical insurge rate for the experiments were from 0.2 inch/ sec to 0.8 inch/sec (based on the pressurizer inside area). In order to obtain the same jet to ambient density ratio for the experiment and a pressurizer, insurged water temperature was maintained at 70°F while the initial pool temperature was at 303°F.

A complete discription of experiments involving insurge to a partially filled tank is given in Appendix A. Sections A.1 and A.2 are data for insurge rates of 0.5 in/sec an 0.24 in/sec using three different radial thermal thermocouple locations in the pool. Section A.4 contains the data taken using only pool center line temperature measurements for an insurge rate of 0.4 in/sec.

3.1.1 Radial Temperature Gradient

The experimental runs using the three radial TC locations were intended to detect the radial temperature distribution in the liquid and vapor regions. Results of all the experiments performed indicated that no significant radial temperature gradient exists in any of the regions. The only exception to this was during the insurge when a plume was shed at the entrance due to the baffle (Fig. 6). The thickness of the region which there was a radial temperature variation was found to be proportional to the insurge rate, since radial temperature differences of 10°F to 50°F were

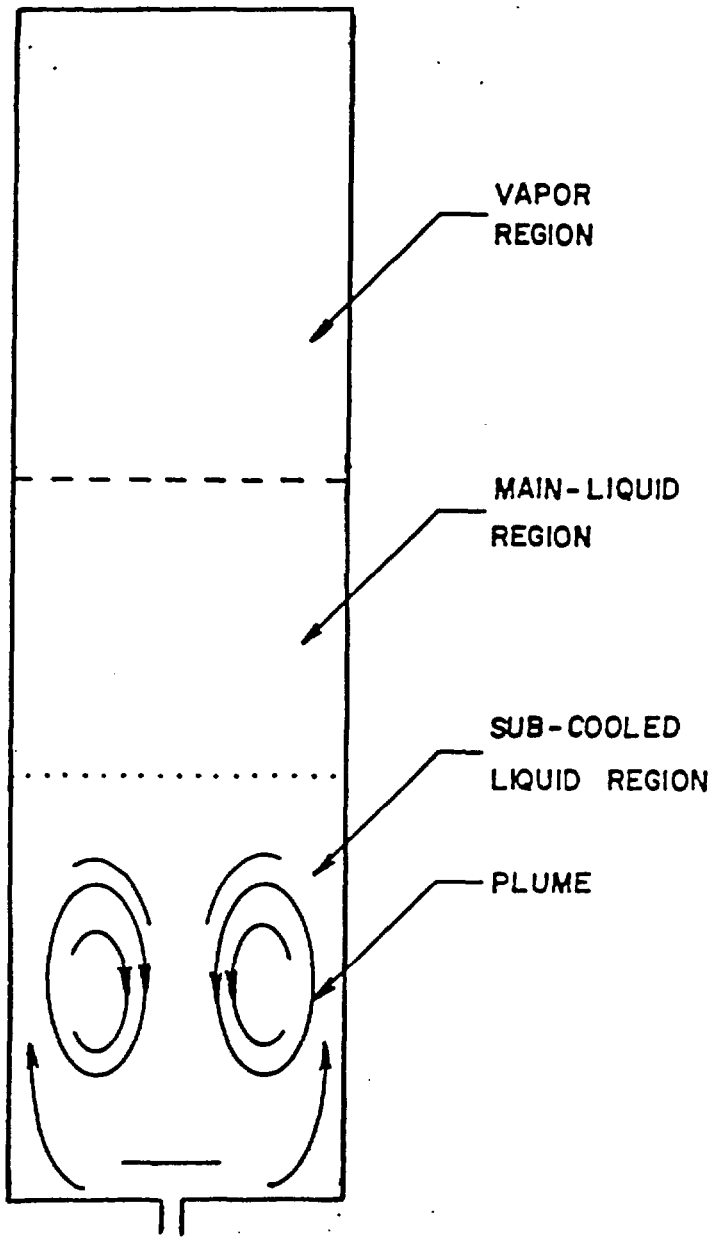

FIG. 6

PLUME GEOMETRY

observed depending on how rapid the insurge was. See Figs. 7,8. As the insurge was stopped, the plume and along with it the radial temperature differences faded away. Throughout the insurge and after, the vapor region showed no sign of a radial temperature difference (see Fig. A.1.2 through A.1.11 in Appendix A).

3.1.2 Liquid Region and Mixing of the Jet

For the cases of an insurge when the tank was initially one-third full, the insurged liquid failed to break through the interface. This was observed to be true for all the allowable insurge rates. Failure of the jet to break through the interface resulted into the stratification of the liquid region in the bottom of the tank. This stratification was caused by the negative buoyancy due to the density difference and because of the baffle at the inlet pipe. Two distinct liquid regions, Fig. 6, were observed to exist: one being the main liquid region which refers to the original amount of the liquid. Throughout the transient this region maintained its original temperature. The other region consists of the subcooled liquid which was insurged. This region is further subdivided in a few stratified layers of subcooled liquid. This can be readily seen from Figs. A.4.4 through A.4.11 in Appendix A.

These stratified layers of liquid proved to be quite stable because after the insurge was stopped they retained their temperature profiles. At each instant of time, the region which separated the main liquid from the subcooled region was observed to be a mixing layer at approximately two to three inches in height. A rough sketch of the density variation in the liquid region is given in Fig. 9.

It should be noted that this type of stratification should be expected

LEGEND

△	CENTRE LINE
□	1/4" AWAY FROM WALL
○	OUTSIDE WALL
- - -	WATER LEVEL
.....	SATURATION TEMPERATURE

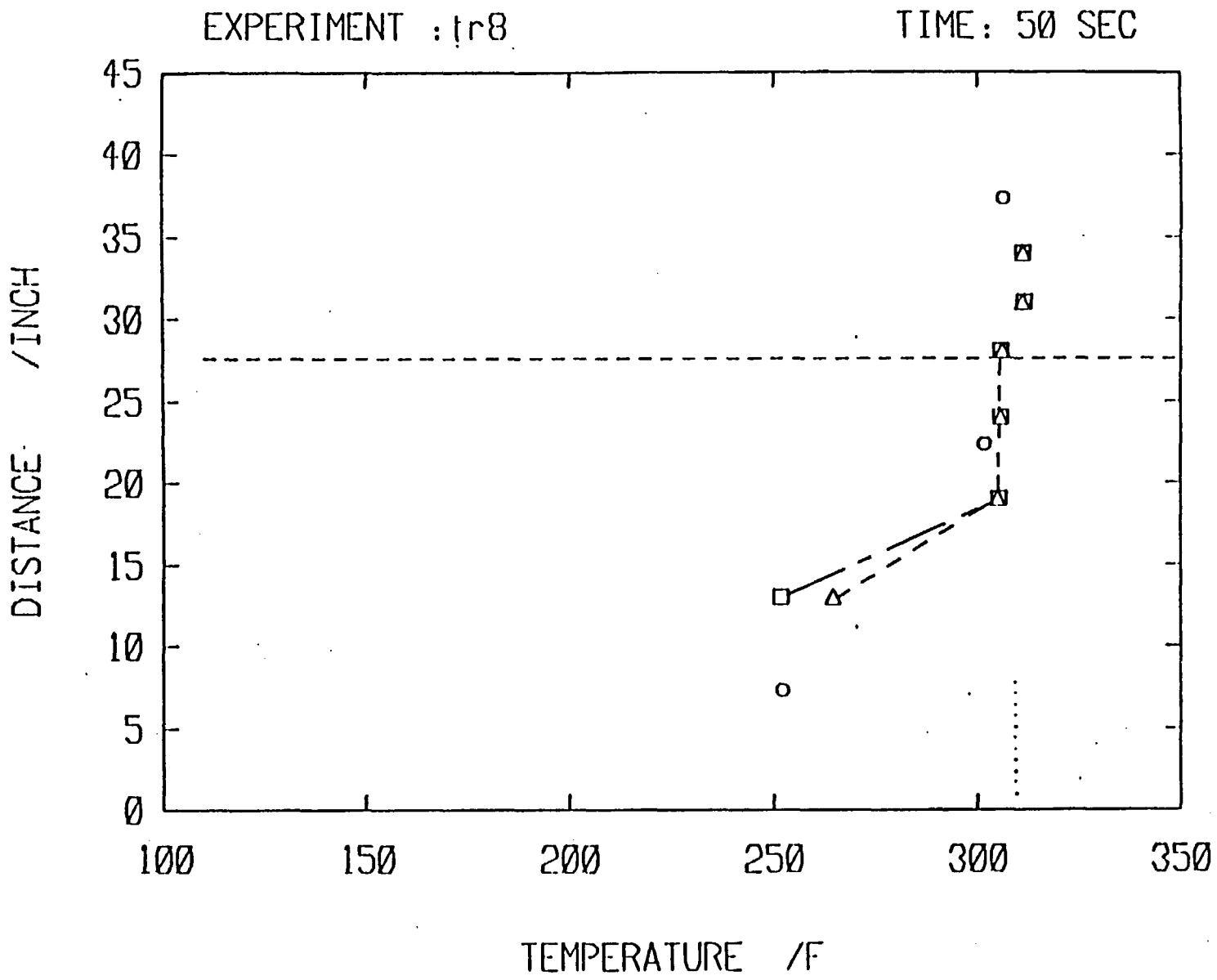

FIG. 7

RADIAL AND AXIAL TEMPERATURE DISTRIBUTION : INSURGE RATE=0.25 in/sec

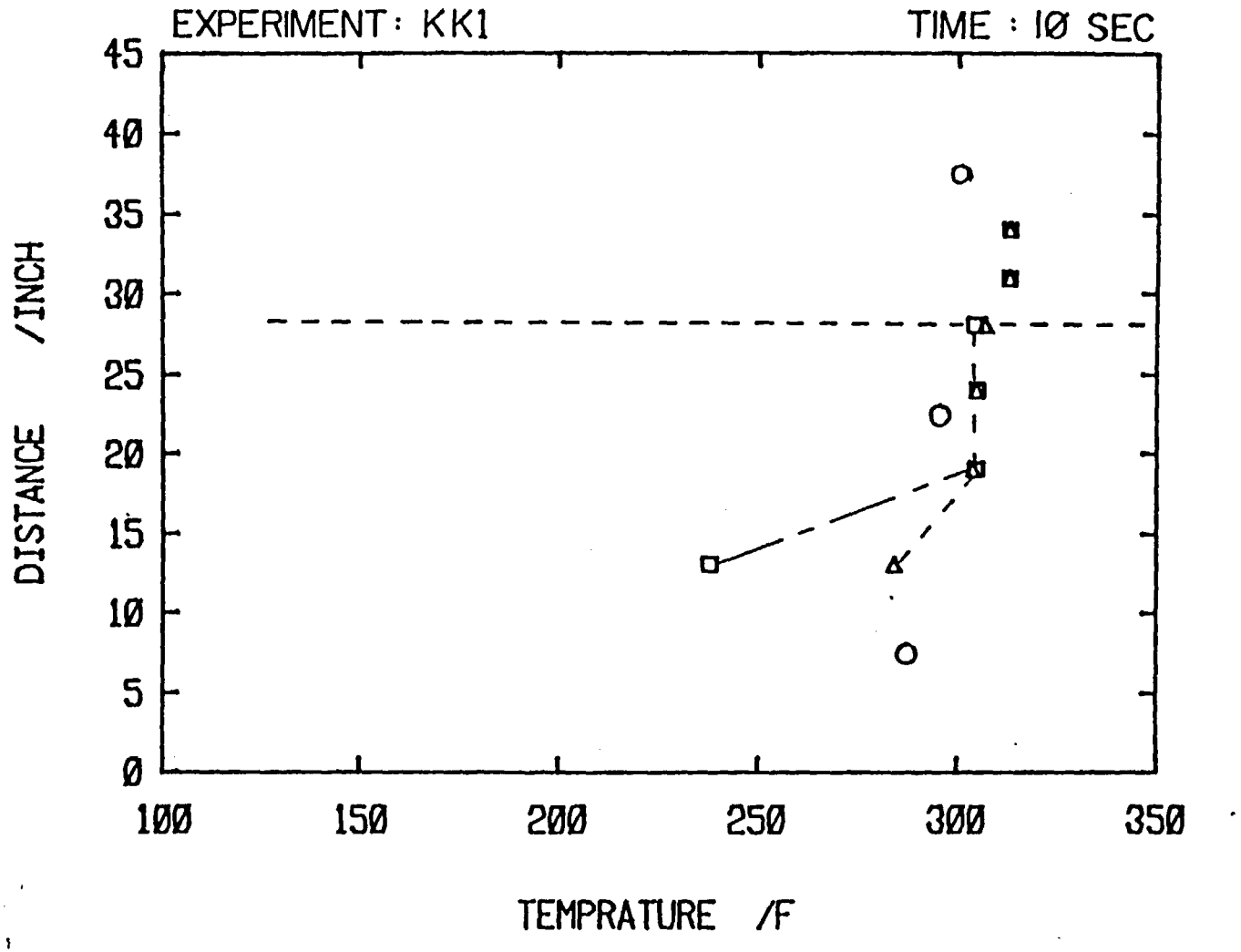

FIG. 8

RADIAL AND AXIAL TEMPERATURE DISTRIBUTION : INSURGE RATE=0.5 in/sec

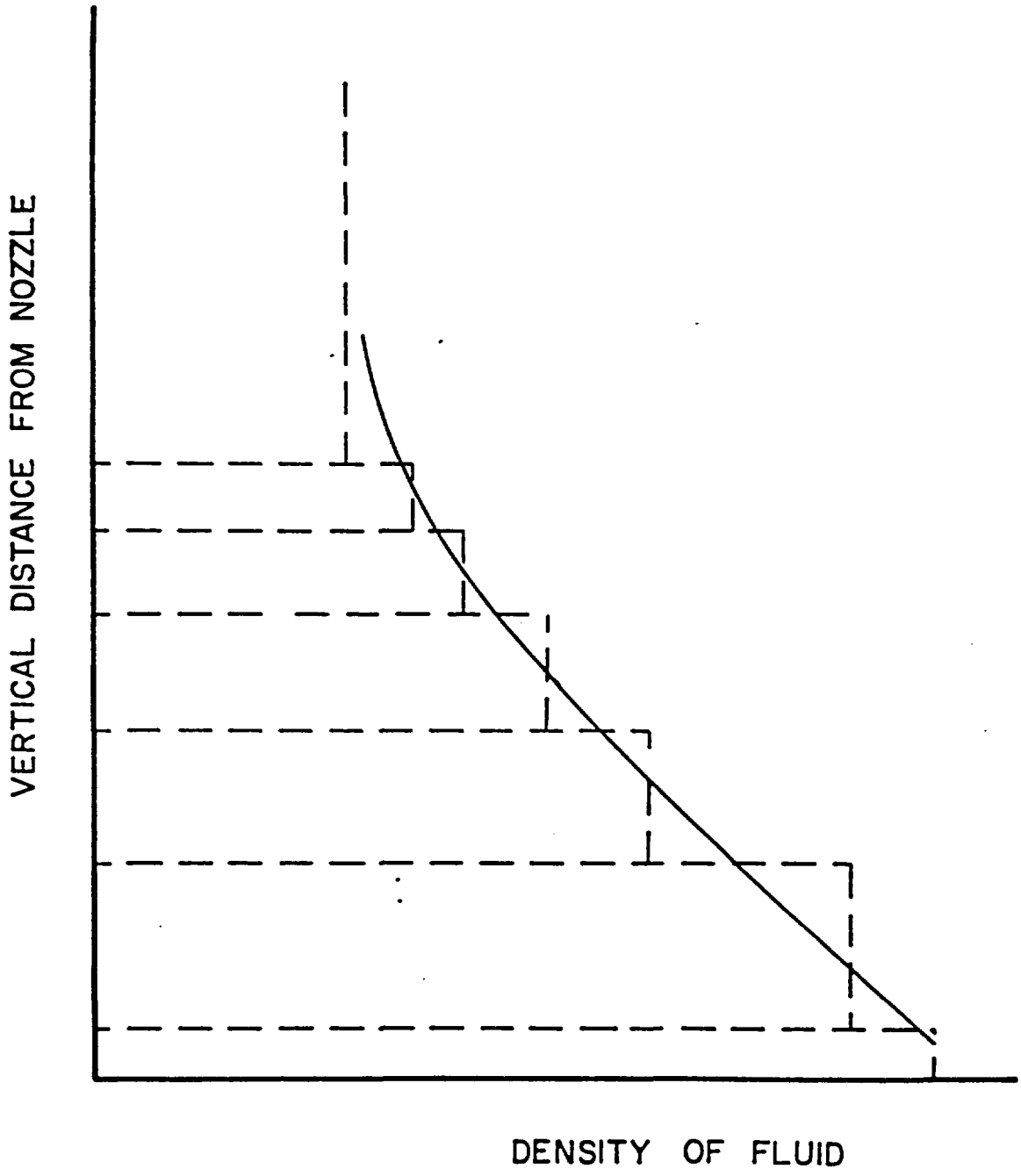

DENSITY VARIATION IN LIQUID

FIG. 9

in an actual pressurizer. This is again due to the negative buoyancy on the jet and the baffle at the inlet. Furthermore, some pressurizers such as B & W are equipped with a horizontal bank of heaters which further block the axial mixing.

3.1.3 Vapor Region

As it was pointed out earlier (§3.1.1), no radial temperature gradient existed in the vapor region except in a boundary layer on the wall. Furthermore, no axial temperature gradient was detected in the vapor region except very close to the interface. The temperature signals also indicated a few degrees of superheat to exist in the vapor. See Fig. 7 for instance.

3.1.4 Wall Temperature Response

As Figures A.4.6 through A.4.11 show, wall temperature changes at two locations, at the liquid-vapor interface and at the hot and cold liquid interface. The former acquires the same temperature as the vapor after a time lag, while the latter cools down very rapidly to a temperature close to the ajoining liquid temperature.

3.2 Insurge into the Empty Tank

As before, two types of experiments were run for the case of the insurge into the empty tank. The range of the insurge rates were from 0.4 inch/sec to 0.7 inch/sec. Temperature of the insurged liquid was at 70°F.

3.2.1 Liquid Region

The experimental runs using the radial TC's showed that the only radial temperature gradient was because of the plume. As before, this gradient faded away as the insurge was stopped. The radial temperature

difference was observed to increase as the insurge rate was increased.

Using the centerline TC's, it was observed that complex pool temperature profile was produced, see Fig. A.5.5 through A.5.14 in Appendix A. After the transient was stopped these layers tended to maintain their last temperature and remain stagnant.

3.2.2 Vapor Region

Regardless of the insurge rate, no radial temperature gradient was observed. Furthermore, no axial temperature gradient was detected, Fig. A.3.3 through A.3.9, except very close to the interface. A few degrees of superheat was detected in the body of the vapor.

3.2.3 Pressure Response

In this case, the jet was able to break through the interface. This gave rise to direct condensation on the subcooled liquid interface. As a result of this the pressure dropped severely during the first few seconds and then it started rising, Fig. 10. At this point, the liquid level was sufficiently high so that the jet no longer break through the interface. This height at which the jet was no longer able to break thru was observed to be roughly equal to the baffle height.

Different types of pressure responses were observed for different insurge rates, Fig. 11. It can be safely postulated that the pressure response depends on variables such as the insurge rate, baffle geometry, tank and other components geometry, etc. It should be noted that the sudden drop in pressure at time, t = 14 sec, (Fig. 11), is probably due to the presence of the window; see Fig. 2. It is postulated that due to an area increase, a new surface is formed hence an increase in the interfacial

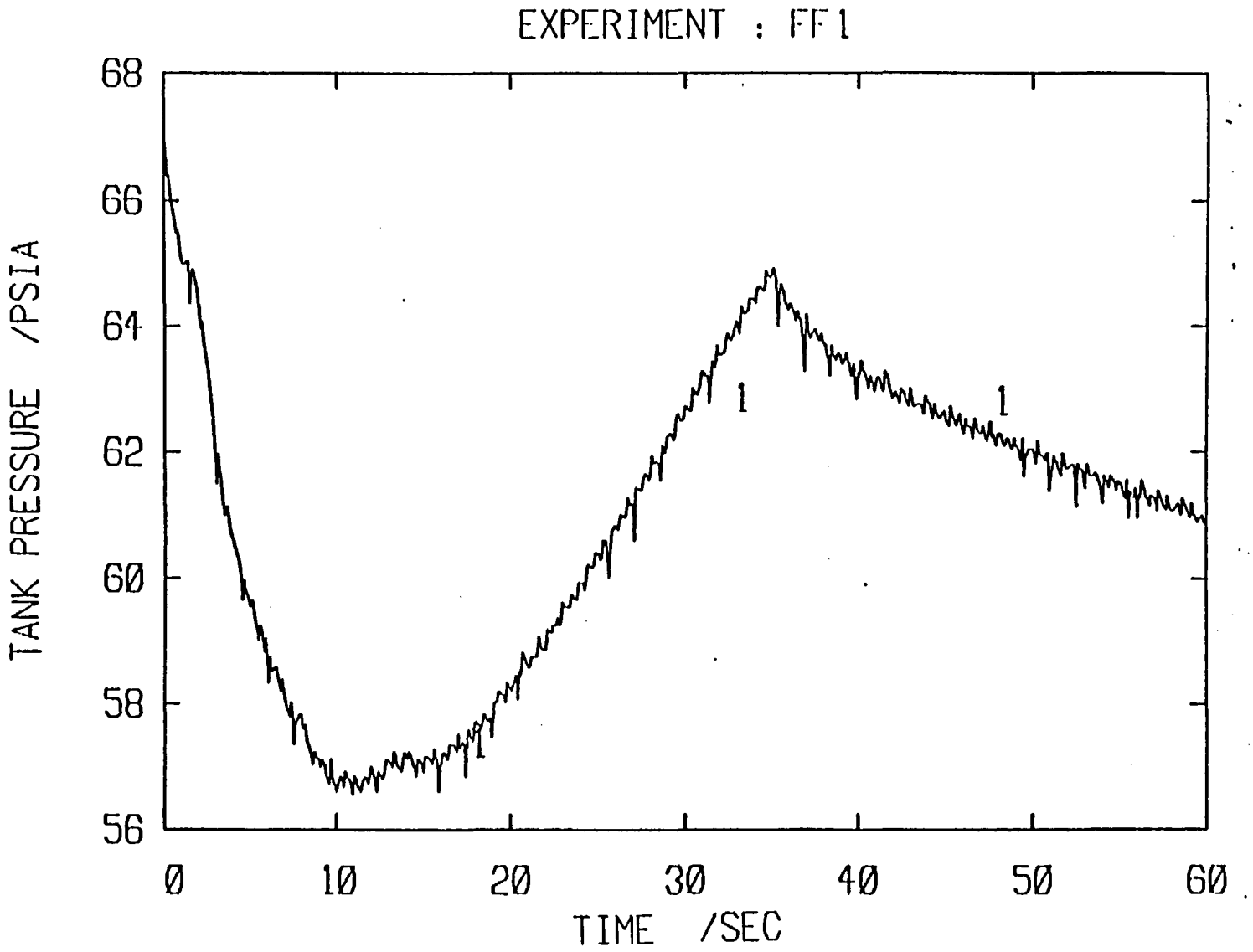

FIG. 10

PRESSURE RESPONSE FOR INSURGE TO EMPTY TANK: INSURGE RATE=0.5 in/s

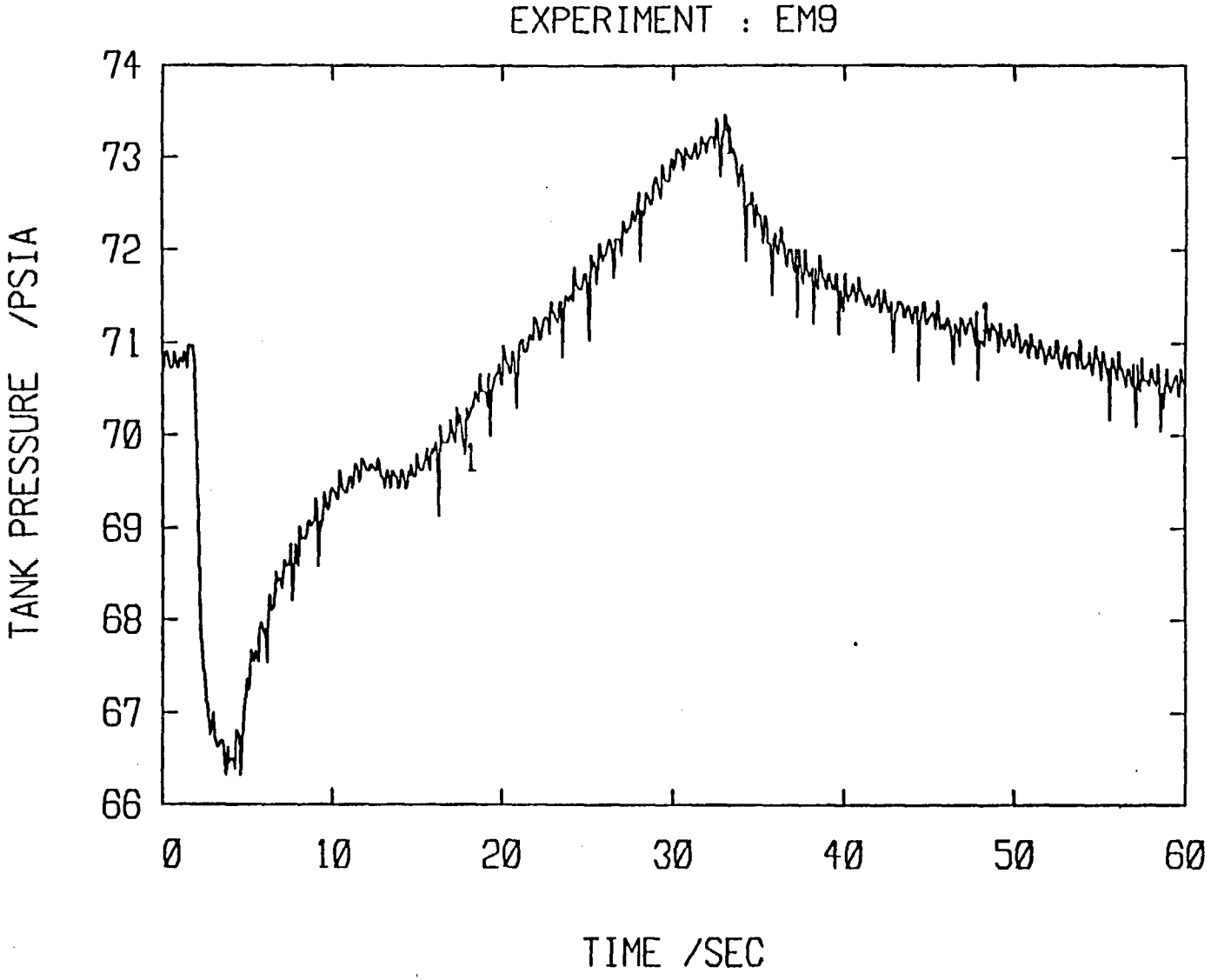

FIG. 11

PRESSURE RESPONSE FOR INSURGE TO EMPTY TANK: INSURGE RATE=0.7 in/s

heat transfer and a drop in pressure. It's not clear why this disturbance is not evident in Figure 10.

3.3 Summary

Experimental observations indicated that the liquid region is divided into two distinct regions. One being the main liquid region wich corresponds to the original amount of the liquid in the tank. This region remains at its original temperature during the insurge with no radial temperature gradient. The other region is the insurged subcooled liquid which itself is consisted of small layers of liquid at different temperatures.

The vapor phase becomes superheated by a few degees during the insurge and has no radial or axial temperature gradient. As the experiments showed, the only regions of wall which responded to the transient were the parts adjacent to the vapor and to the subcooled liquid region.

Insurge experiments to the empty tank showed that a complex condensation phenomena takes place at the interface. It was seen that the latter and hence the pressure response could be a function of the insurge rate and surge line and sparger geometry.

CHAPTER 4

ANALYTICAL MODEL

4.1 Previous Works

Lack of adequate experimental work could have played a major role in the failure of the previous models, as has been pointed out by Nahavandi [6] in late 60s and by Bonaca [4] more recently. One of the earliest models made the assumption of an adiabatic compression of vapor. This kind of crude modeling which neglects any kind of heat transfer results in an erroneous response. Later, a series of models were developed which considered saturation line process along with heat transfer to the vessel [7]. In some other pressurizer analysis, some workers [8,9,1] came up with calculation methods involving several isothermal control volumes. Such a model needs a method of evaluating heat transfer between control volumes, a method which we don't yet have.

In recent years, new digital programs, such as RETRAN or RELAP-5 are being used to describe the overall behavior of the system. The latter and the previously mentioned models were intended only for slow transients and they have proved to be unsuccessful for more complex and faster transients.

4.2 General Discussion

To describe all the phenomena occuring in the pressurizer during a transient, the following processes should be considered:

(1) Mixing of the subcooled jet below the free surface

(2) Condensation or natural convection on the walls of the pressurizer in the vapor

(3) Heat transfer to and from the wall in the liquid

(4) Condensation heat transfer at the free surface

(5) Condensation on the spray entering from the top of the pressurizer

In the next section, individual points relevant to the insurge transient which are mentioned above will be discussed in the light of these experimental observations. As it will be shortly discussed, §4.7, the only dominant process, for insurge duration of order of wall conduction time constant, is the wall heat transfer. Later they will be put together into a pressurizer model suitable for calculating the peak pressure during an insurge transient.

4.3 Mixing of the Subcooled Jet

One of the most significant observations in the pressurizer experiments is the stable stratification which is produced when there is an insurge of subcooled liquid. This stratification was detected in the experiments reported earlier (§3.1.2).

The existance of the stratification can be understood analytically by considering mixing in an ideal case. Let us imagine a dense jet entering a large pool of less dense liquid. Dimensional analysis shows that the local velocity, v, and the local density, ρ, depend on the other variables as [10]:

$$\frac{v}{v_o} = f\left(\frac{z}{D}, \frac{r}{D}, \frac{\rho_s - \rho_o}{\rho_o}, Fr, Re\right) \qquad (1)$$

and

$$\frac{\rho_s - \rho}{\rho_s - \rho_o} = f\left(\frac{z}{D}, \frac{r}{D}, \frac{\rho_s - \rho_o}{\rho_o}, Fr, Re\right) \qquad (2)$$

where

$$Re = \frac{v_o D}{\nu} \quad ; \quad Fr = \frac{v_o^2}{\frac{\rho_s - \rho_o}{\rho_o} gD}$$

Near the ceiling level; i.e., the highest level reached by fluid of the jet (Fig. 12), jet fluid leaves the upflow region and enters the down flow region. Thus, near the ceiling level the vertical flux of the jet decreases with height.

The jet can be thought as three zones: zone with positive entrainment near the jet entrance, zone with negative entrainment near the ceiling level, and transition level between zones, z_t [11] (see Fig. 12). The following conditions have to be satisfied for the above zones:

$$\frac{d}{dz} \int_A v dA = 0 \quad ; \quad z = z_t \tag{3}$$

$$\frac{d}{dz} \int_A vc dA = 0 \quad ; \quad z < z_t \tag{4}$$

$$\frac{dc_m}{dz} = 0 \quad ; \quad z > z_t \tag{5}$$

where concentration, $c \equiv \frac{\rho_s - \rho}{\rho_s - \rho_o}$

and subscript, m, means value at the axis of jet.

The momentum equation in vertical direction is,

$$\int_A \rho v^2 \, dA = \left[\int \rho v^2 \, dA\right]_{z=z_t} + g \int_{z_t}^{z} dz \int_A (\rho_s - \rho) dA \quad ; \quad z > z_t \tag{6}$$

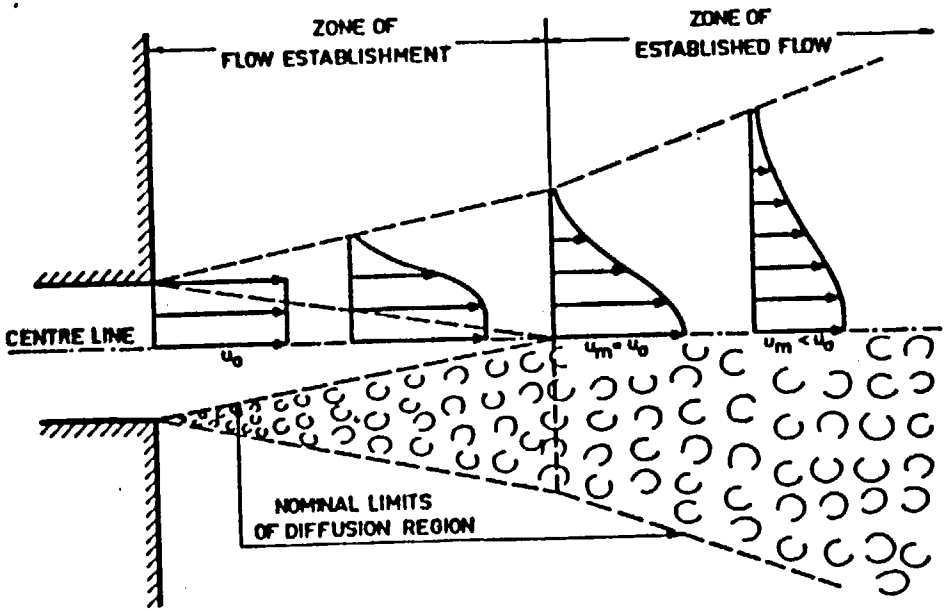

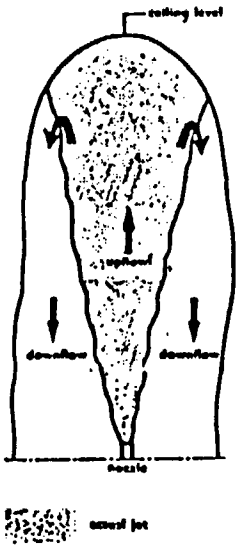

SCHEMATIC REPRESENTATION OF FLOW ESTABLISHMENT

FIG. 12

and

$$\int_A \rho v^2 \, dA = \left[\int_A \rho v^2 \, dA\right]_{z=z_e} + g \int_{z_e}^{z} dz \int_A (\rho_s - \rho) dA \quad ; \quad z < z_t \tag{7}$$

where z_e = length of zone of establishment (see Fig. 12).

Momentum at zone of establishment can be expressed as:

$$M_e = M_o + g \int_o^{z_e} dx \int_A (\rho_s - \rho) dA \tag{8}$$

and according to Albertson et al;

$$\frac{\int_A c \, dA}{\frac{\pi}{4} D^2_{nozzle}} = 1 + \frac{\{(2\pi)^{1/2} - z\}}{C_2} \frac{z}{D_{nozzle}} + \frac{\{3 - (2\pi)^{1/2}\}}{C_2^2} \frac{z^2}{D^2_{nozzle}} \tag{9}$$

From the last two equations, M_e can be written as,

$$M_e = M_o\left[1 + \frac{\{6 + (2\pi)^{1/2}\}}{6} \frac{C_2}{F_r}\right] \tag{10}$$

where C_2 is a dimensionless coefficient given in Fig. 13. The case considered here involves a negative buoyancy which corresponds to a negative Froude number. So, the left hand plane of Fig. 13 applies to this analysis.

Finally, value of zone of establishment can be found as,

$$z_e = C_2 D_{nozzle} \tag{11}$$

For the zone with positive entrainment, the velocity and concentration profiles can be regarded to be similar at all heights. Using the Gaussian distributions;

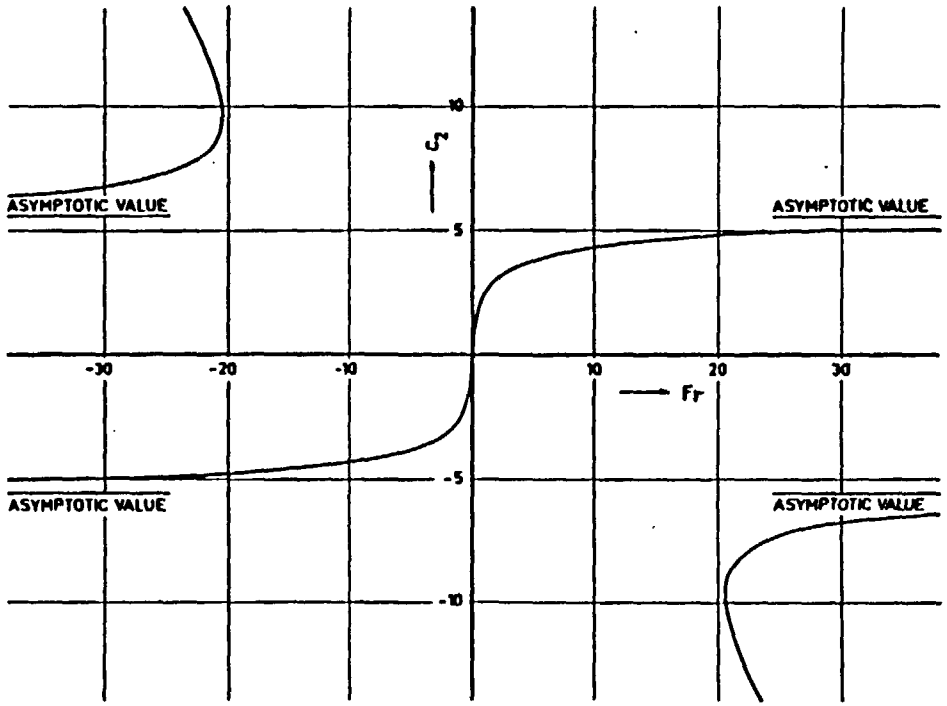

C_2 AS A FUNCTION OF FROUDE NO.

FIG. 13

$$\frac{v}{v_m} = e^{-k(r/z)^2} \qquad (12\text{-i})$$

and

$$\frac{\rho - \rho_s}{\rho_m - \rho_s} = e^{-\mu K(r/z)^2} , \qquad (12\text{-ii})$$

where μ and K are numerical constants. Using equations (12-i), (12-ii) in (8) and noting that ceiling level occurs when $u_m = 0$; one can solve for z_L;

$$\frac{z_L}{D_{nozzle}} = 1.94|Fr|^{1/2} \qquad (13)$$

Using numerical values, it can be seen that the ceiling level will never reach the free surface for the operational range of insurge rates. Therefore, if the jet cannot make it to the free surface without the presence of the baffle, it definitely will not reach the interface in the actual case.

4.4 Wall Condensation

During an insurge transient, the vapor temperature increases corresponding to an increase in the pressure. Due to the wall heat capacitance, there will be a time lag in temperature response. The temperature difference between wall and vapor causes condensation to occur on the wall. It should be noted that less wall condensation can occur during accidents in which a considerable pressure drop is followed by a rapid system refill (repressurization).

In order to obtain the heat transfer to the wall, an expression for the condensation coefficient of heat transfer should be arrived at. Nusselt's theory based on laminar film condensation can estimate the

coefficient of heat transfer within reasonable accuracy. The following assumptions should be made for this model:

1) neglecting effect of non-condensible gases present in the pressurizer
2) neglecting any shear stress at the condensation interface
3) assuming a fully developed laminar flow.

The resulting coefficient of heat transfer can be expressed as:

$$h_{avg} = \frac{1}{L} \int_0^L h_z \, dz \tag{14}$$

$$(h_{cond})_{avg} = 0.943 \sqrt[4]{\frac{g\rho \, (\rho - \rho_v) \, K^3 h_{fg}}{L\mu\Delta T}} \tag{15}$$

where L is the instantaneous length of vapor region plus the equivalent length of the top flange, i.e.

$$L(t) = L_v(t) + \frac{A_{top}}{\pi d} \tag{16}$$

4.5 Heat Transfer to the Wall

The wall heat transfer in the vapor space turns out to be the most significant heat transfer in the problem. This heat transfer was evaluated in the following manner. The heat diffusion equation can be regarded as the governing equation for wall temperature distribution,

$$\frac{\partial T_w}{\partial t} = \alpha \frac{\partial^2 T_w}{\partial x^2} \tag{17}$$

B.C.

(i) Condensation on the inner face

$$q''(x = 0) = h_{cond} \, (T_v - T_w \, (x = 0)) \tag{18}$$

(ii) Perfect insulation on the outside

$$\overset{"}{q}\ (x = x_o) = -\ K\ (\frac{\partial T_w}{\partial x})\Big|_{x=xo} = 0 \qquad (19)$$

where x_o is wall thickness, and h_{cond} is condensation coefficient of heat transfer calculated as described in the previous section.

Using the observations from insurge experiments to partially filled tank, it can be deduced that vapor temperature increases in an approximately linear fashion (see Fig. 14). Mathematically this can be written as;

$$Tv = Tv(t=0) + (\frac{dTv}{dt})\Big|_t \Delta t + (\frac{d^2 T_v}{dt^2})\Big|_t \frac{(\Delta t)^2}{2} + \ldots \qquad (20)$$

$$\approx Tv(t=0) + (\frac{dTv}{dt})\Big|_t \Delta t \qquad (21)$$

For mild transients the dependancy of wall temperature on time and position can be approximated by a fully developed parabolic profile [13],

$$\frac{Tw}{T_{w(x=o)}} = a_o + a_1\ (\frac{x}{xo}) + a_2\ (\frac{x}{xo})^2 \qquad (22)$$

where a_i ; i = 1,2,3 are constants.

Invoking the boundary conditions,

$$\overset{"}{q} = -\ K\ (\frac{dT_w}{dt})\Big|_{x=o} = -\ \frac{Ka_1}{x_o}\ T_w\ (x=o) \qquad (23)$$

and

$$0 = -\ K\ (\frac{dT_w}{dx})\Big|_{x=xo} = -\ K\ [\frac{a1}{xo} + 2\ \frac{a_2}{x_1}]\ T_w(x=o) \qquad (24)$$

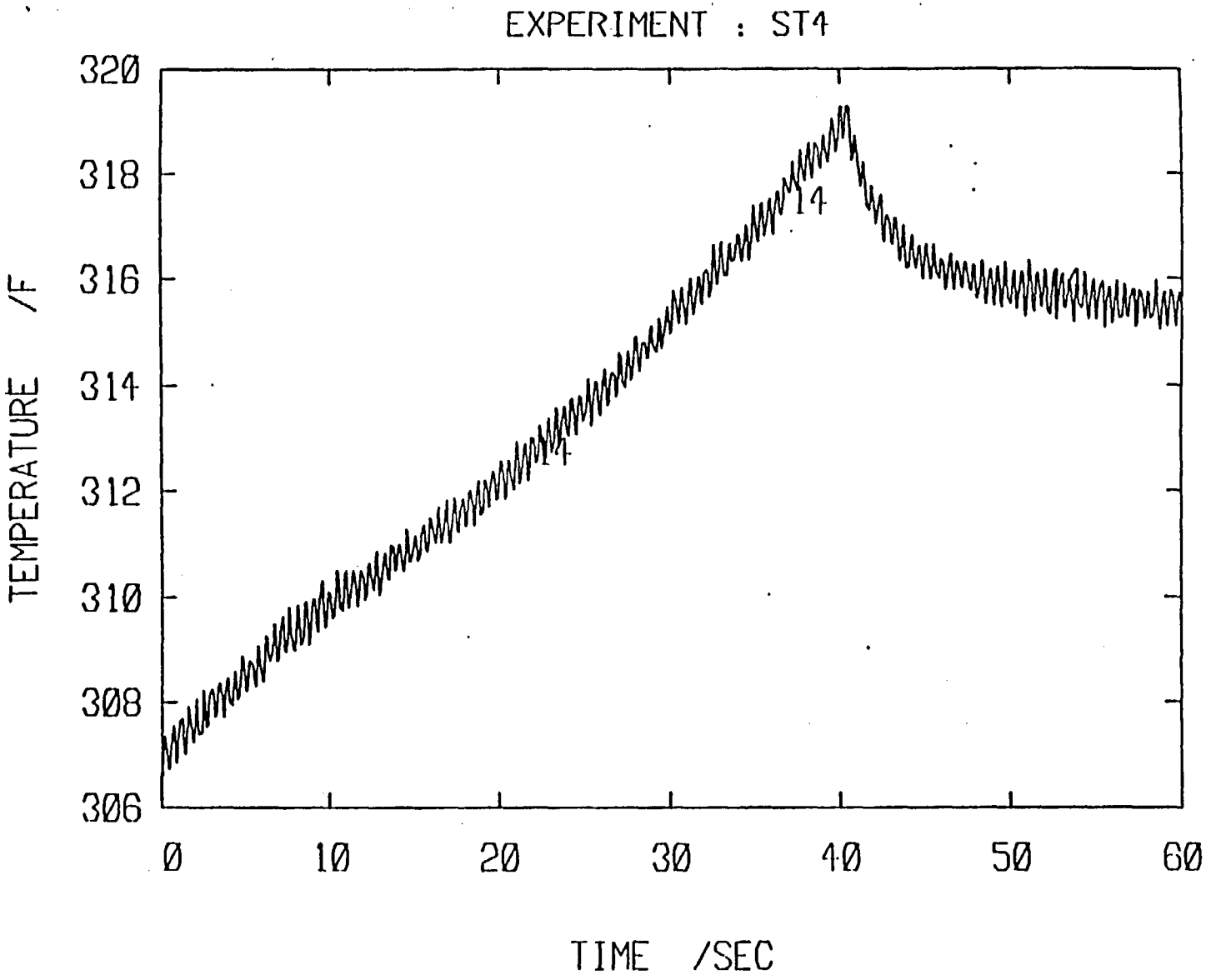

FIG. 14

VAPOR TEMPERATURE RESPONSE : INSURGE RATE=0.44 in/sec

Heat transfer to the wall can be also expressed as,

$$\overset{"}{q} = \lim_{\Delta x \to o} \rho c_p \frac{d}{dt} \sum_{n=1}^{n} T_w \, \Delta x \tag{25}$$

$$= \rho \, c_p \frac{d}{dt} \int_o^{x_o} T_w(x=o)\left[a_o + a_1\left(\frac{x}{x_o}\right) + a_2\left(\frac{x}{x_o}\right)^2\right] dx \tag{26}$$

and,

$$\left.\frac{T_w}{T_w(x=o)}\right|_{x=o} = 1$$

therefore, $$a_o = 1 \tag{27}$$

Using equations (23), (24), (27) and (18), equation (26) reduces to,

$$\overset{"}{q} = \rho c_p x_o \left[\left(\frac{dTw}{dt}\right)\Big|_{x=o} - \frac{x_o \, h_{cond}}{3K} \left(\dot{T}_v - \dot{T}_w\right)\Big|_{x=o}\right] \tag{28}$$

equating (18) and (28) results into an ordinary differential equation with $T_w(x=o)$ as the dependant variable,

$$\left[\left(1 + \frac{xo \, h_{cond}}{3K}\right) (\rho c_p xo)\right] \left.\frac{dT_v}{dt}\right|_{x=o} + h_{cond} \, T_w\Big|_{x=o}$$

$$= \left[\left(\frac{xo \, h_{cond}}{3K}\right) (\rho \, c_p \, xo)\right] \frac{dT_v}{dt} + h_{cond} \, T_v \tag{29}$$

The right hand side of equation (29) is simply a function (linear) of time (invoke equation (21)), i.e.

$$R.H.S. = \left[\left(\frac{xo \, h_{cond}}{3K}\right)(\rho c_p \, x_o)\right] \frac{dTv}{dt} + h_{cond} \left[Tv(t=o) + \left(\frac{dTv}{dt}\right)t\right] \tag{30}$$

Solving for homogeneous and particular solution,

$$T_w(x=o) = T_v + \left(\frac{\rho c_p x_o}{h_{cond}}\right)\left(e^{bt} - 1\right)\left(\frac{dT_v}{dt}\right) \qquad (31)$$

where

$$b = h_{cond}/\left[(\rho c_p x_o)\left(1 + \frac{h_{cond}\, x_o}{3K}\right)\right]$$

The accuracy of this model was checked against data by evaluating equation (6) at $x=x_o$. The discripency was found to be negligible within thermocouple's accuracy. The overall utility of this model will be shown shortly.

Using equations (15), (18) and (31), one can easily calculate the vapor wall heat transfer. A typical calculated wall heat transfer rate is shown in Fig. 15. From the above analysis it can be deduced that thicker walls simply mean a longer time constant and a larger percent error in the final result. This is due to a possible "hot region" in the wall.

4.6 Interface Heat Transfer Model

When the heaters are not in use; the only heat source to the main liquid is the vapor region. The heat and mass transfer from vapor to the main liquid region occurs at the interface. Due to the low thermal diffusivity of water, depth of pentration of heat below the interface is very small. In view of this short penetration, the main liquid region can be considered as a semi-infinite body. In order to find the importance of this phenomena, i.e. by comparing values of the different kinds of heat transfer, the heat diffusion equation must be solved.

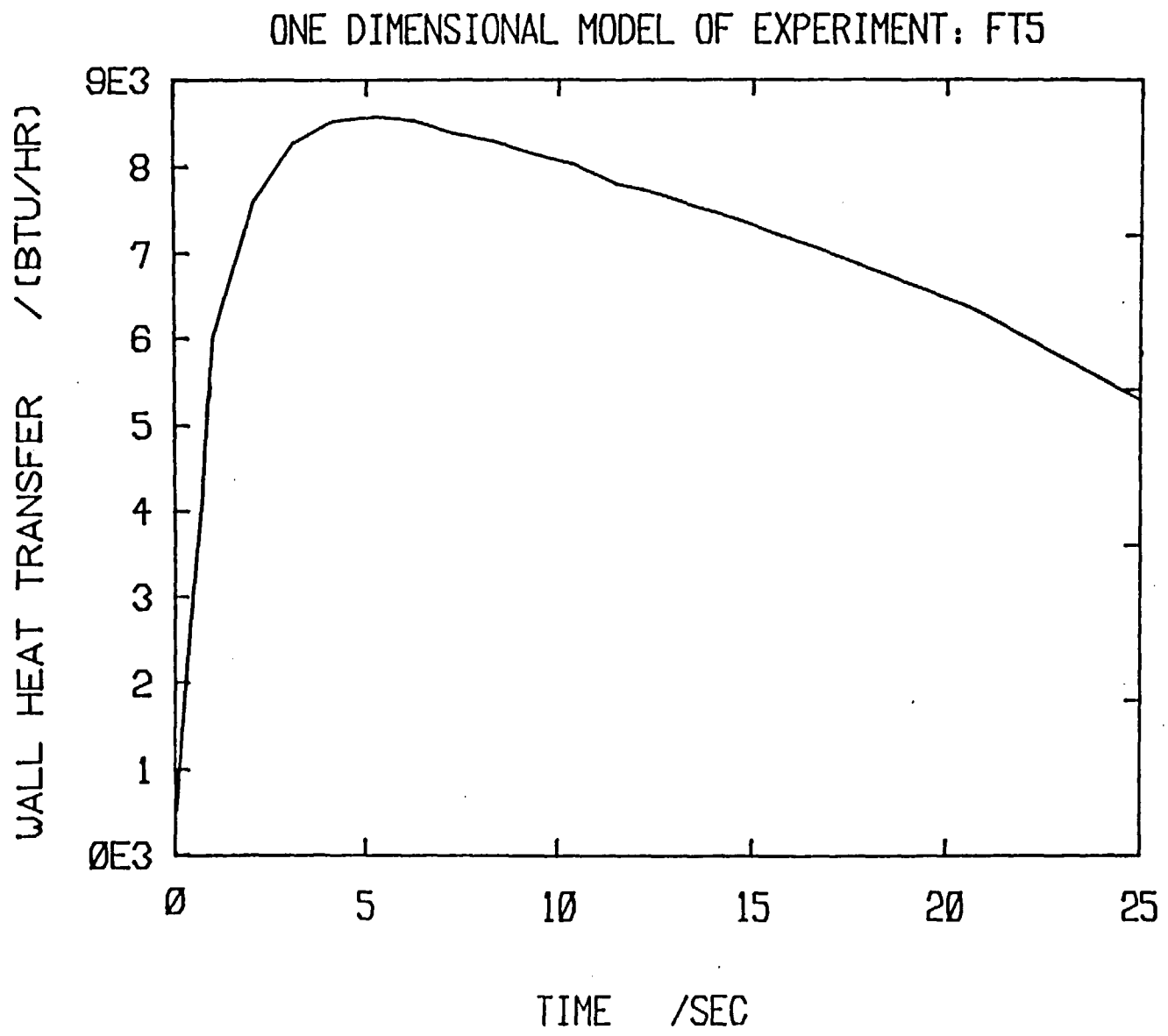

WALL HEAT TRANSFER : INSURGE RATE=0.78 in/sec

FIG. 15

The constitutive equation is;

$$\frac{\partial T}{\partial t} = \alpha \frac{\partial^2 T}{\partial x^2} \tag{32}$$

With conditions,

$$T(x,o) = T_v(o) \quad : \quad 0 < x < \infty$$

$$T(o,t) = T_v(t) \quad : \quad t > 0$$

This equation was solved by finite difference technique using an implicit relationship (Crank-Nicolson);

$$T_n^{i+1} = rT^i_{n-1} + (1 - 2r)T_n^i + rT^i_{n+1} \tag{33}$$

for $r = \alpha\Delta T/(\Delta x)^2$ and $0 < r < 1/2$

using conditions,

$$T_1^i = T_v^i$$

So,

$$(q/A)^{i+1} \cong (T_1^{i+1} - T_3^{i+1})/2\Delta x \tag{34}$$

The result of this calculation is shown in Fig. 16 for the experiment FT2. As it can be seen, the interface heat transfer is negligible.

The same result was obtained using a simple order of magnitude analysis. In this case, the energy equation at the interface was considered (Fig. 17):

$$q = KA \left(\frac{\Delta T}{\delta}\right) \tag{35}$$

Total heat transfer, Q, can be written as:

$$Q = (A\delta)\cdot\rho c \frac{\Delta T}{2} \tag{36}$$

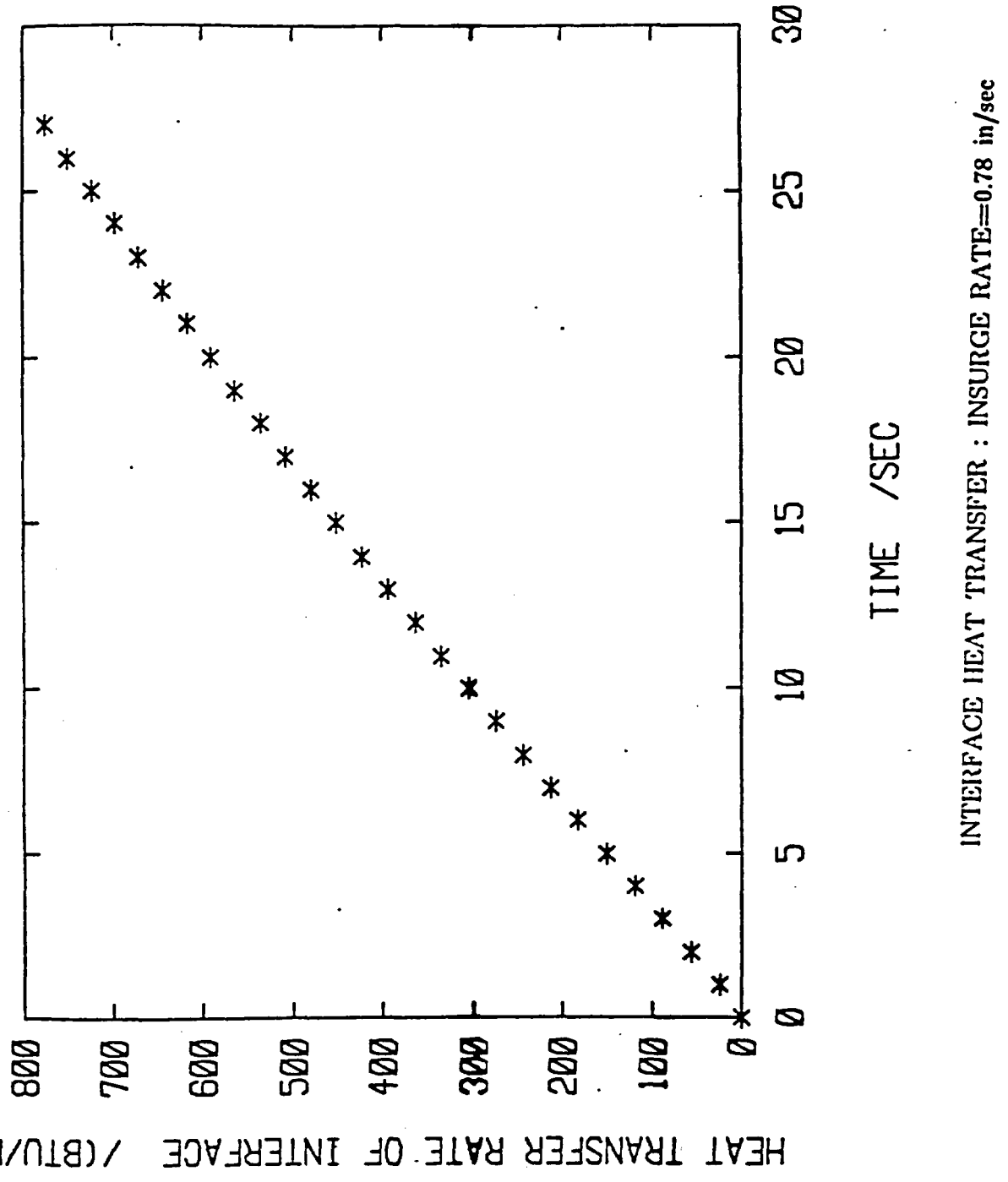
INTERFACE HEAT TRANSFER : INSURGE RATE=0.78 in/sec
HEAT TRANSFER RATE OF INTERFACE /(BTU/HR)
800
700
600
500
400
300
200
100
0
0
5
10
15
20
25
30
TIME /SEC

FIG. 16

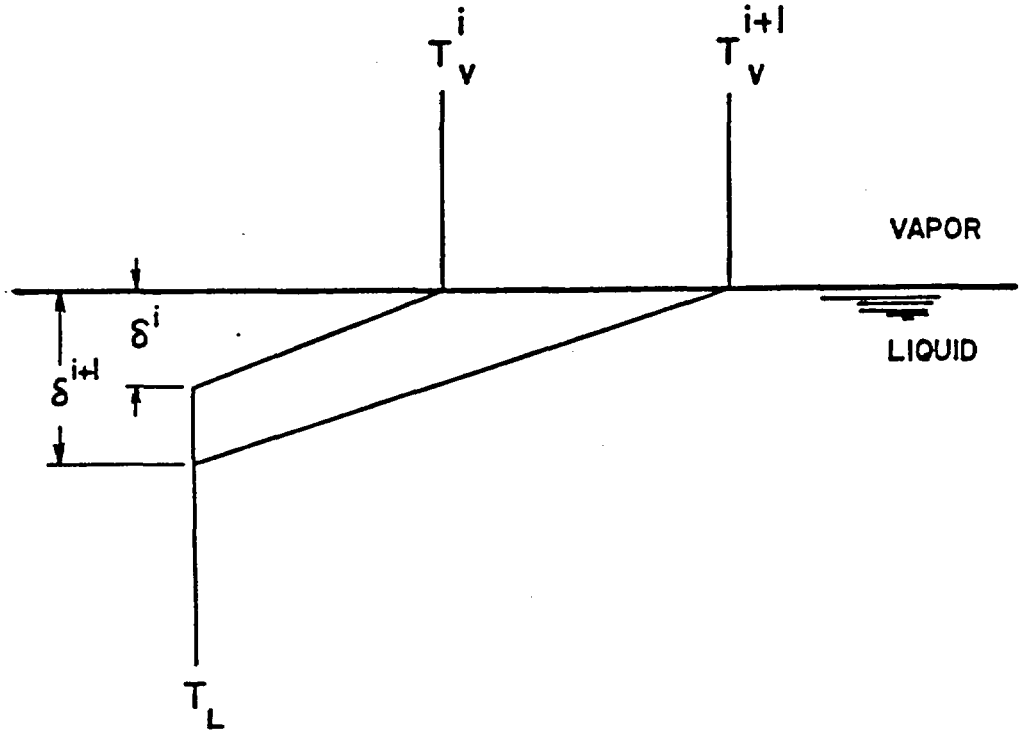

TEMPERATURE DISTRIBUTION USED FOR THE SIMPLE ANALYSIS

FIG. 17

$$q \simeq A\rho c \left(\frac{\Delta T}{2}\right) \frac{d\delta}{dt} \tag{37}$$

separating and then integrating we obtain,

$$\delta \sim 2\sqrt{\frac{K}{\rho c} t} \tag{38}$$

Heat transfer to the pool of liquid can now be calculated by substituting eqn. (38) in (36). The heat transfer for a period of 30 seconds was calculated using finite difference and simple analysis. The simple analysis gave a value within 10% of the result obtained by finite difference.

As Figs. 15 and 16 examplify, interface heat transfer is negligible. Yet, the above calculation of heat transfer can be regarded as an upper limit, since a reduction of heat transfer due to accumulation of the condensate should be expected. This accumulation is caused by both the free surface condensation and by the wall condensation which carries down and accumulate on the interface.

4.7 Comparison Between Different Modes of Heat Transfer

In a pressurizer many other processes take place such as, constant dribble of spray; one or more banks of heaters heating the subcooled liquid; axial heat transfer from vapor to the liquid through the wall; radial heat transfer due to conduction to the liquid; heating the pool from vapor region. Therefore, one must show that the effect of these processes are inconsequential, so that the overall model about to be discussed can be justified.

Such a calculation was made for Experiment: FT5 (see Appendix A.6). The result of the quantative comparison between different kinds of heat

transfer is shown in Table 4.1. It is obvious that the interfacial heat transfer and axial conduction at the wall is negligible compared to the heat transfer from the vapor to wall.

Another set of calculations were made using the dimensions of a Westinghouse pressurizer (see Appendix D for details on geometry). Table 4.2 shows the approximate time constant for each heat transfer process. From these results, it can be seen that for insurge transients of the order of 20 minutes or less; only the conduction from vapor to wall should be considered in the model.

4.8 Overall Model

In order to calculate the pressure response during an insurge, it is necessary to apply the 1st law to the steam volume. In this section, the conservation equations (derived in Appendix B) will be written using results of previous sections to account for the processes. As it is was explained in Chapter 3, experimental observations showed that the only non-equilibrium regions are the vapor and the subcooled liquid. Therefore, the pressure response can be calculated by considering the vapor region as a thermodynamic system (see Fig. 18). The first law applied to this region can be expressed as,

$$\sum \dot{Q}_i + \sum \dot{m}_i h_i = \dot{U} + p\dot{V} \tag{39}$$

$$= \dot{m}u + m\dot{u} + p\,\dot{m}v + pm\dot{v}$$

$$= \dot{m}\,(u + pv) + m\,(\dot{u} + p\dot{v})$$

$$= \dot{m}h + m\,(\dot{h} - v\dot{p}) \tag{40}$$

TABLE 4.1: Order of Magnitude for Different Types of Heat Transfer Occuring During the Insurge Experiments

Wall conduction time constant - 50 sec.

Type of heat transfer:		$Q(\Delta t = 30 \text{ sec})$
Conduction from vapor to wall	-	230 BTU
Conduction from vapor to pool	-	3 BTU
Wall axial conduction from vapor to cold liquid	-	3 BTU

TABLE 4.2: Order of Magnitude for Time Constants of Different Types of Heat Transfer in the Case of a Westinghouse Pressurizer

Time constant for:

		τ
Conduction from vapor to wall	-	1/2 hr.
Axial conduction in the wall from vapor to subcooled liquid region	-	25 hrs.
Radial conduction from wall to subcooled liquid	-	60 hrs.
One bank of heaters	-	1 hr.
Dribble from spray nozzle	-	4 hrs.
Conduction from vapor to liquid	-	18000 hrs.

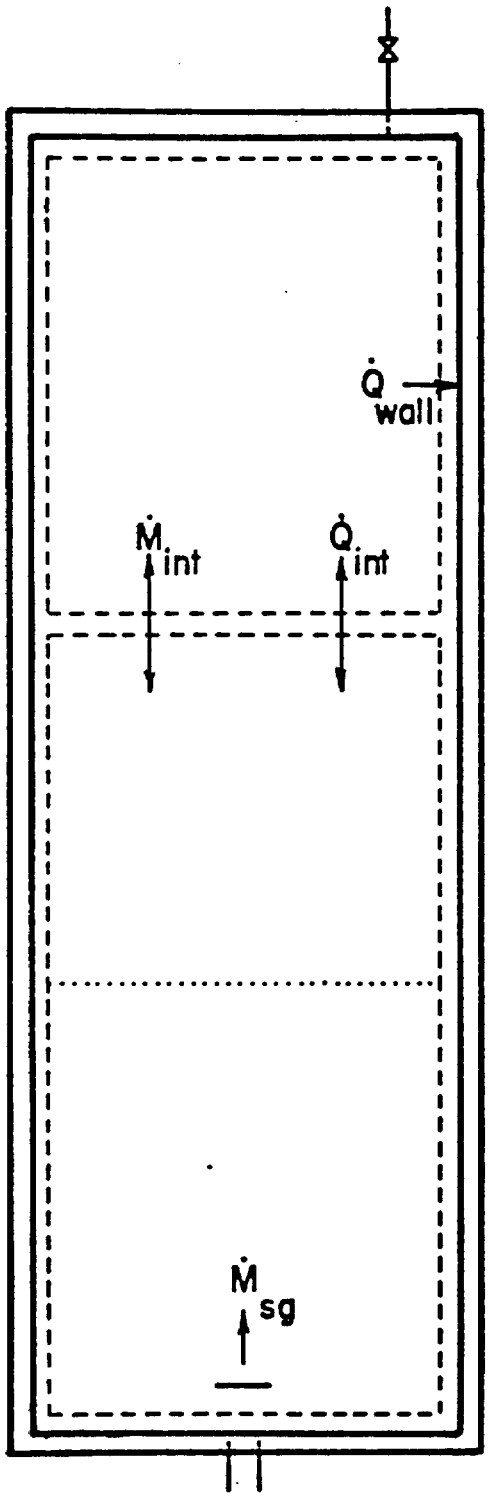

CONFIGURATION OF THE SYSTEM

FIG. 18

Therefore,

$$- \dot{Q}_{int} - \dot{Q}_{wall} - \dot{m}_{cond} h_{cond} = m_v (\dot{h}_v - v_v \dot{p}) + \dot{m}_v h_v \quad (41)$$

Conservation of mass yields;

$$\dot{m}_v = - \dot{m}_{cond} \quad (42)$$

From (41) and (42);

$$- \dot{Q}_{int} - \dot{Q}_{wall} + \dot{m}_v h_{cond} = m_v (\dot{h}_v - v_v \dot{p}) + \dot{m}_v h_v \quad (43)$$

Conservation of volume gives,

$$\dot{V}_v = - \dot{V}_{sg} \quad (44)$$

$$= m_v \dot{v}_v + \dot{m}_v v_v \quad (45)$$

Therefore,

$$\dot{m}_v = \frac{\dot{V}_{sg} - m_v \dot{v}_v}{v_v} \quad (46)$$

also,

$$h_v = h_v (p,T) \quad (47)$$

$$v_v = v_v (p,T) \quad (48)$$

$$T = T(p) \quad (49)$$

From the above equations, it can be seen that equation (41) is a function of prerssure. In order to solve for pressure, an explicit, numerical scheme can be used. Equation (41) can be written as (and neglecting $\dot{Q}_{int}$):

$$- (Q_{wall}^{i+1} - Q_{wall}^{i}) - h_{cond} (m_v^{i+1} - m_v^{i}) - m_v [(h_v^{i+1} - h_v^{i}) - v_v (p^{i+1} - p^{i})] - (m_v^{i+1} - m_v^{i}) h_v = 0 \quad (50)$$

Using curved-fit properties for steam and water, and employing results of §.4.4 and 4.5, equation (50) can be solved iteratively.

4.9 Comparison Between Model Prediction and Data

The model described in the previous section was compared against experiments ran at different insurge rates. This was done by solving equation (50) and using insurged mass of water as input. For each of the runs, (descriptions given in Appendix A), the model approximated the experimental data quite well, Figs. 19,20,21. The small discrepancy seen is probably due to the parabolic temperature profile assumption; i.e. having no thin "hot" region right at the inside wall early in the transient. Although the method of analysis was checked against data from low pressure experiments, this should not matter since the amount of condensation and the percentage pressure rises are smaller at higher pressures. Therefore, this study should be applicable to high pressure processes.

A comparison of the limiting cases; i.e. adiabatic and equilibrium models, was made against experiment data, Fig. 22. Not only these predictions showed a large difference in magnitude compared to each other (as was mentioned in §1.3), but they also failed to estimate the pressure response behavior satisfactorily.

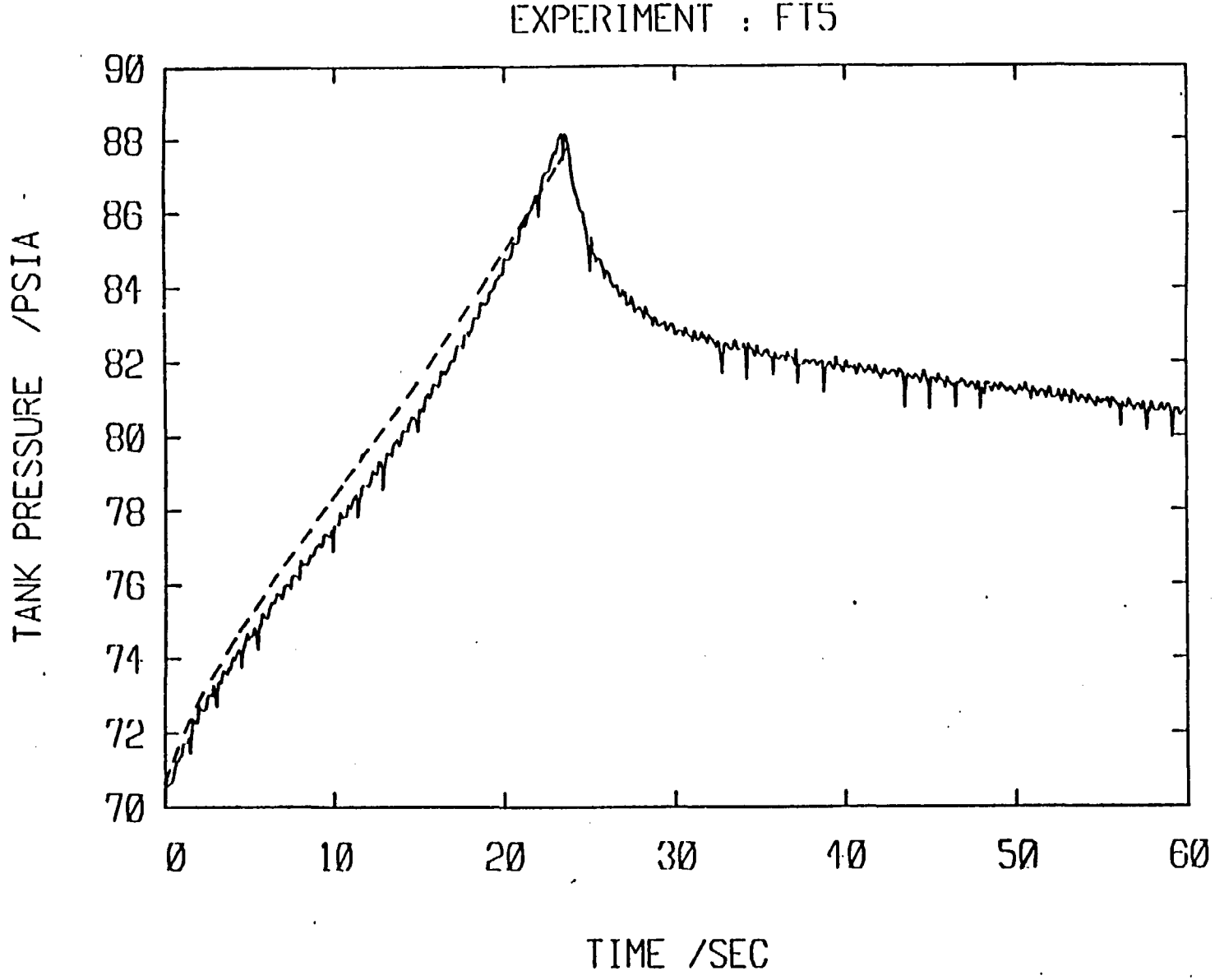

FIG. 19

COMPARISON BETWEEN DATA AND MODEL : INSURGE RATE=0.78 in/sec

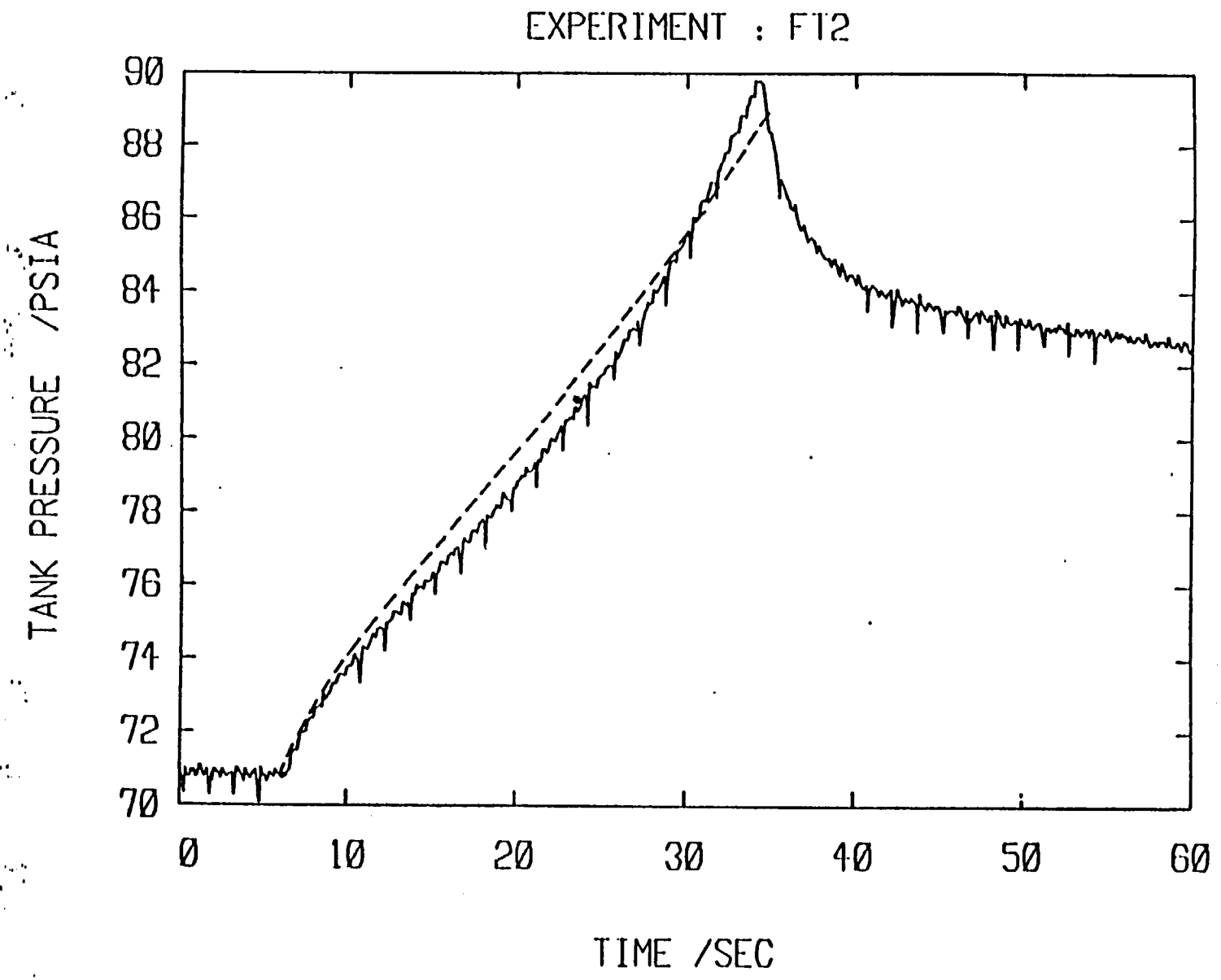

FIG. 20

COMPARISON BETWEEN DATA AND MODEL : INSURGE RATE=0.6 in/sec

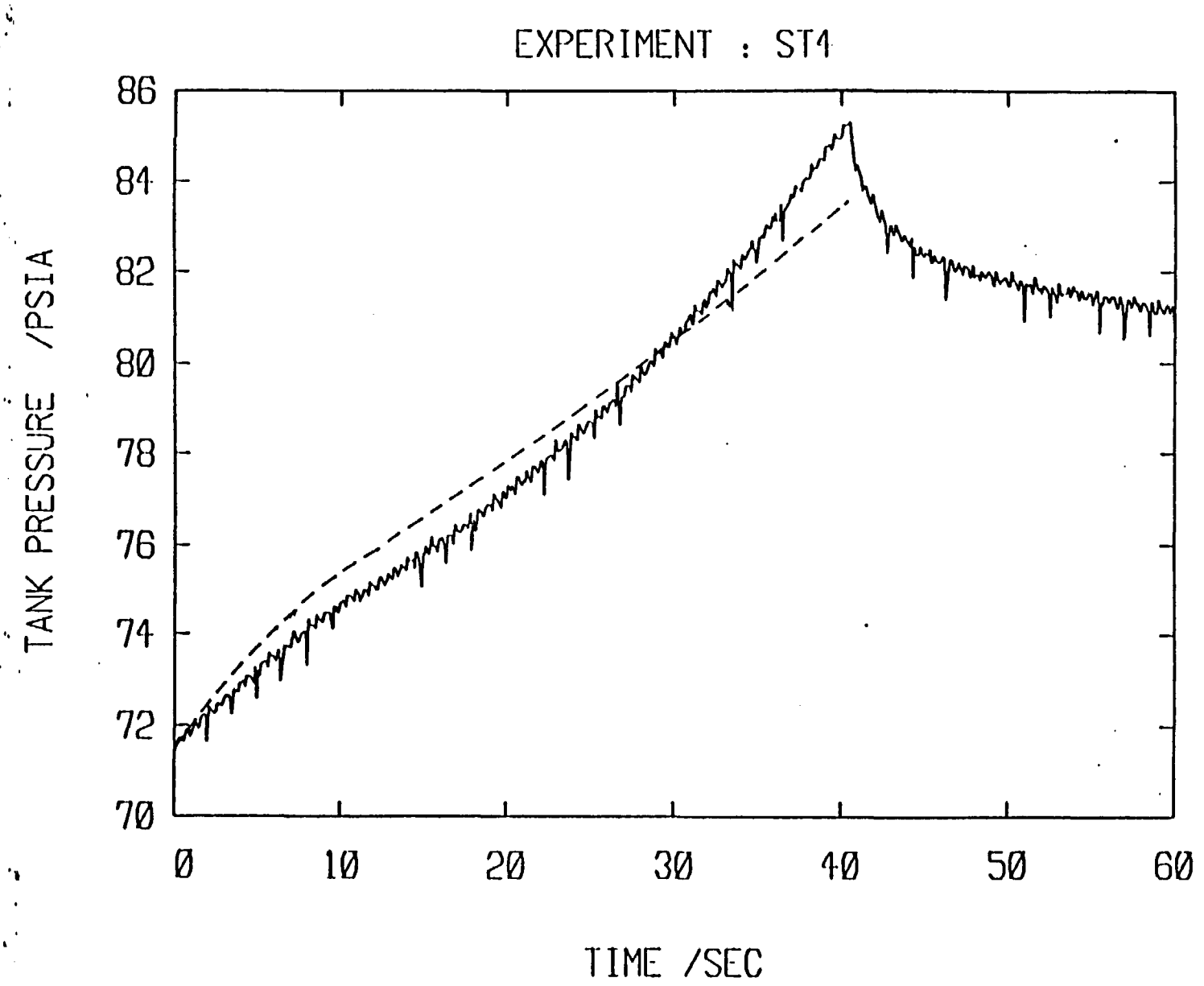

FIG. 21

COMPARISON BETWEEN DATA AND MODEL : INSURGE RATE=0.44 in/sec

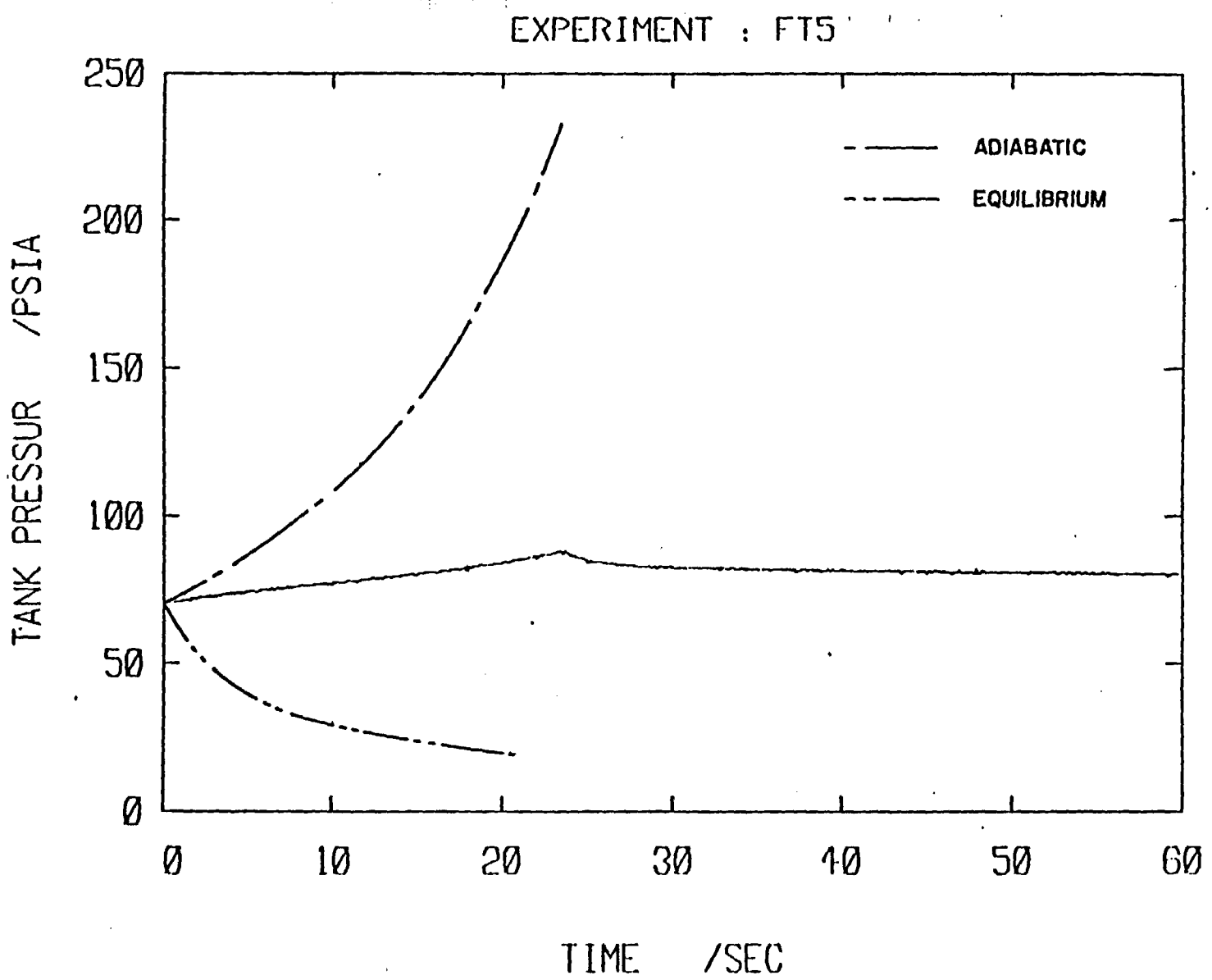

FIG. 22

COMPARISON BETWEEN LIMITING CASES : INSURGE RATE=0.78 in/sec

CHAPTER 5

CONCLUSIONS

1) The limits of perfect mixing in the pressurizer and adiabatic compression of the steam bubble yield very different pressure responses. These pressure responses are so different in magnitude that they don't yield a reliable limit when calculating pressures during an insurge transient.
2) Wall heat transfer substantially reduces the peak pressure during an insurge transient.
3) Interface condensation is entirely negligible during an insurge transient of 5 minutes or less duration and for pool depths sufficient to submerge the inlet sprarger.
4) Wall axial conduction is quite negligible during an insurge transient of 5 minutes duration or less.

REFERENCES

1. Redfield, J.A., "Pressurizer Performance During Loss-Of-Load Tests at Shipping Port", Nuclear Applications, V.4, March 1968.

2. Demuth, N.S., et al, "Effects of Condensation Modeling on Transient Behavior of Pressurized Water Reactors," Los Almos National Lab, LA-UR-82-2661.

3. Reeder, D.L., "Quick-Look Report on LOFT Nuclear Experiments," L6-1, L6-2, L6-3, EGG-LOFT-5270, Project No. P394, October 1980.

4. Bonaca, M.V., "PWR Transient Pressurizer Pressure Behavior," ANS Winter Meeting, 1981.

5. Retran II - A Program for One-Dimensional Transient Thermal-Hydraulic Analysis of Complex Fluid Flow Systems, Vol. 1, EPRI NP-408, 1977.

6. Nahavandi, A.N., et al., "A Comparison of Equilibrium and Non-equilibrium Thermodynamic Models in a Water-Reactor Pressurizer," ANS (1967, Winter Meeting).

7. Glasser, T.H., "Basic Equations for Predicting Performance of a Nuclear Power Plant Pressurizer," ASME - S7-NESC-95.

8. Cunningham, J.P., et al., "PRESTO, A Pressurizer Transient Program for the IBM-704," YAEC-141.

9. Thomas, A.W. and Findlay, "PRE- A Pressurizer Transient Program for the Philco 2000 Computer, KAPL-M-E7-7.

10. Abraham, G., "Jet Diffusion in Stagnant Ambient Fluid," No. 29.

11. Turner, J.S., "Jet with Negative or Reserving Buoyancy," Journal of Fluid Mechanics, 26, pp.779-792.

12. Albertson, et al., "Diffusion of Submerged Jets," American Civil Engineers, 115, p.639-697.

13. Reynolds, W.C., Report No. 58-A-248.

14. Potter, Foss, "Fluid Mechanics," Wiley, 1975.

15. Honan, T., Personal Communications.

16. RELAP5/MOD 1 Code Manual, Volume 1: "System Models and Numerical Methods," NUREG/CR-1826, March 1982.

APPENDIX A

Experimental Data

Results of 5 different insurge experiments are shown in this Appendix. Sections A.1 through A.3 include data taken with thermocouple at three different radial locations. Section A.3 is data for insurge to empty tank. Sections A.4 and A.5 include data showing axial temperature distribution with only centerline temperature measurements. Section A.4 shows data for insurge to partially filled tank and Section A.5 shows data for insurge into empty tank.

A.1 Experiment: BB4

Water level at t = 0 sec : L = 17 in.

Water level increase : ΔL = 16 in.

Insurge time : t = 31 sec.

This experiment was ran using the first type of top flange (§2.1). The presence of the plume was detected from Figs. A.1.6 through A.1.8. From these plots, the plume speed was estimated. As calculations showed, the plume travels with a speed slightly less than that of the insurged liquid level rise.

The pressure spikes, Fig. A.1.1, appear to be due to pickup in the leads. Though they confuse the data, they are not important.

LEGEND

△	CENTRE LINE
□	1/4" AWAY FROM WALL
○	OUTSIDE WALL
- - -	WATER LEVEL
.....	SATURATION TEMPERATURE

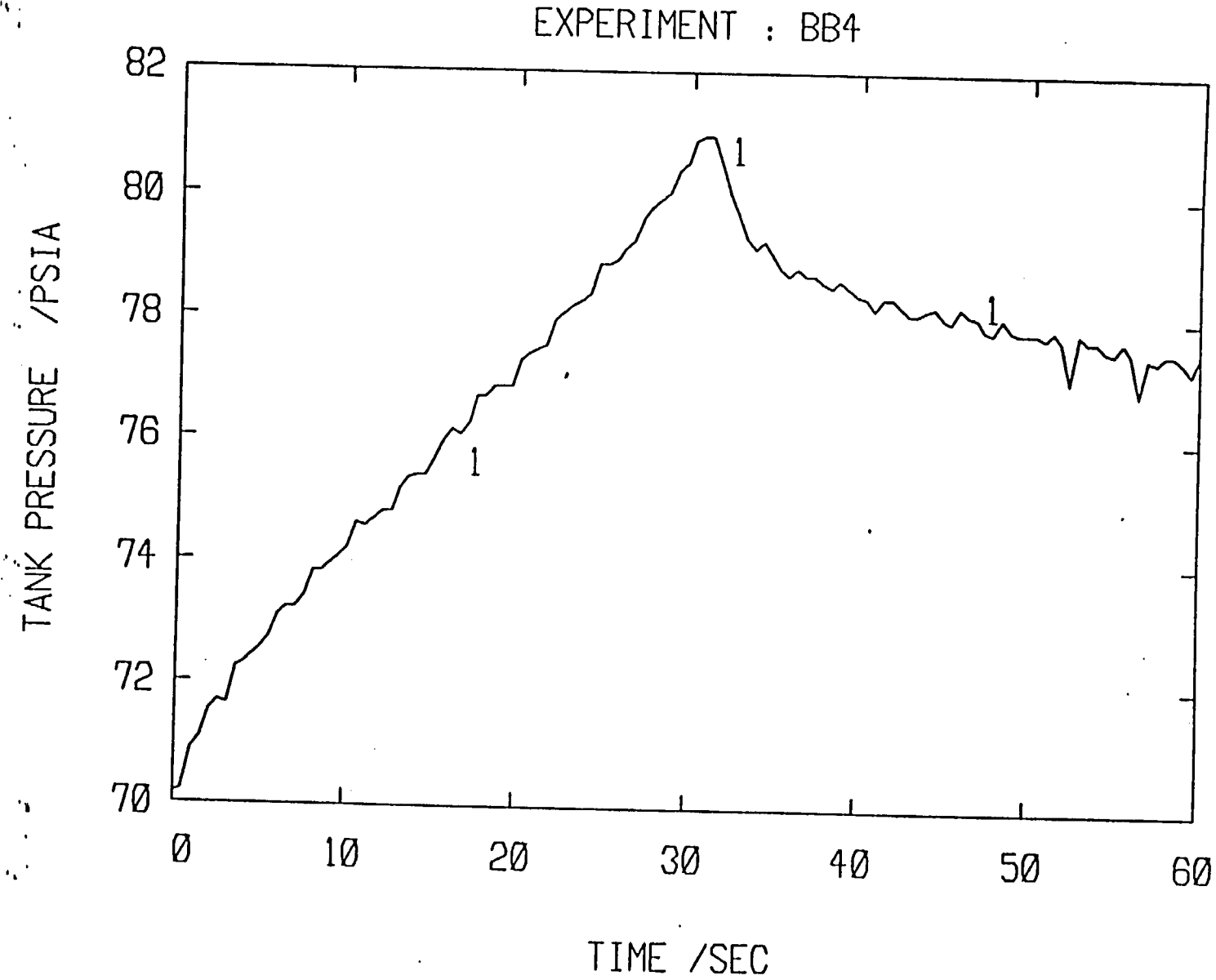
EXPERIMENT : BB4
TANK PRESSURE /PSIA
82
80
78
76
74
72
70
0
10
20
30
40
50
60
TIME /SEC
1
1
1

Fig. A.1.1

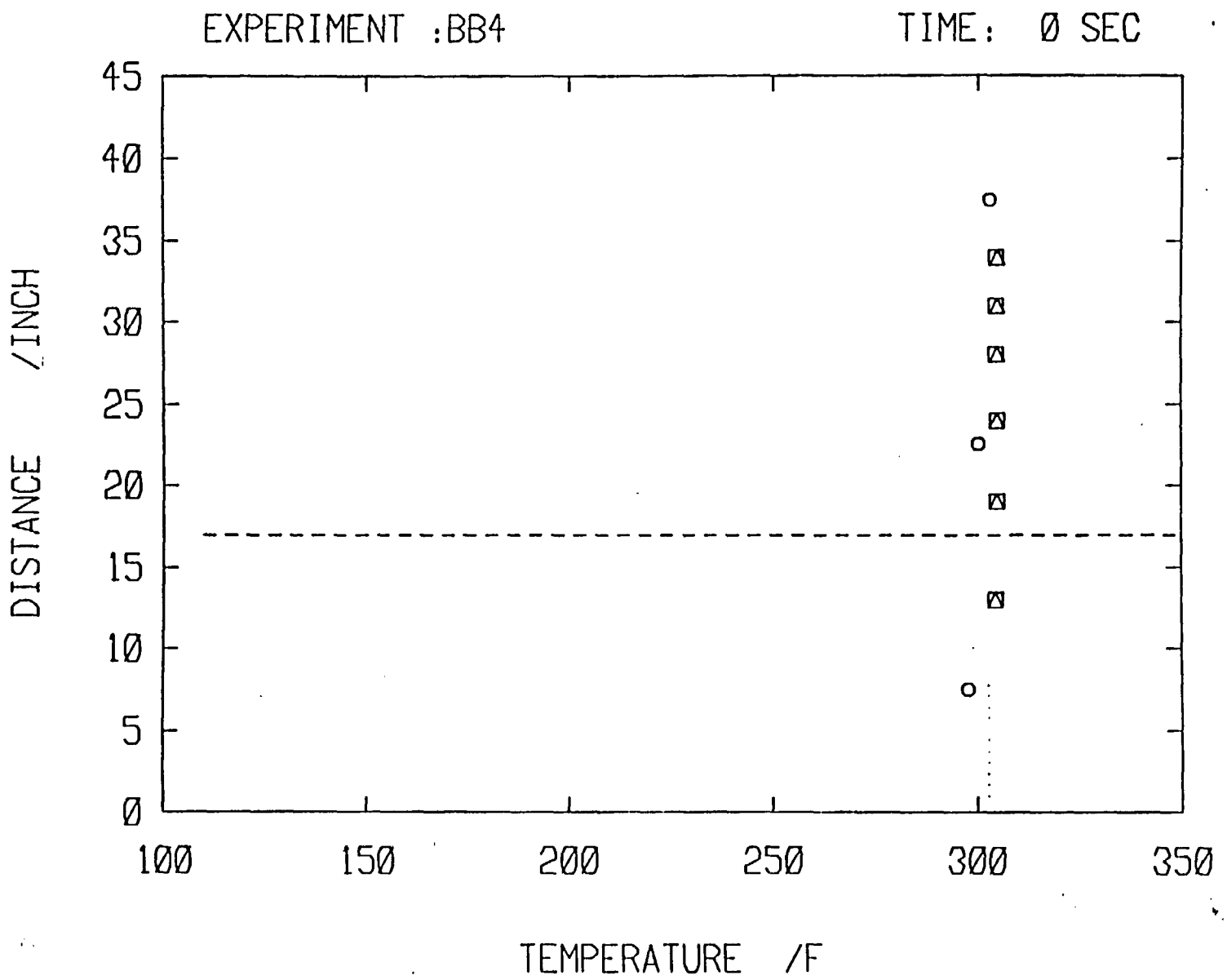
EXPERIMENT :BB4
TIME: Ø SEC
DISTANCE /INCH
45
40
35
30
25
20
15
10
5
Ø
100
150
200
250
300
350
TEMPERATURE /F

Fig. A.1.2

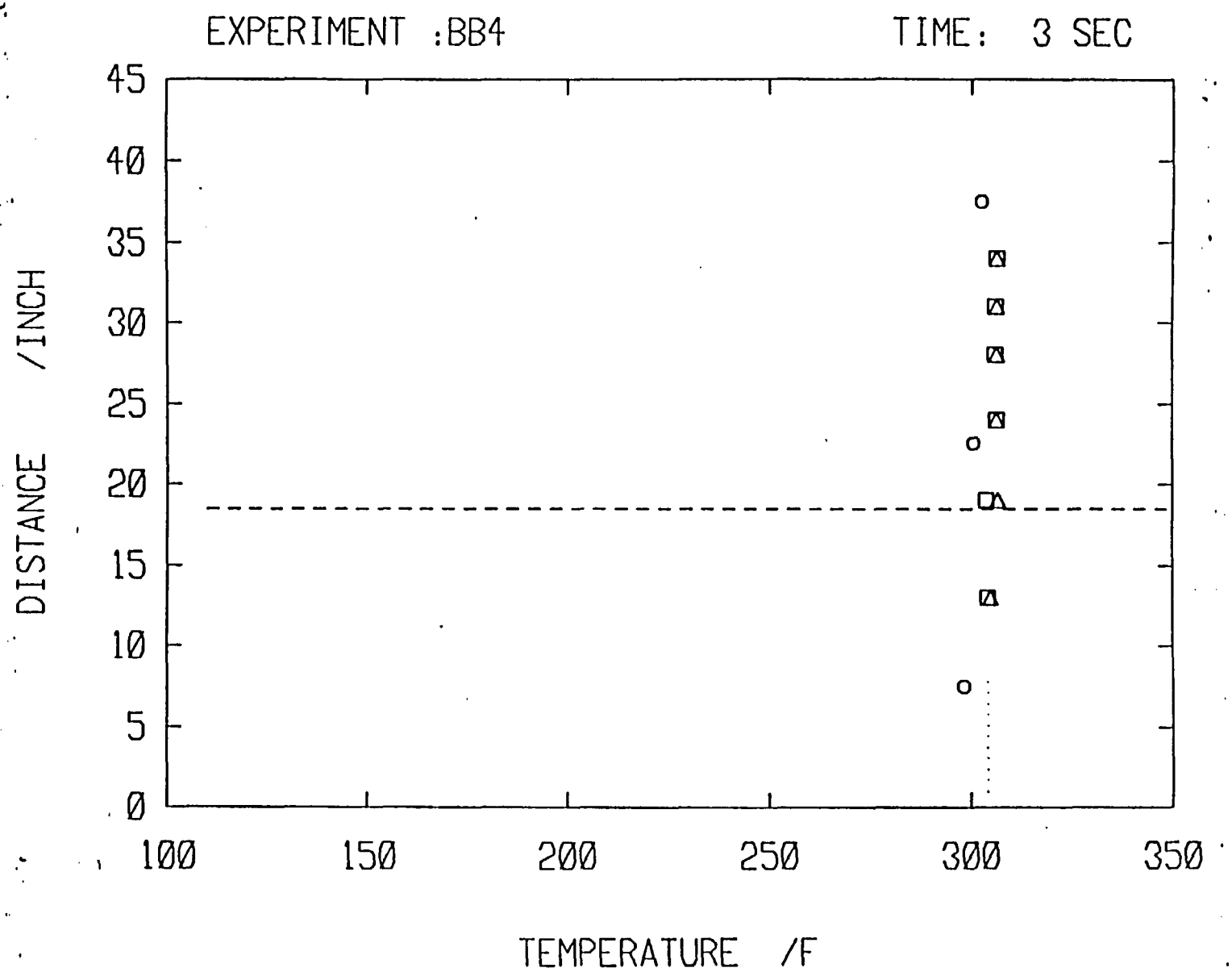
EXPERIMENT :BB4
TIME: 3 SEC
DISTANCE /INCH
45
40
35
30
25
20
15
10
5
0
100
150
200
250
300
350
TEMPERATURE /F

Fig. A.1.3

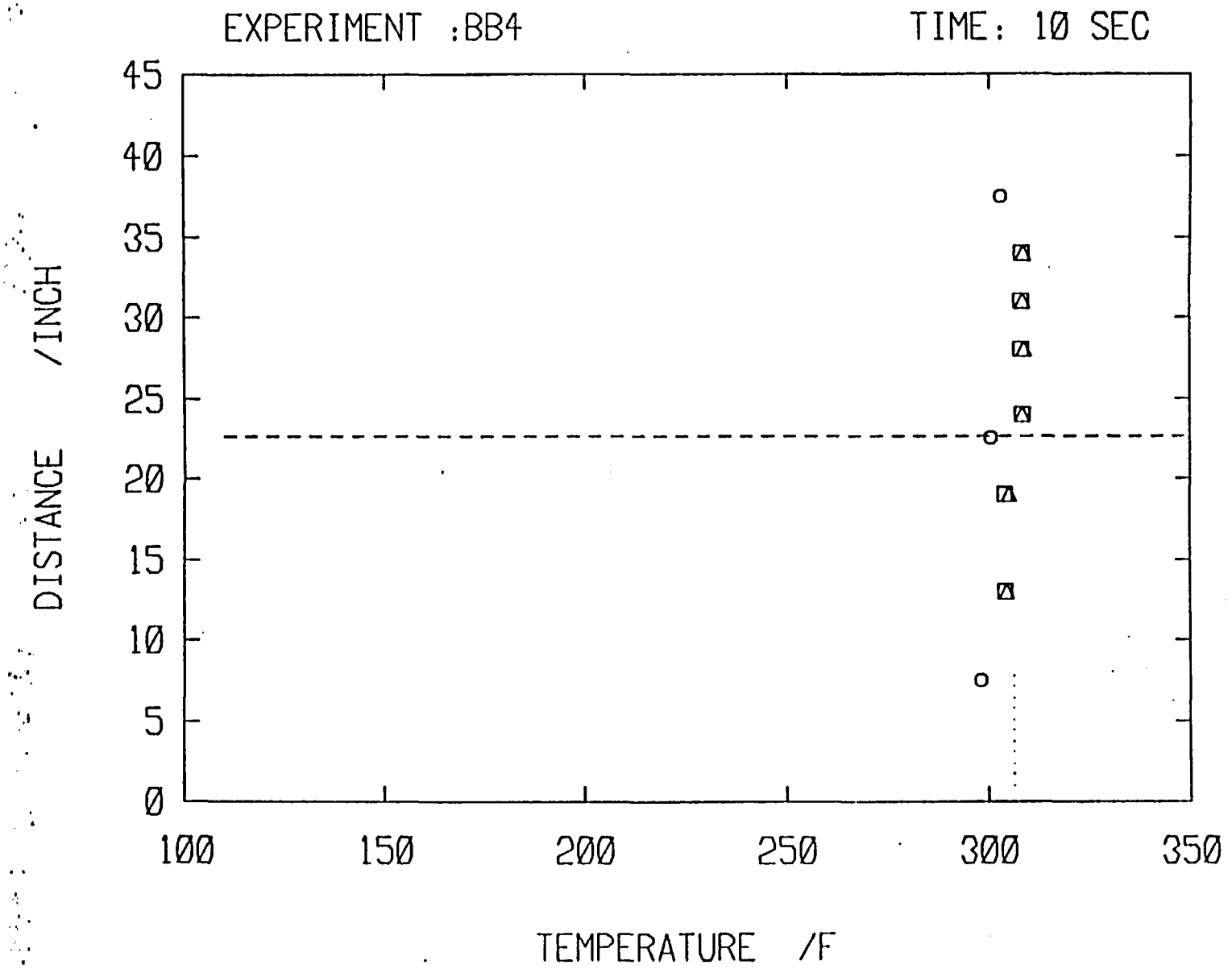
EXPERIMENT :BB4
TIME: 10 SEC
DISTANCE /INCH
45
40
35
30
25
20
15
10
5
0
100
150
200
250
300
350
TEMPERATURE /F

Fig. A.1.4

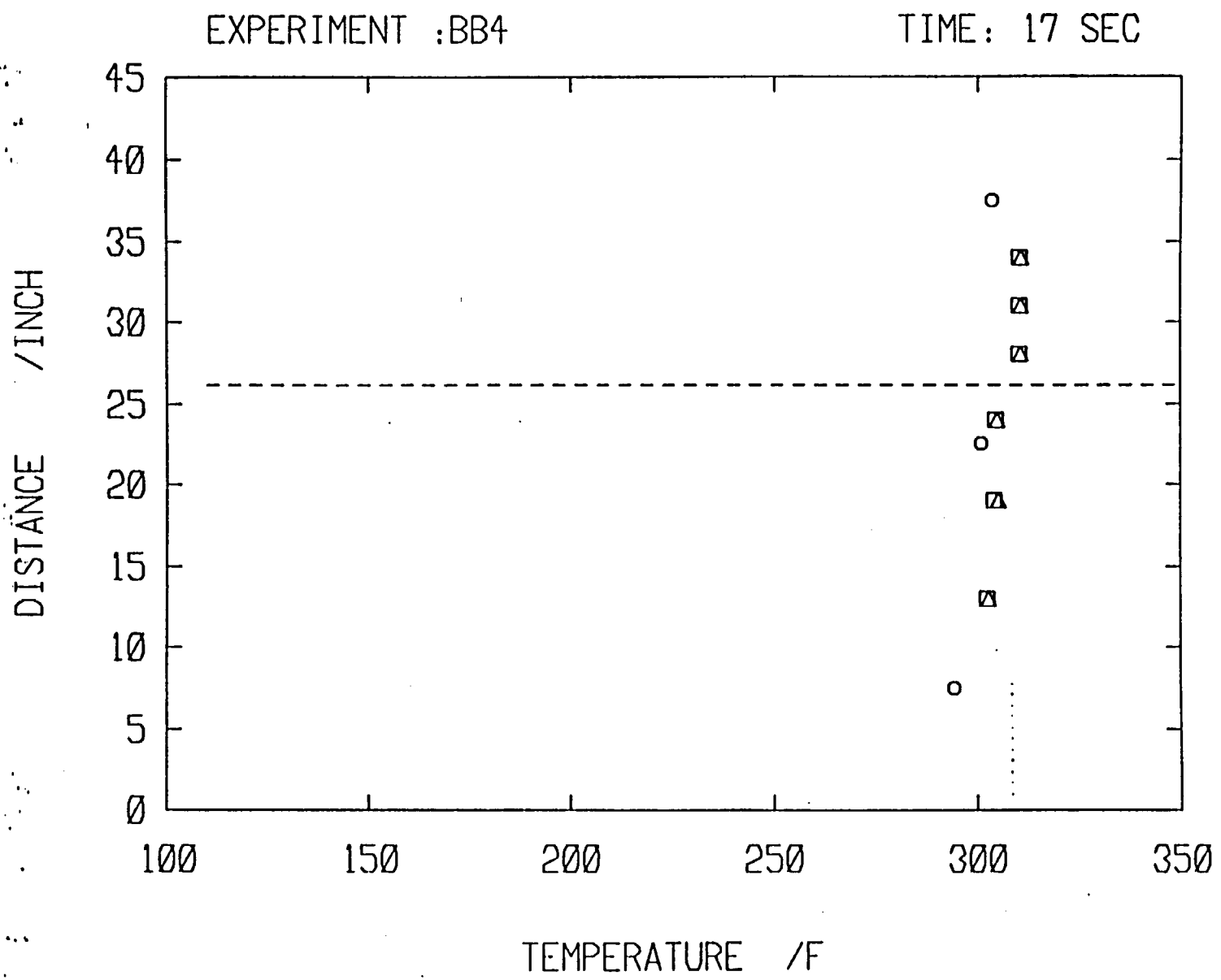
EXPERIMENT :BB4
TIME: 17 SEC
DISTANCE /INCH
45
40
35
30
25
20
15
10
5
0
100
150
200
250
300
350
TEMPERATURE /F

Fig. A.1.5

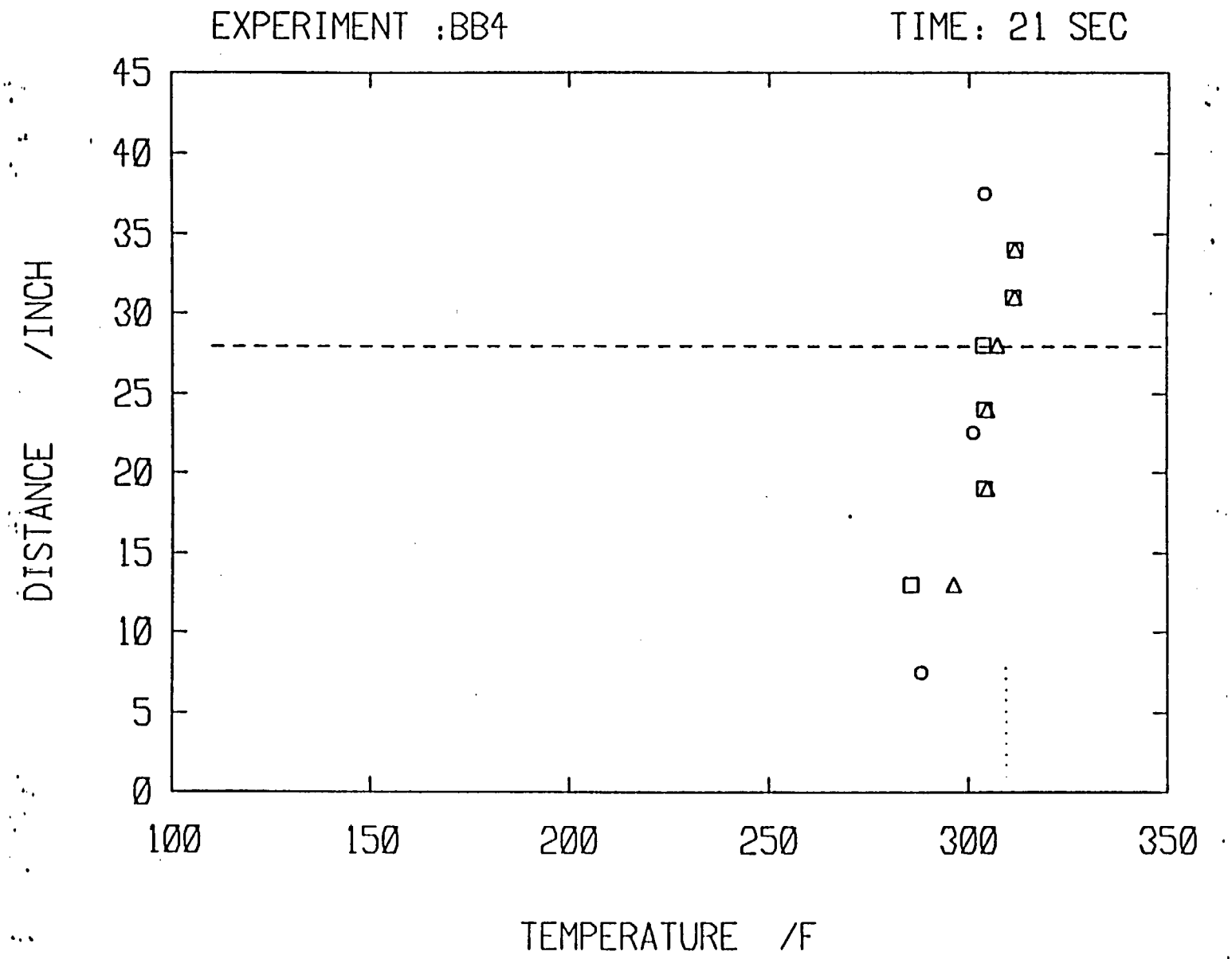
EXPERIMENT :BB4
TIME: 21 SEC
DISTANCE /INCH
45
40
35
30
25
20
15
10
5
0
100
150
200
250
300
350
TEMPERATURE /F

Fig. A.1.6

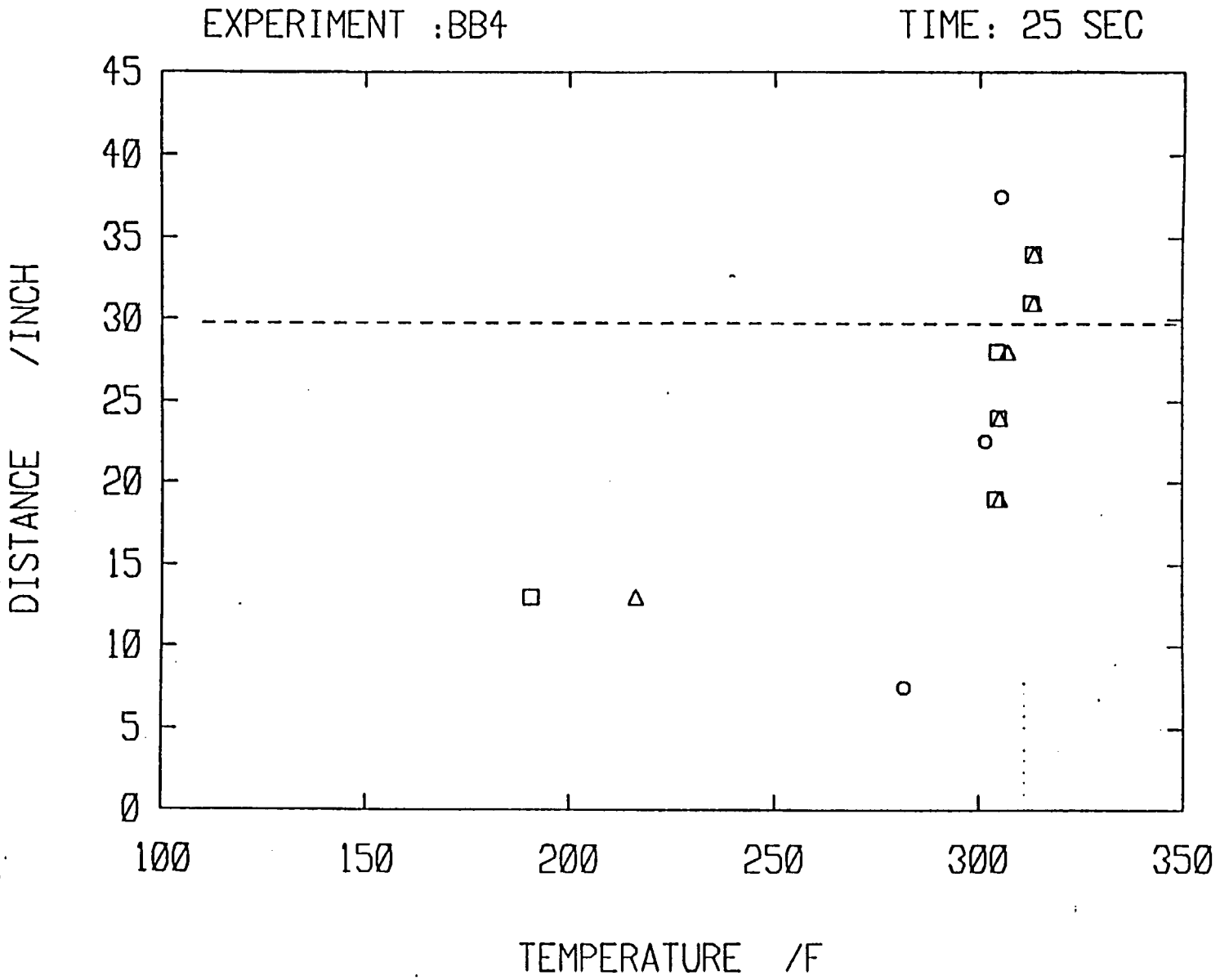
EXPERIMENT :BB4
TIME: 25 SEC
DISTANCE /INCH
45
40
35
30
25
20
15
10
5
0
100
150
200
250
300
350
TEMPERATURE /F

Fig. A.1.7

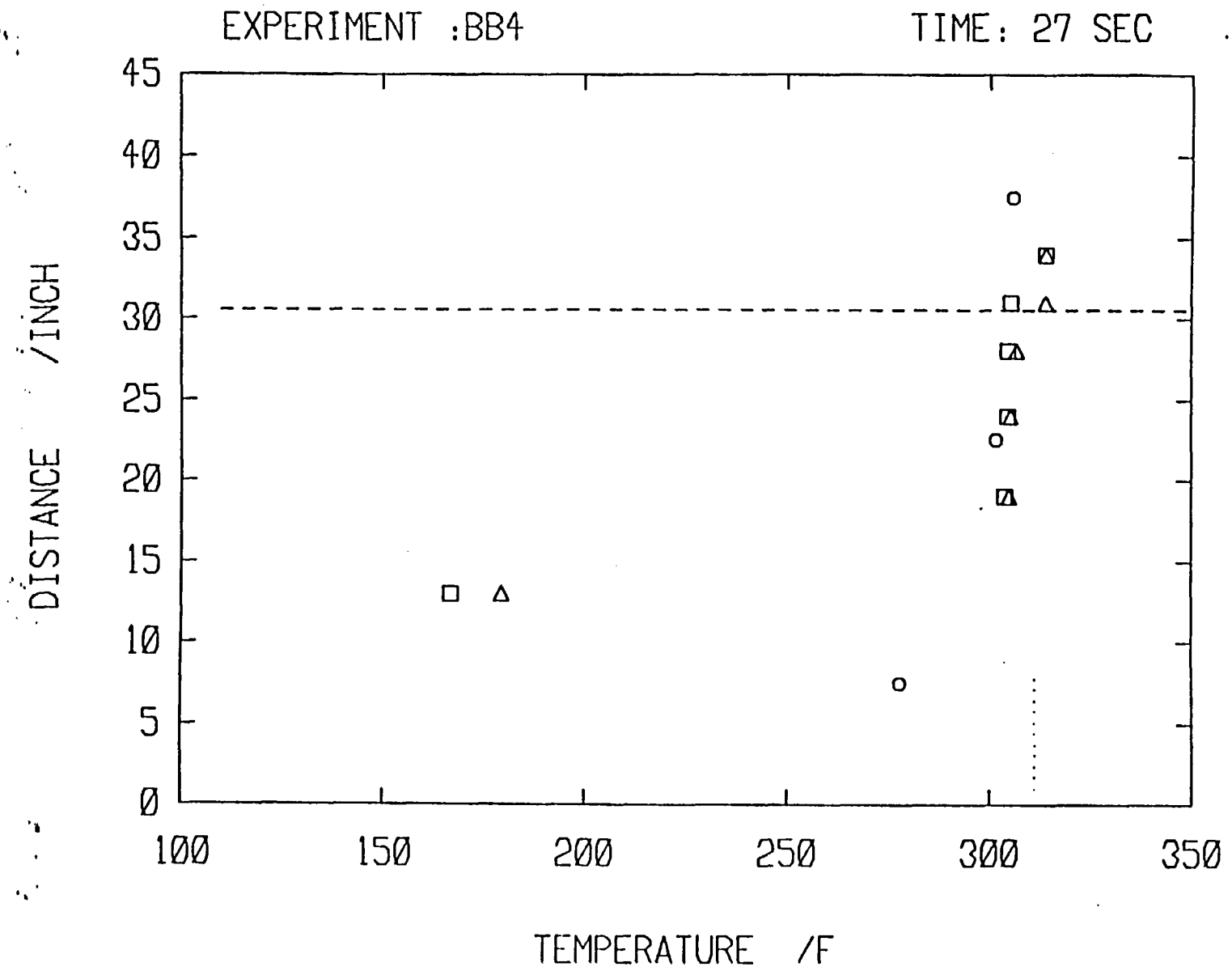
EXPERIMENT :BB4
TIME: 27 SEC
DISTANCE /INCH
45
40
35
30
25
20
15
10
5
0
100
150
200
250
300
350
TEMPERATURE /F

Fig. A.1.8

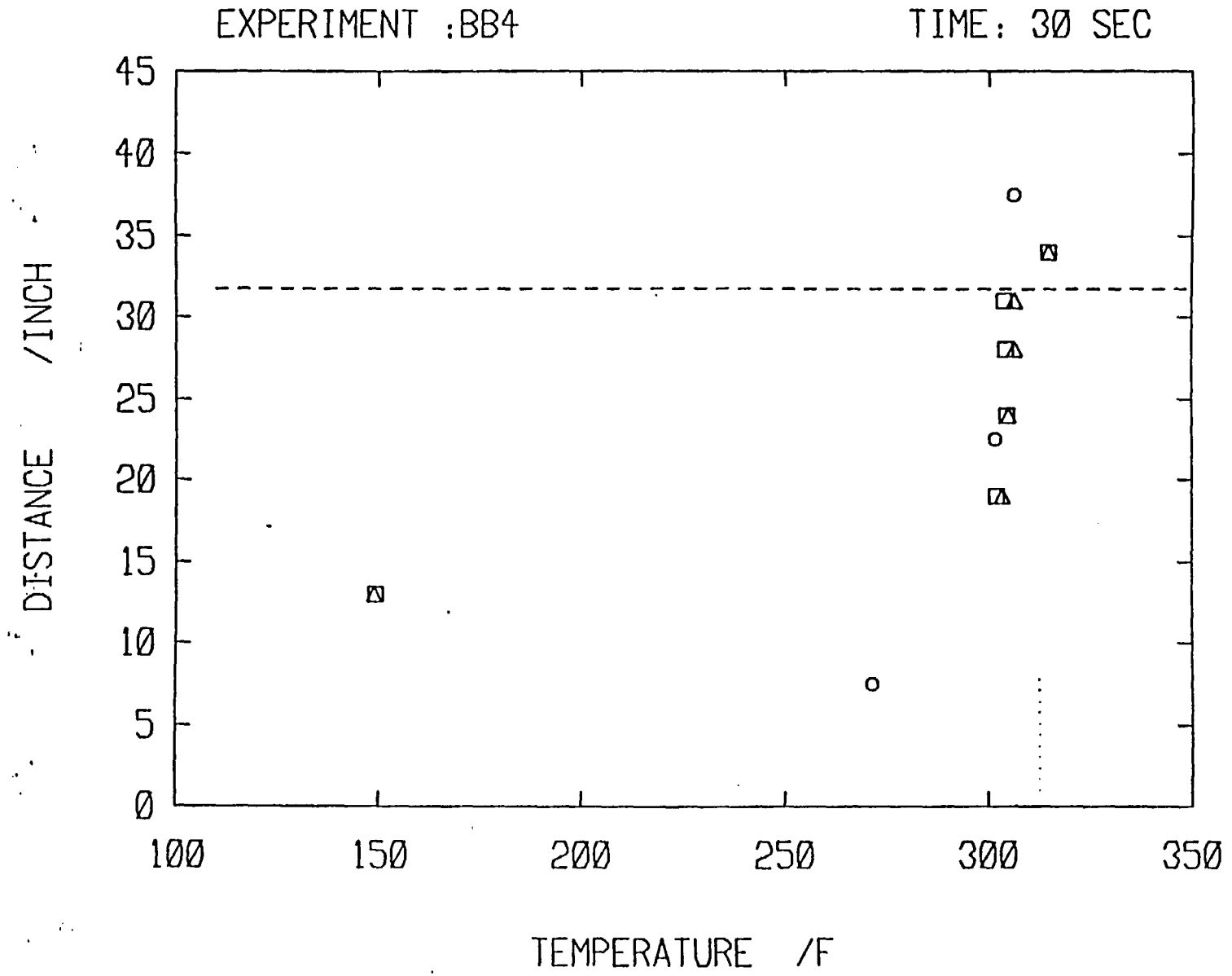
EXPERIMENT :BB4
TIME: 30 SEC
DISTANCE /INCH
45
40
35
30
25
20
15
10
5
0
100
150
200
250
300
350
TEMPERATURE /F

Fig. A.1.9

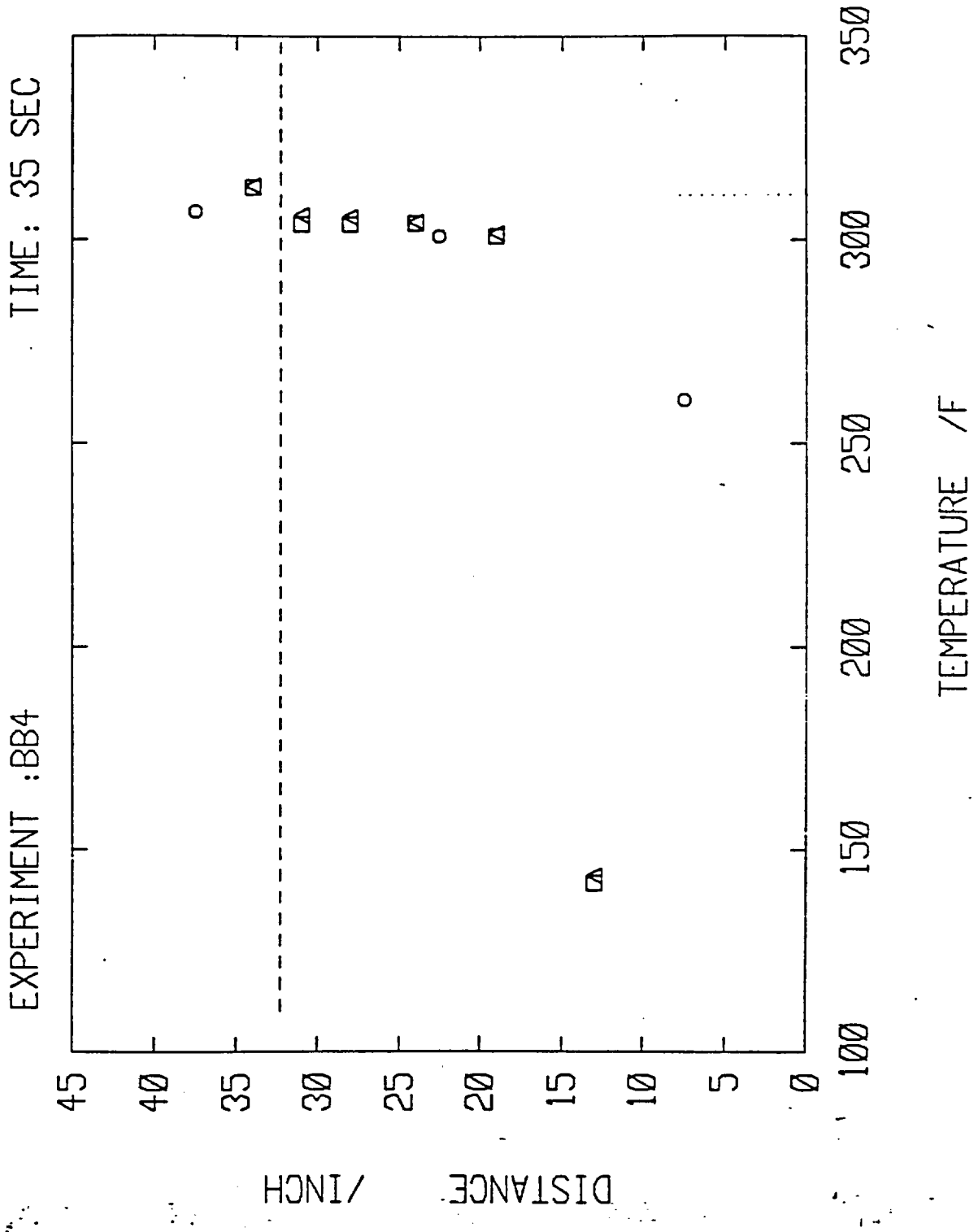
EXPERIMENT :BB4
TIME: 35 SEC
DISTANCE /INCH
TEMPERATURE /F
45
40
35
30
25
20
15
10
5
0
100
150
200
250
300
350

Fig. A.1.10

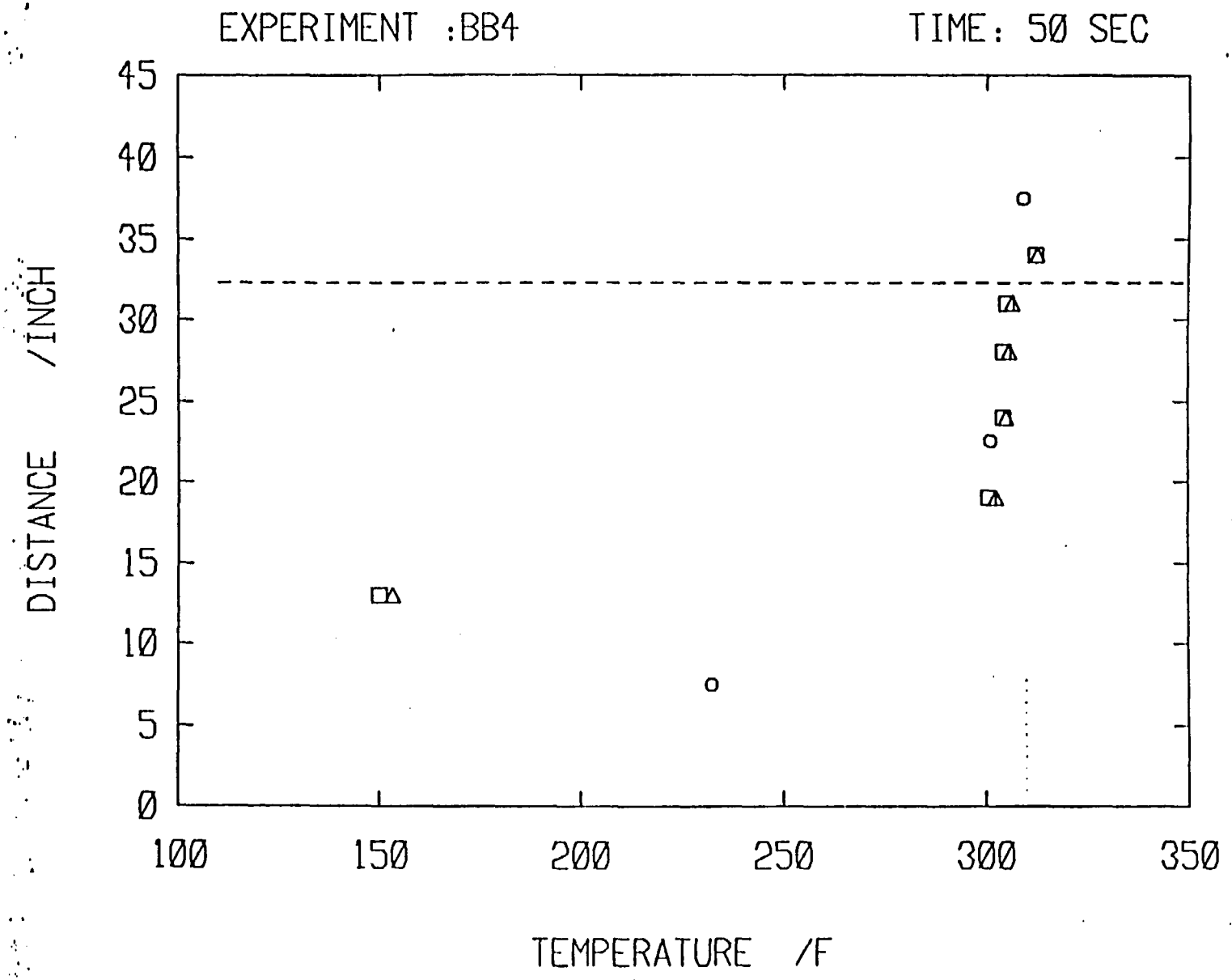
EXPERIMENT :BB4
TIME: 50 SEC
DISTANCE /INCH
45
40
35
30
25
20
15
10
5
0
100
150
200
250
300
350
TEMPERATURE /F

Fig. A.1.11

A.2 Experiment: TR8

Water level at t = 0 sec : L = 17 in.

Water level increase : ΔL = 19 in.

Insurge Time : t = 78 sec.

This was a slow transient and the radially located thermocouples were used. The presence of the plume can be seen from Figs. A.2.9 through A.2.10. After the insurge was stopped; heat transfer from wall to the liquid was done by natural convection mechanism, Fig. A.2.11.

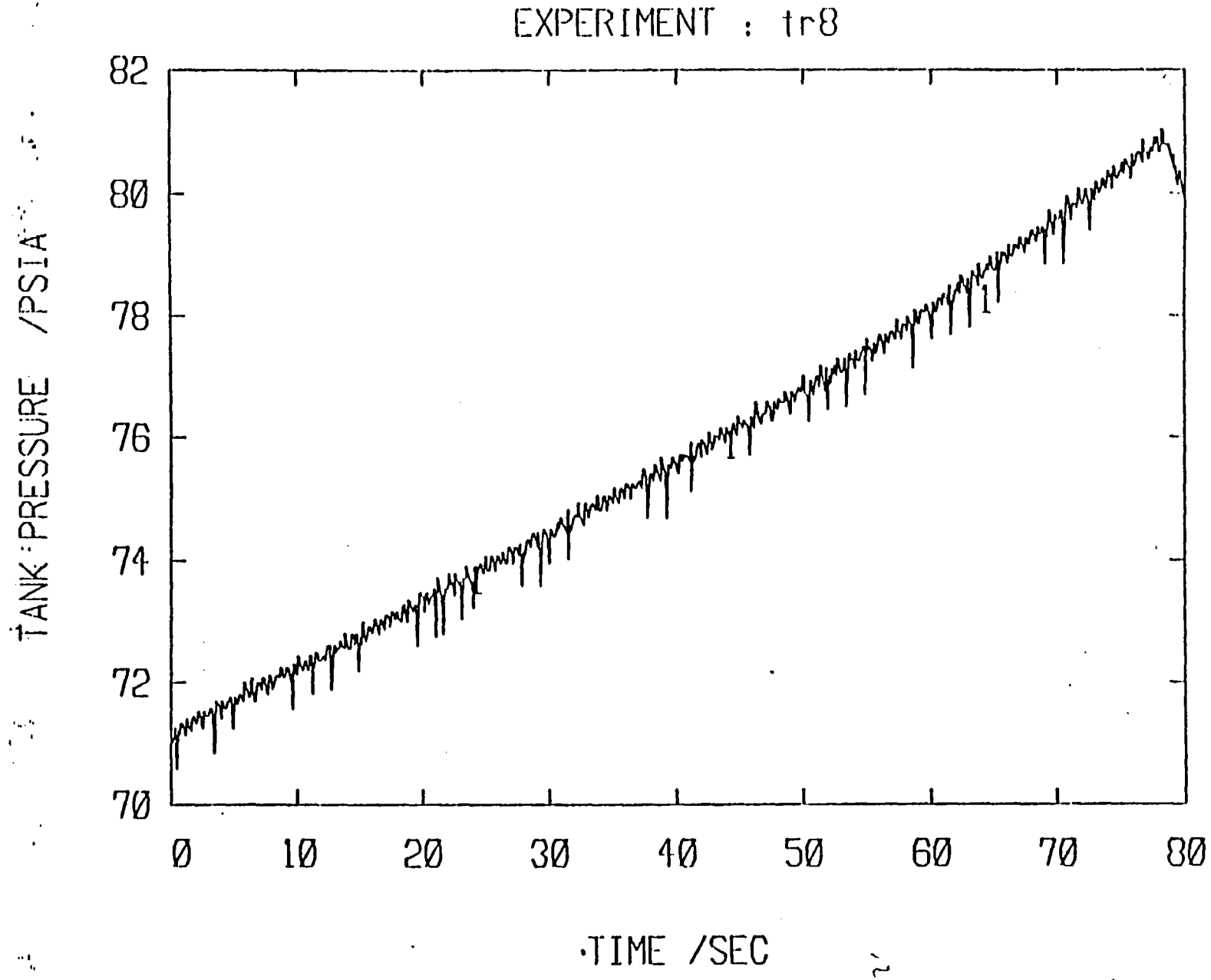
EXPERIMENT : tr8
TANK PRESSURE /PSIA
82
80
78
76
74
72
70
0
10
20
30
40
50
60
70
80
TIME /SEC

Fig. A.2.1

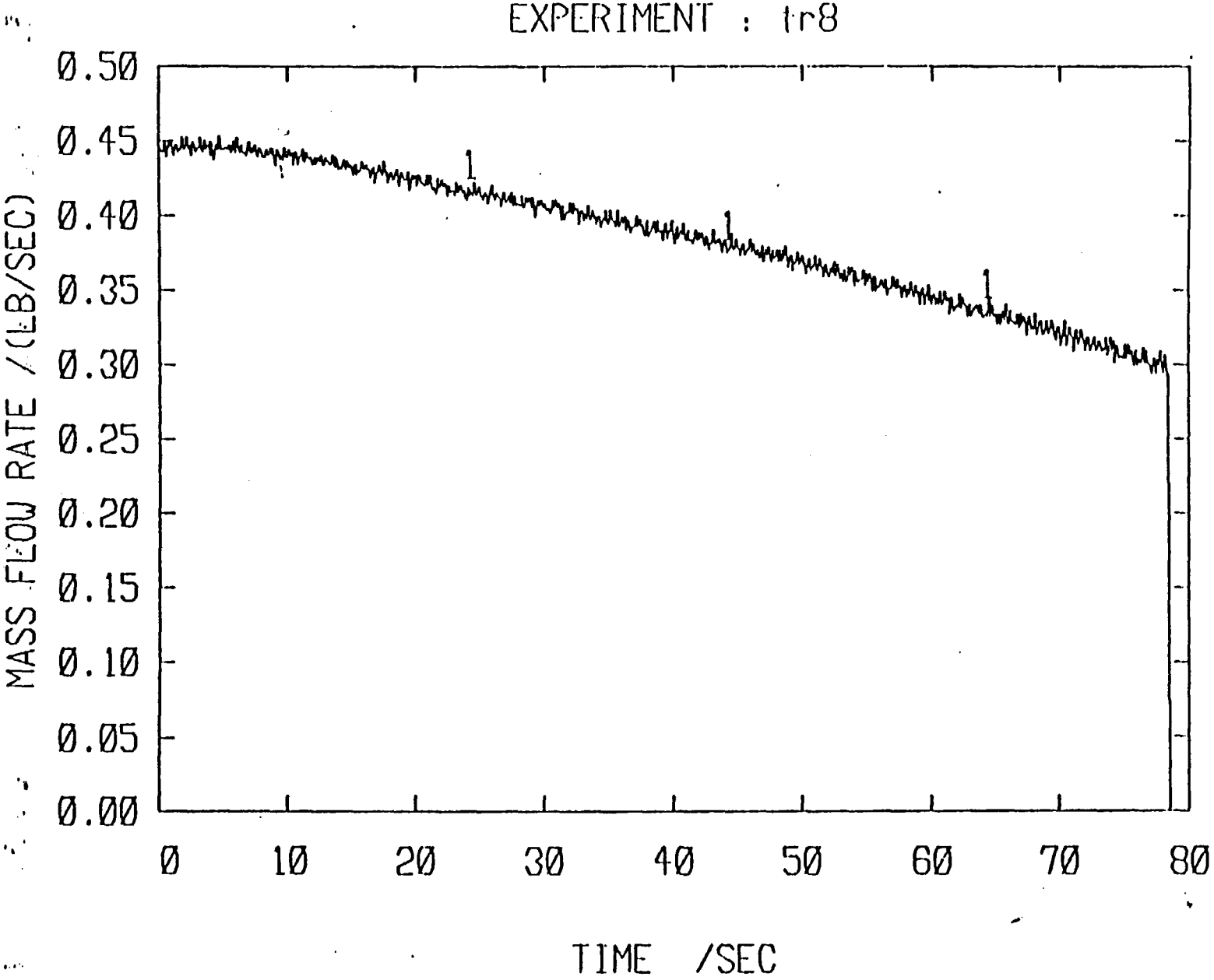
EXPERIMENT : tr8
MASS FLOW RATE /(LB/SEC)
0.50
0.45
0.40
0.35
0.30
0.25
0.20
0.15
0.10
0.05
0.00
0
10
20
30
40
50
60
70
80
TIME /SEC

Fig. A.2.2

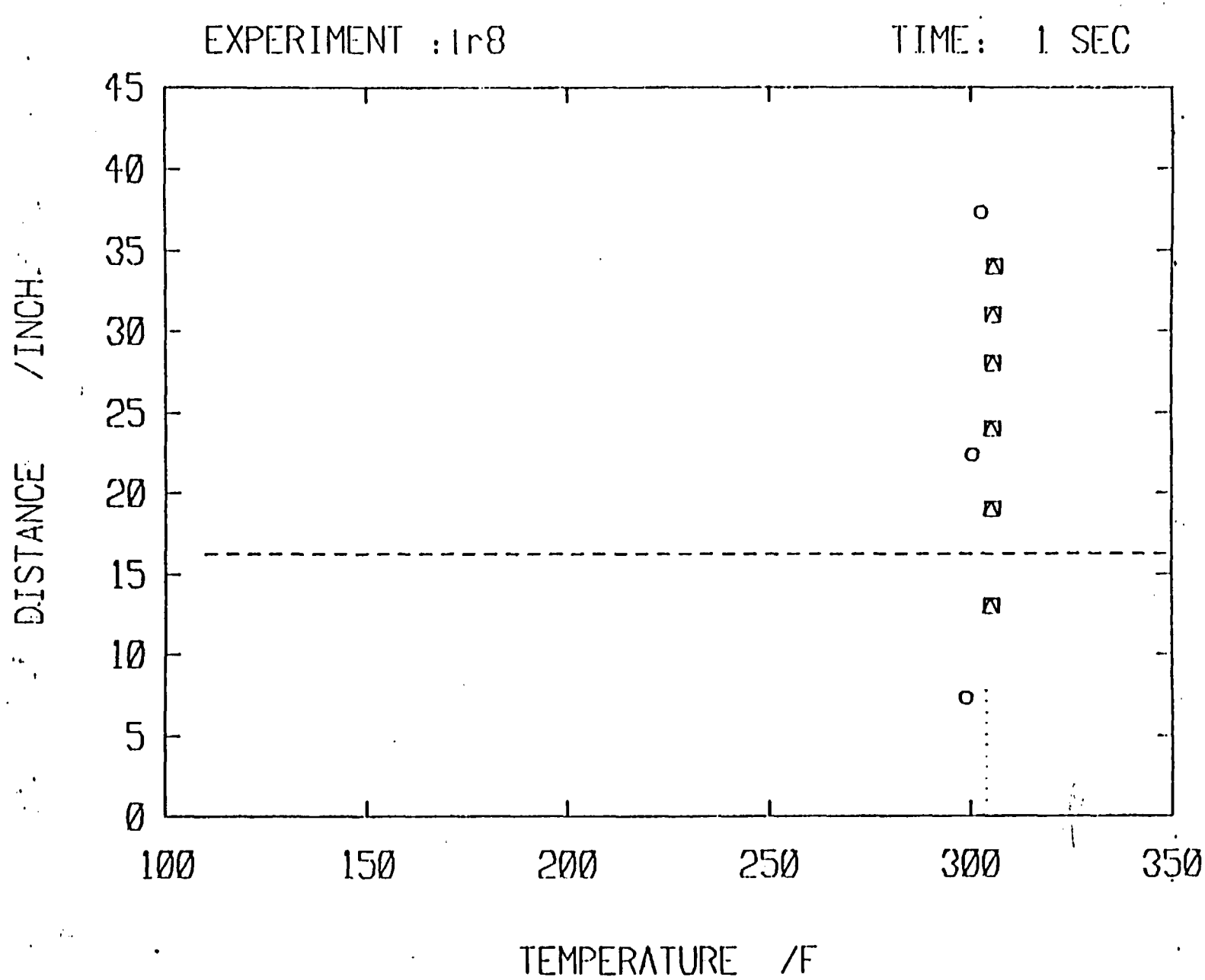
EXPERIMENT : 1r8
TIME: 1 SEC
DISTANCE /INCH
45
40
35
30
25
20
15
10
5
0
100
150
200
250
300
350
TEMPERATURE /F

Fig. A.2.3

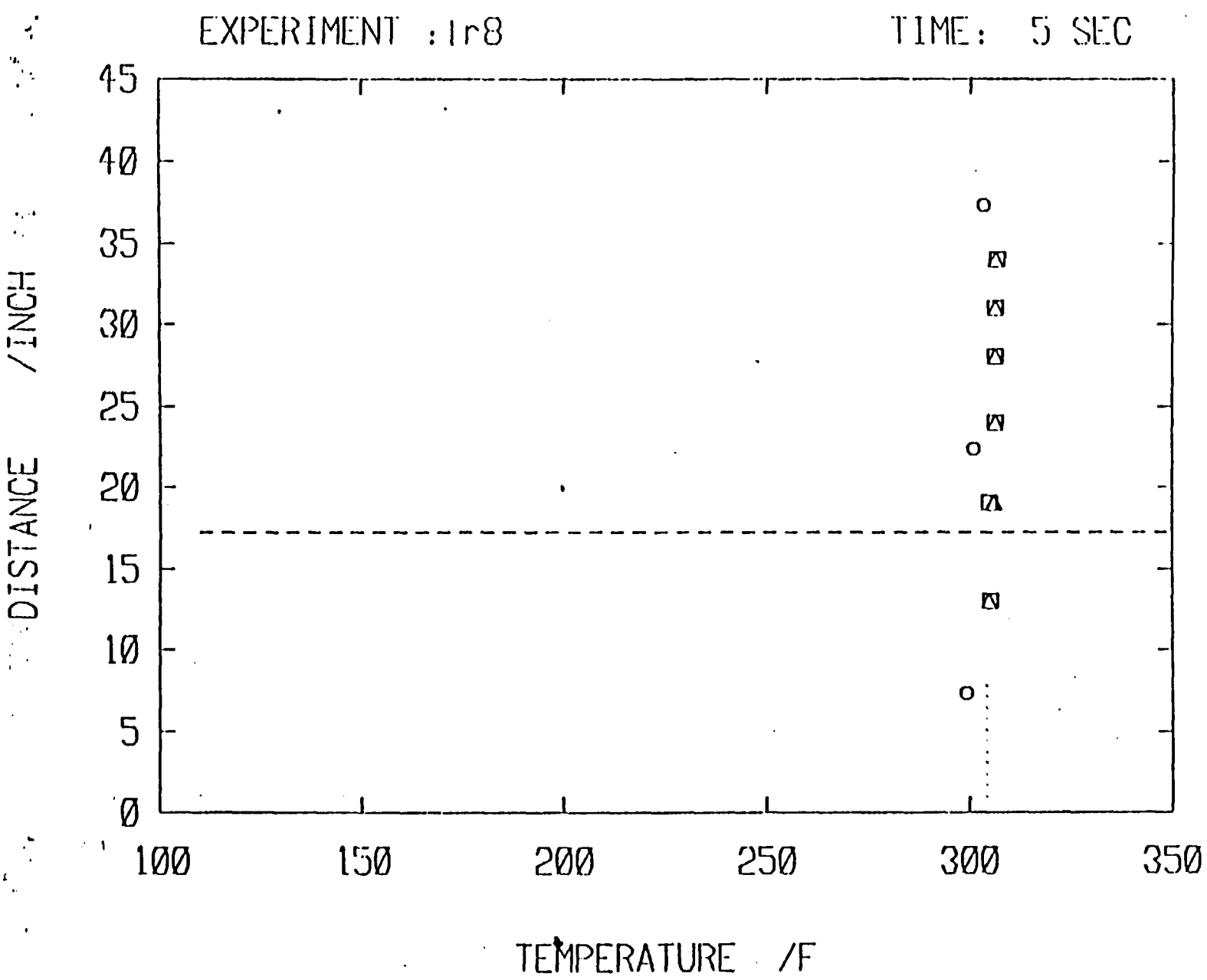
EXPERIMENT : 1r8
TIME: 5 SEC
DISTANCE /INCH
45
40
35
30
25
20
15
10
5
0
100
150
200
250
300
350
TEMPERATURE /F

Fig. A.2.4

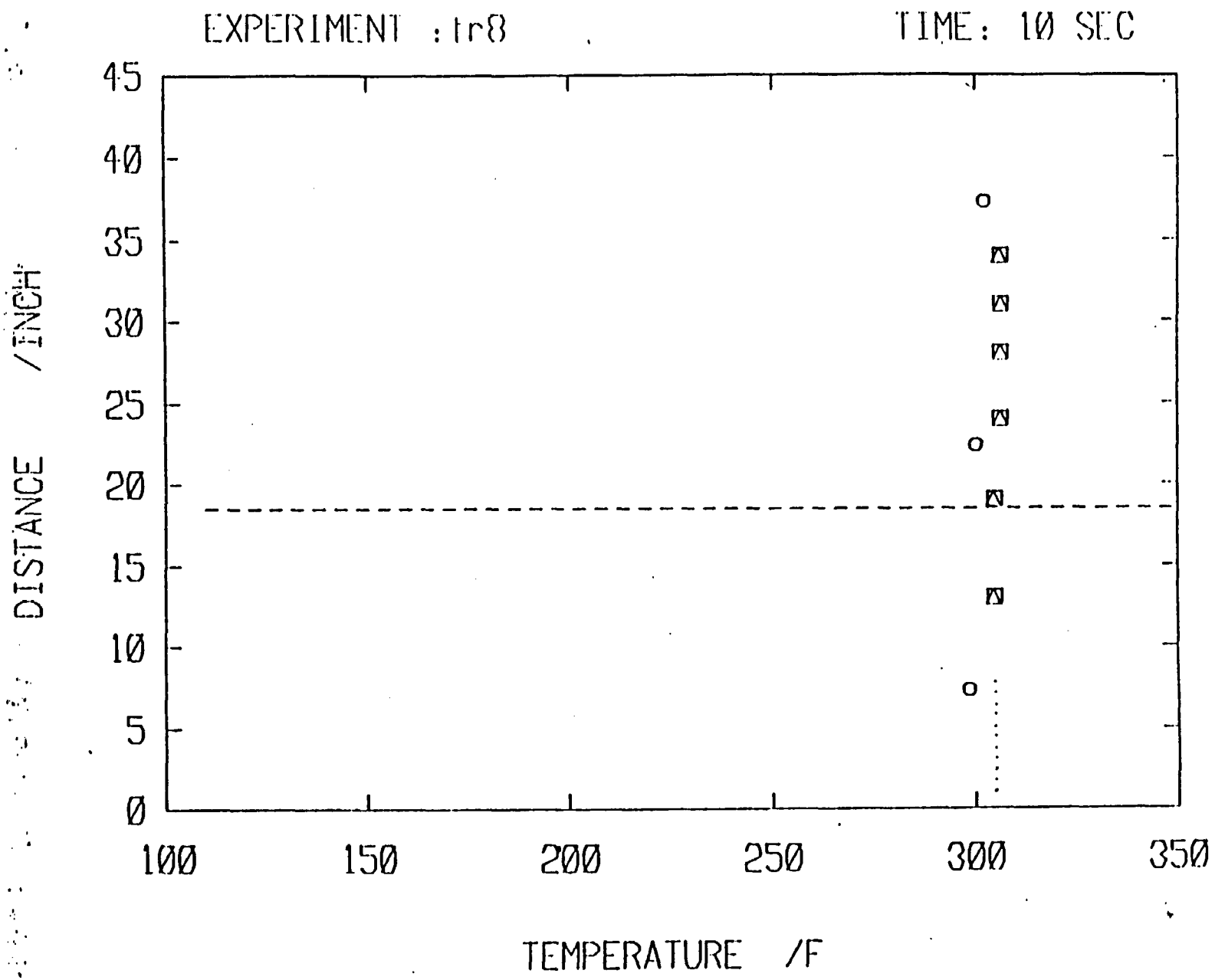
EXPERIMENT : tr8
TIME: 10 SEC
DISTANCE /INCH
45
40
35
30
25
20
15
10
5
0
100
150
200
250
300
350
TEMPERATURE /F

Fig. A.2.5

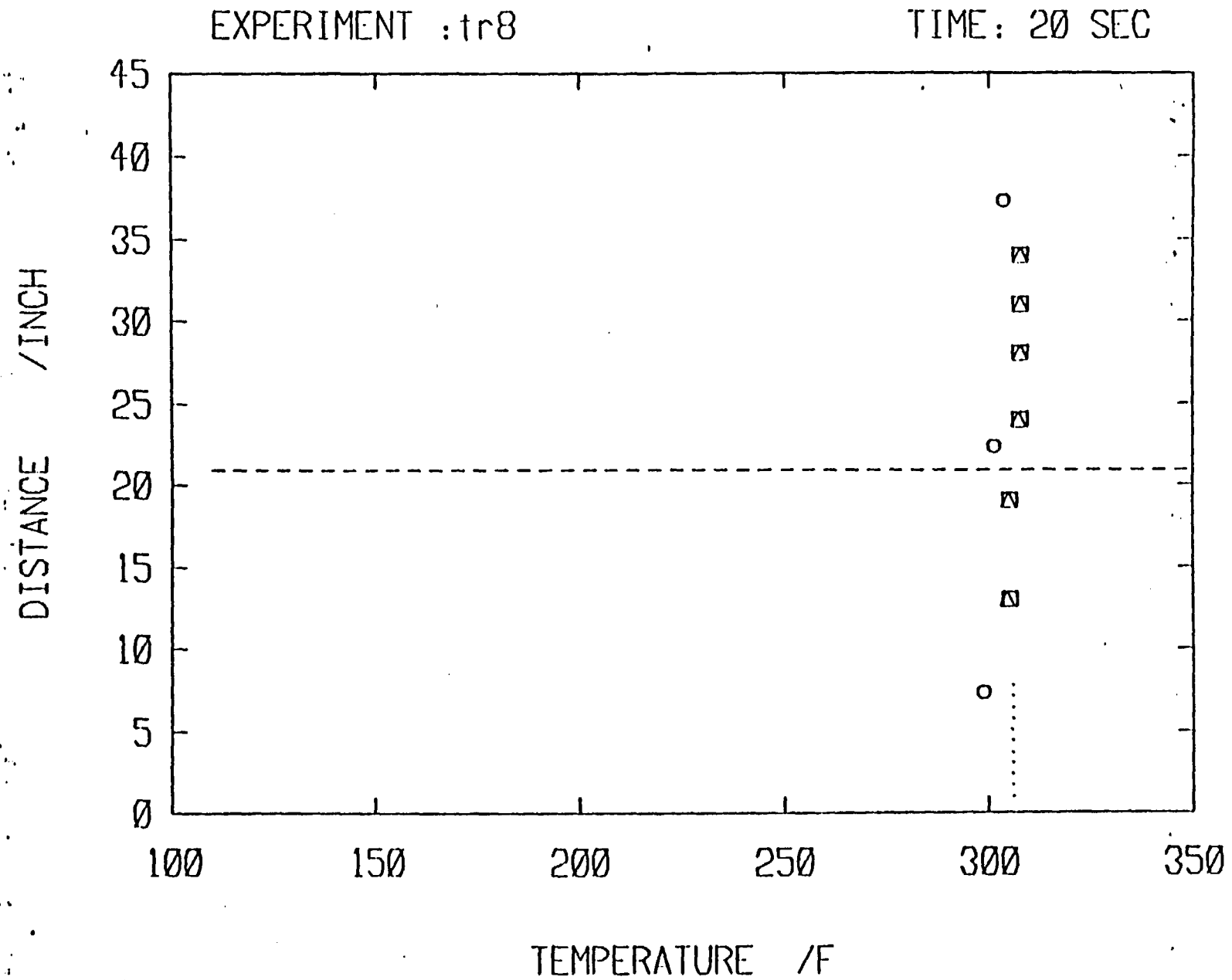
EXPERIMENT :tr8
TIME: 20 SEC
DISTANCE /INCH
45
40
35
30
25
20
15
10
5
0
100
150
200
250
300
350
TEMPERATURE /F

Fig. A.2.6

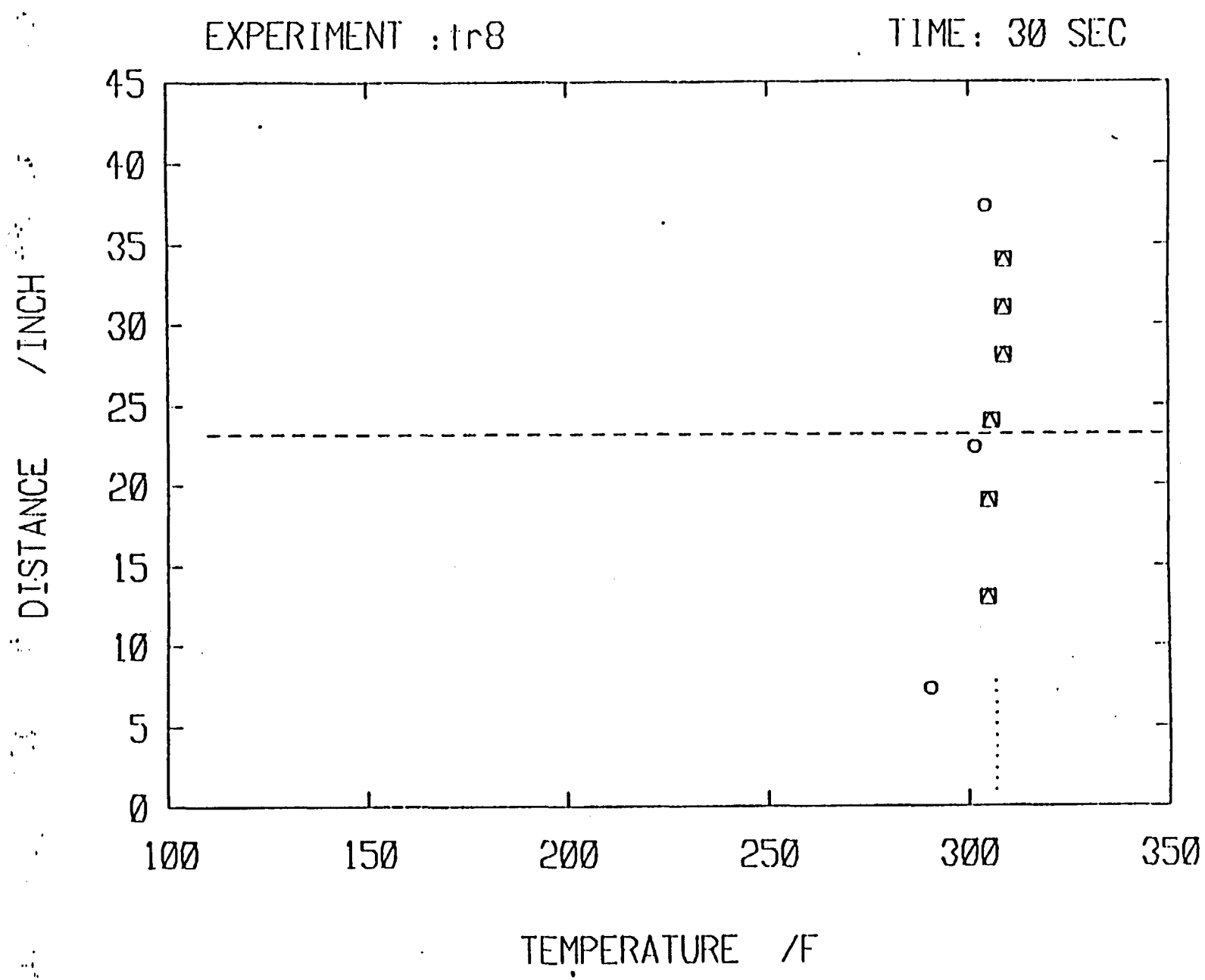
EXPERIMENT : tr8
TIME: 30 SEC
DISTANCE /INCH
45
40
35
30
25
20
15
10
5
0
100
150
200
250
300
350
TEMPERATURE /F

Fig. A.2.7

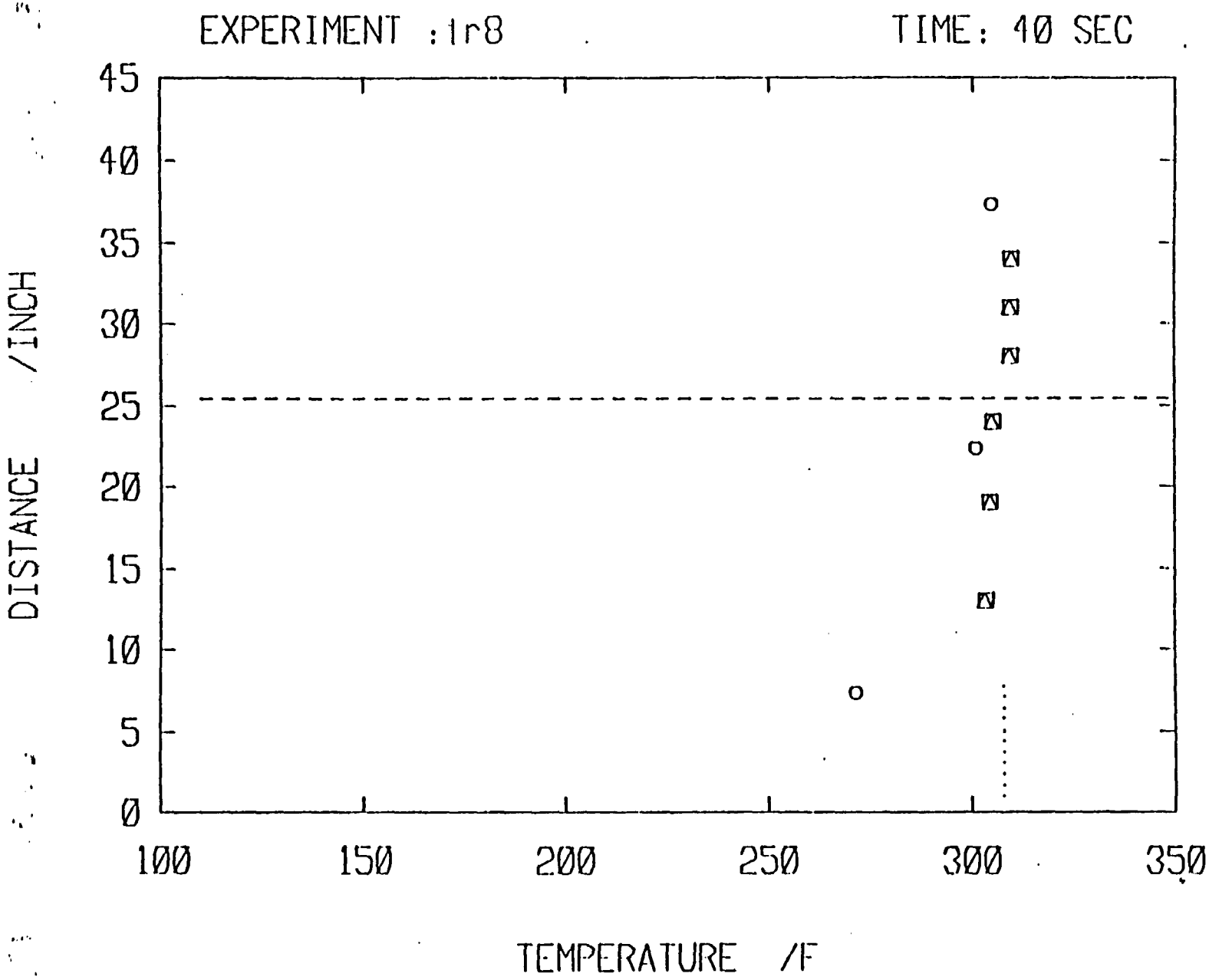
EXPERIMENT :1r8
TIME: 40 SEC
DISTANCE /INCH
45
40
35
30
25
20
15
10
5
0
100
150
200
250
300
350
TEMPERATURE /F

Fig. A.2.8

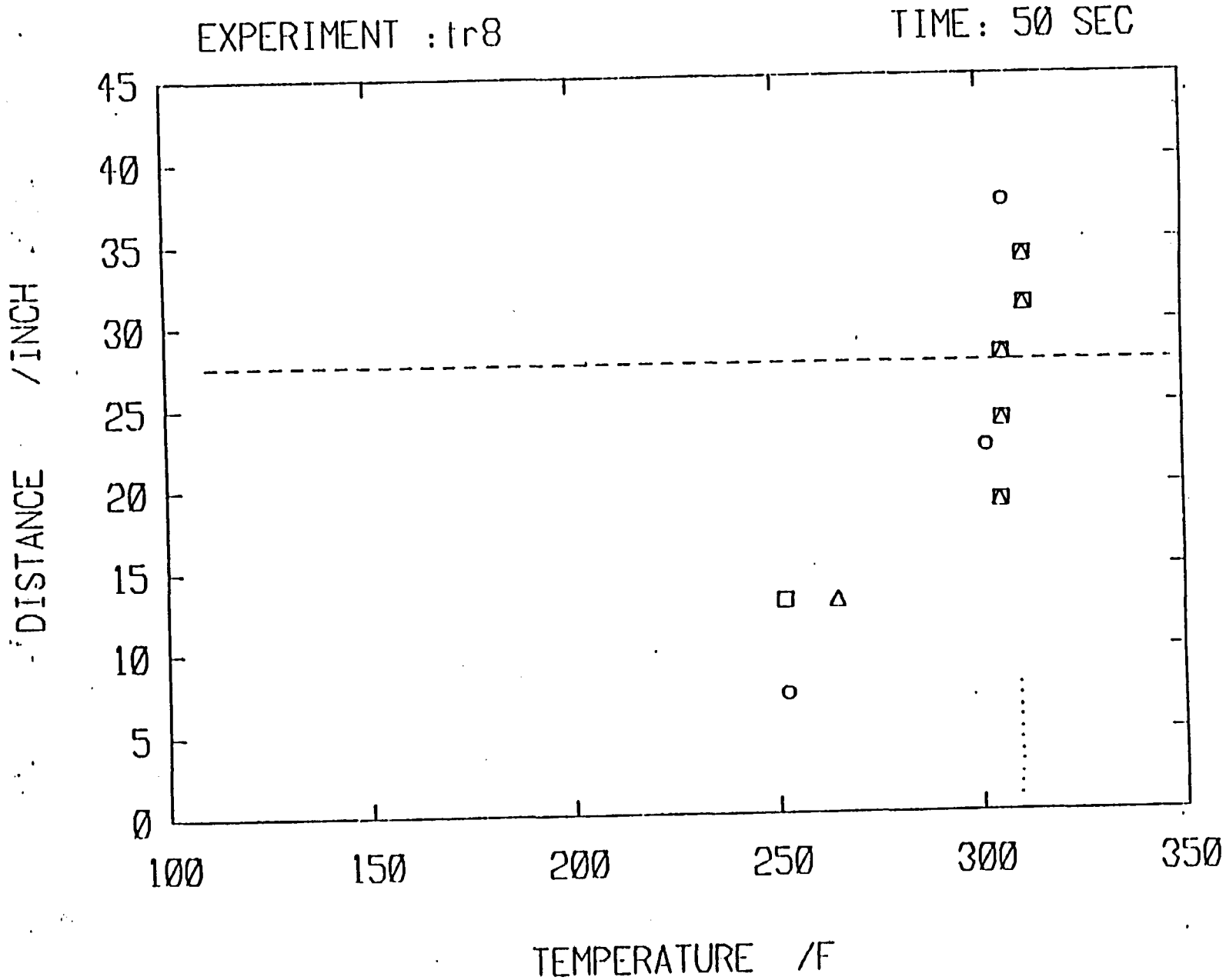
EXPERIMENT : tr8
TIME: 50 SEC
DISTANCE /INCH
45
40
35
30
25
20
15
10
5
0
100
150
200
250
300
350
TEMPERATURE /F

Fig. A.2.9

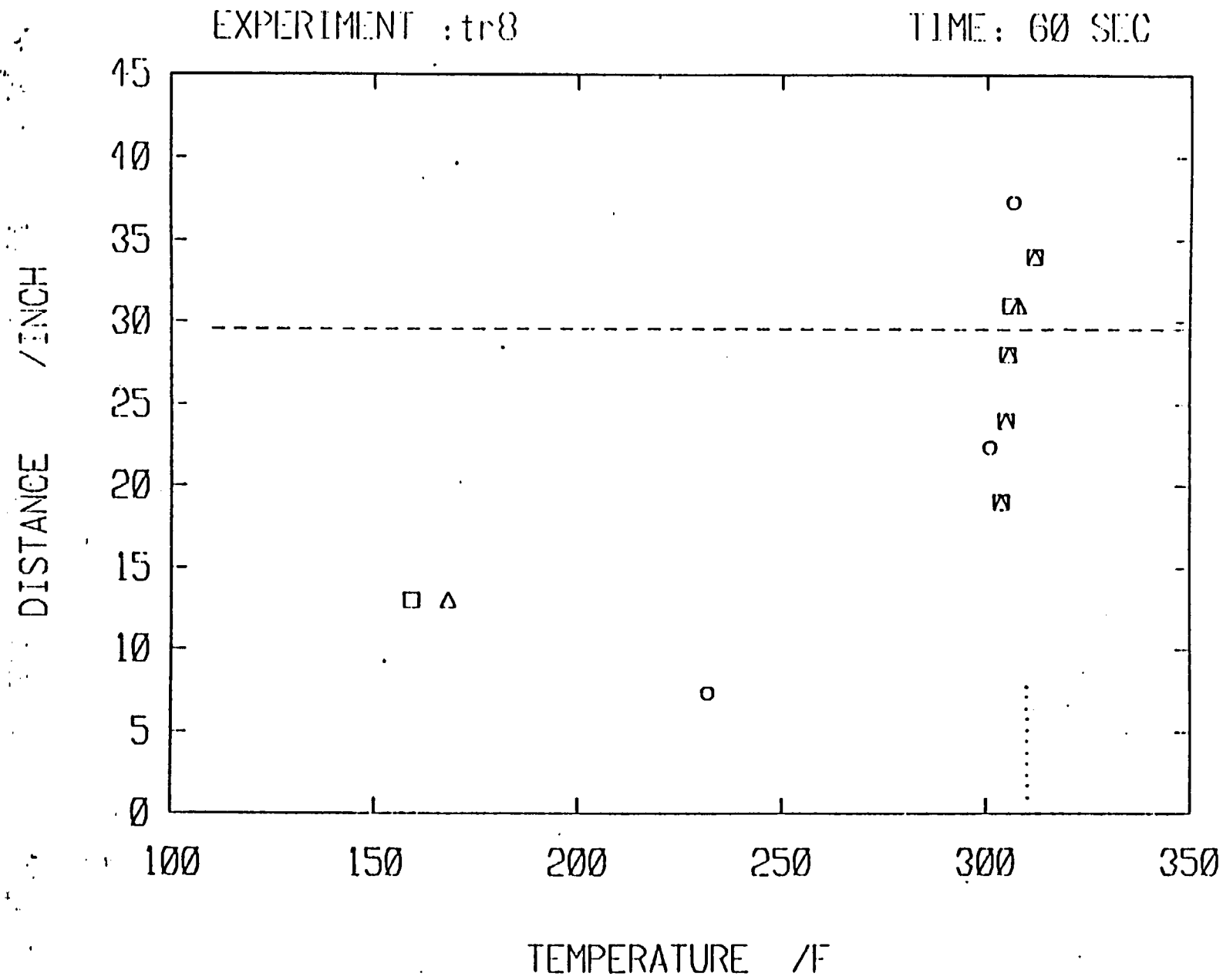
EXPERIMENT : tr8
TIME: 60 SEC
DISTANCE /INCH
TEMPERATURE /F
15
10
35
30
25
20
15
10
5
0
100
150
200
250
300
350

Fig. A.2.10

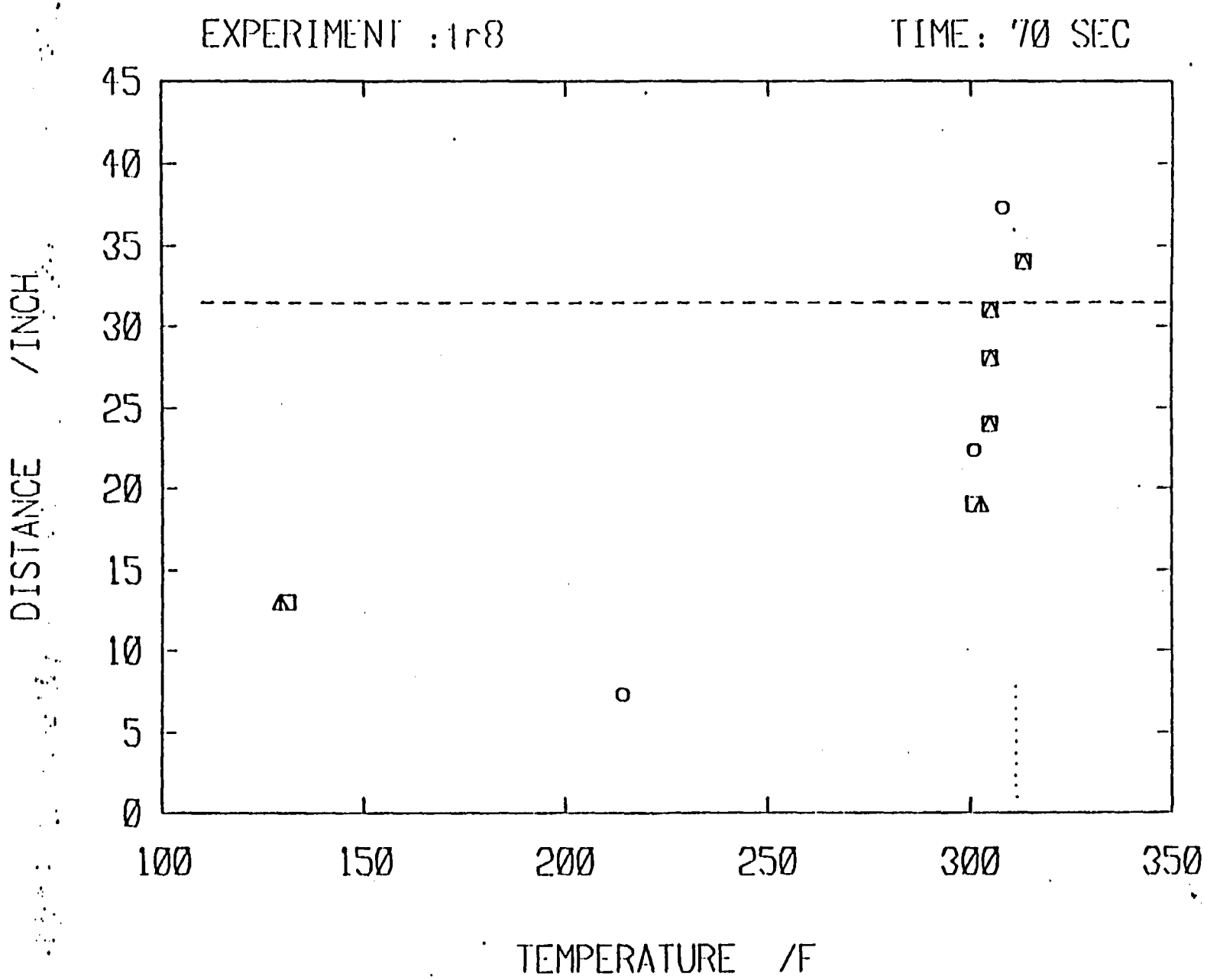
EXPERIMENT :1r8
TIME: 70 SEC
DISTANCE /INCH
45
40
35
30
25
20
15
10
5
0
100
150
200
250
300
350
TEMPERATURE /F

Fig. A.2.11

A.3 Experiment: FF1

Water level at t = 0 sec : L = 0 in.

Water level increase : ΔL = 18 in.

Insurge time : t = 35 sec.

This experiment was ran using the radially located thermocouple arrangement. The transient was initiated by insurging cold water to the tank filled with saturated steam. As Fig. A.3.1 showes; the pressure dropped for the first 10 sec, due to the large heat-transfer at the interface associated with breaking of jet through it. After t = 18 sec; the liquid region acted as a piston and compressed steam, resulting into a pressure rise.

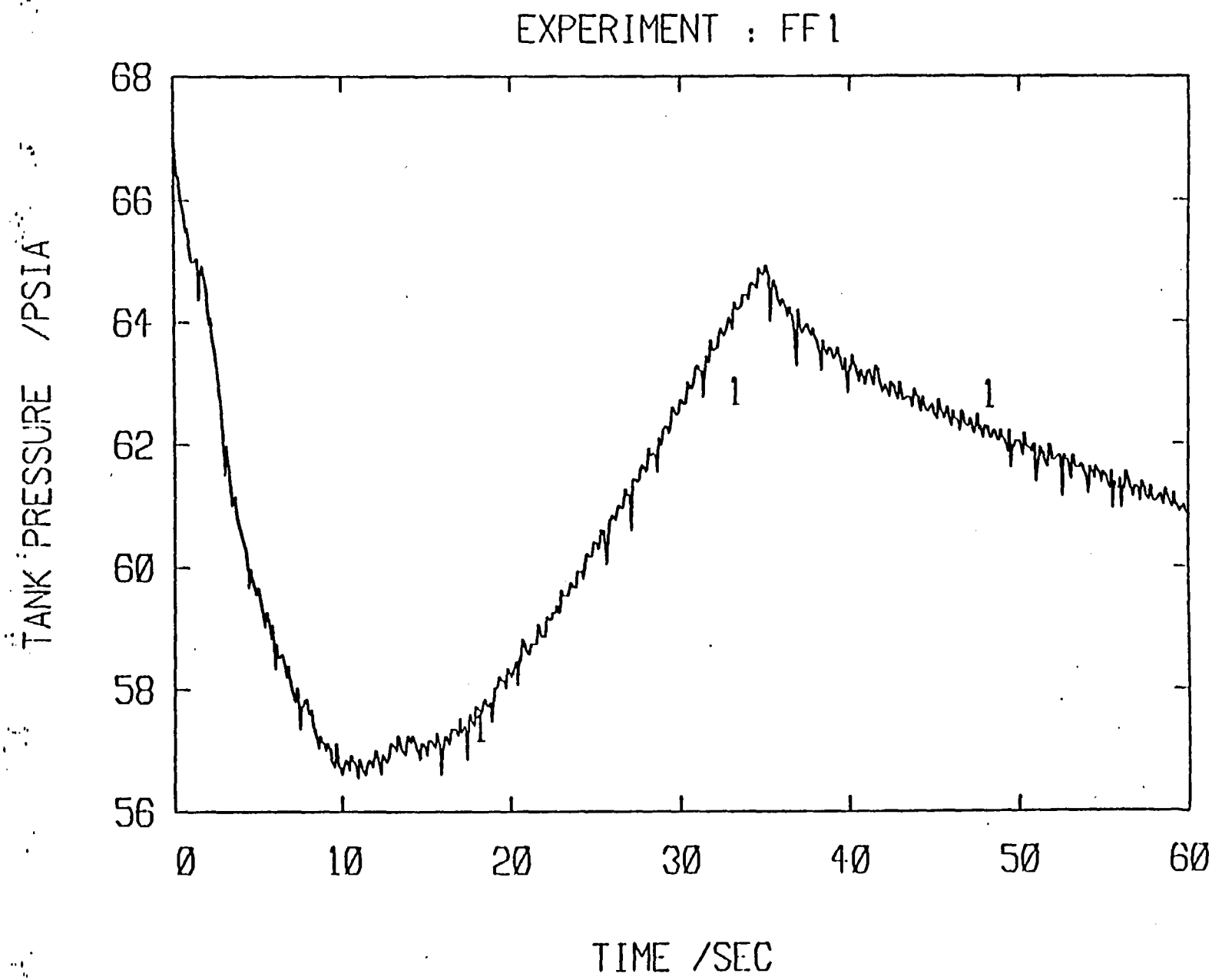
EXPERIMENT : FF1
TANK PRESSURE /PSIA
68
66
64
62
60
58
56
0
10
20
30
40
50
60
TIME /SEC

Fig. A.3.1

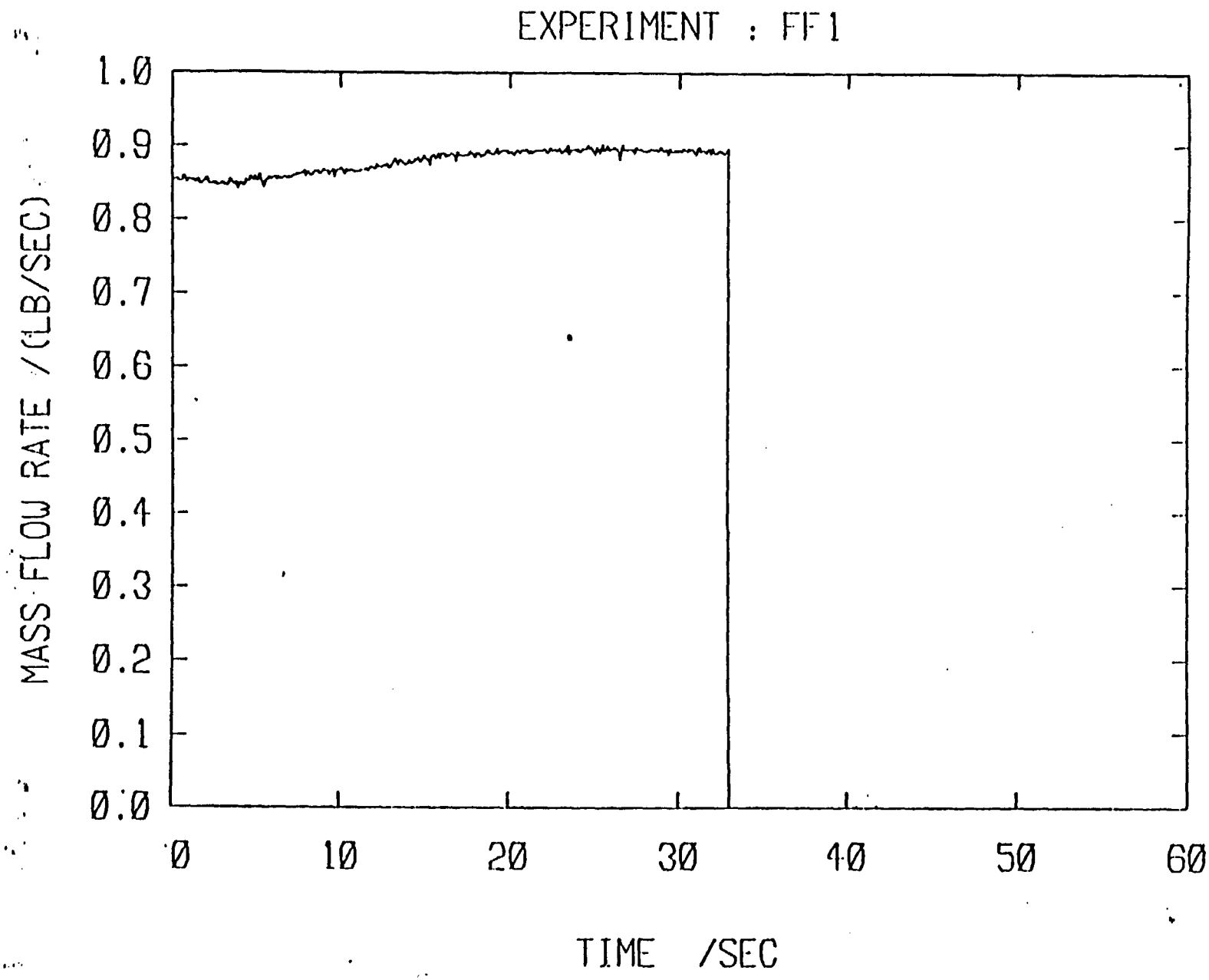
EXPERIMENT : FF1
MASS FLOW RATE /(LB/SEC)
1.0
0.9
0.8
0.7
0.6
0.5
0.4
0.3
0.2
0.1
0.0
0
10
20
30
40
50
60
TIME /SEC

Fig. A.3.2

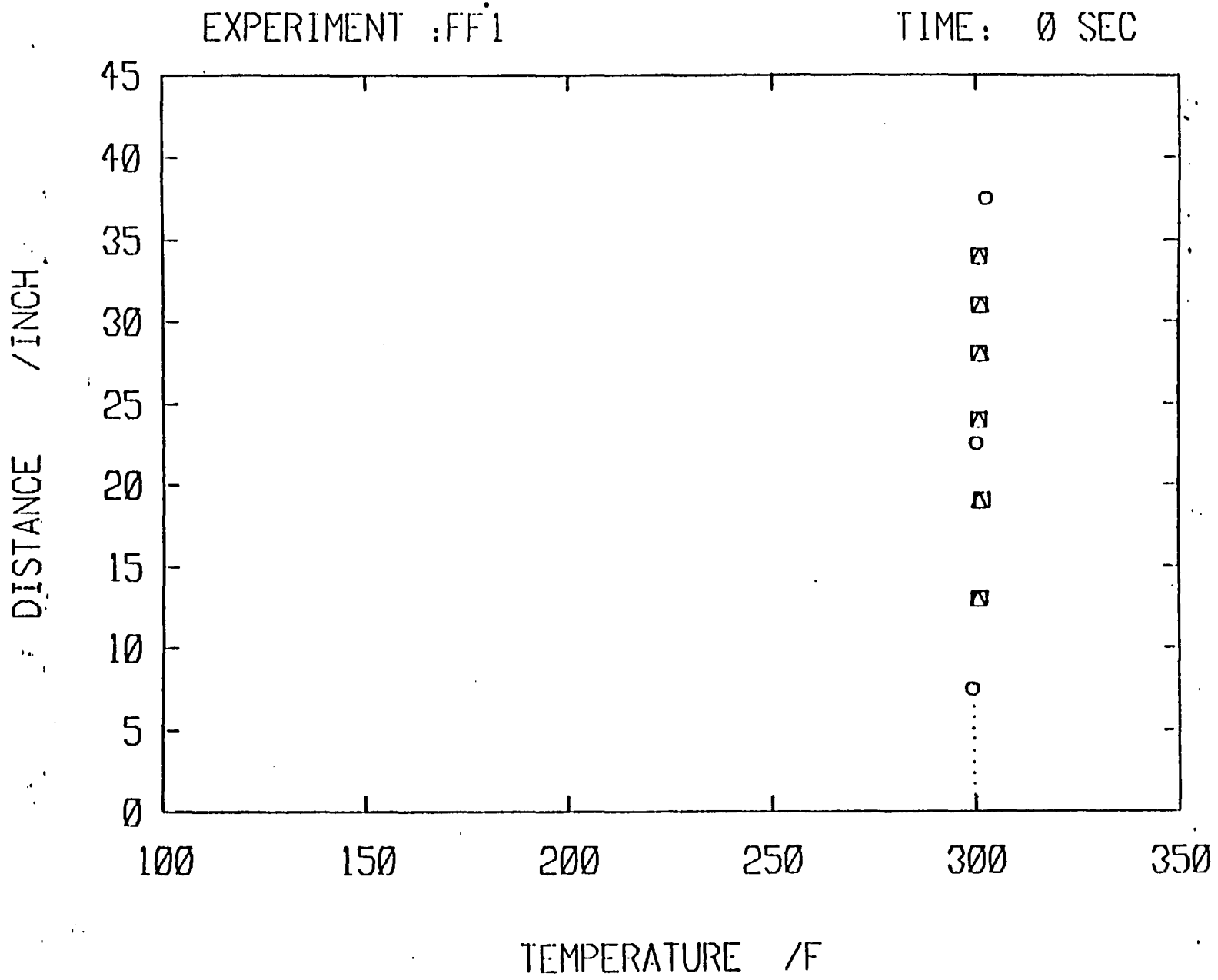
EXPERIMENT :FF1
TIME: Ø SEC
DISTANCE /INCH
45
40
35
30
25
20
15
10
5
Ø
100
150
200
250
300
350
TEMPERATURE /F

Fig. A.3.3

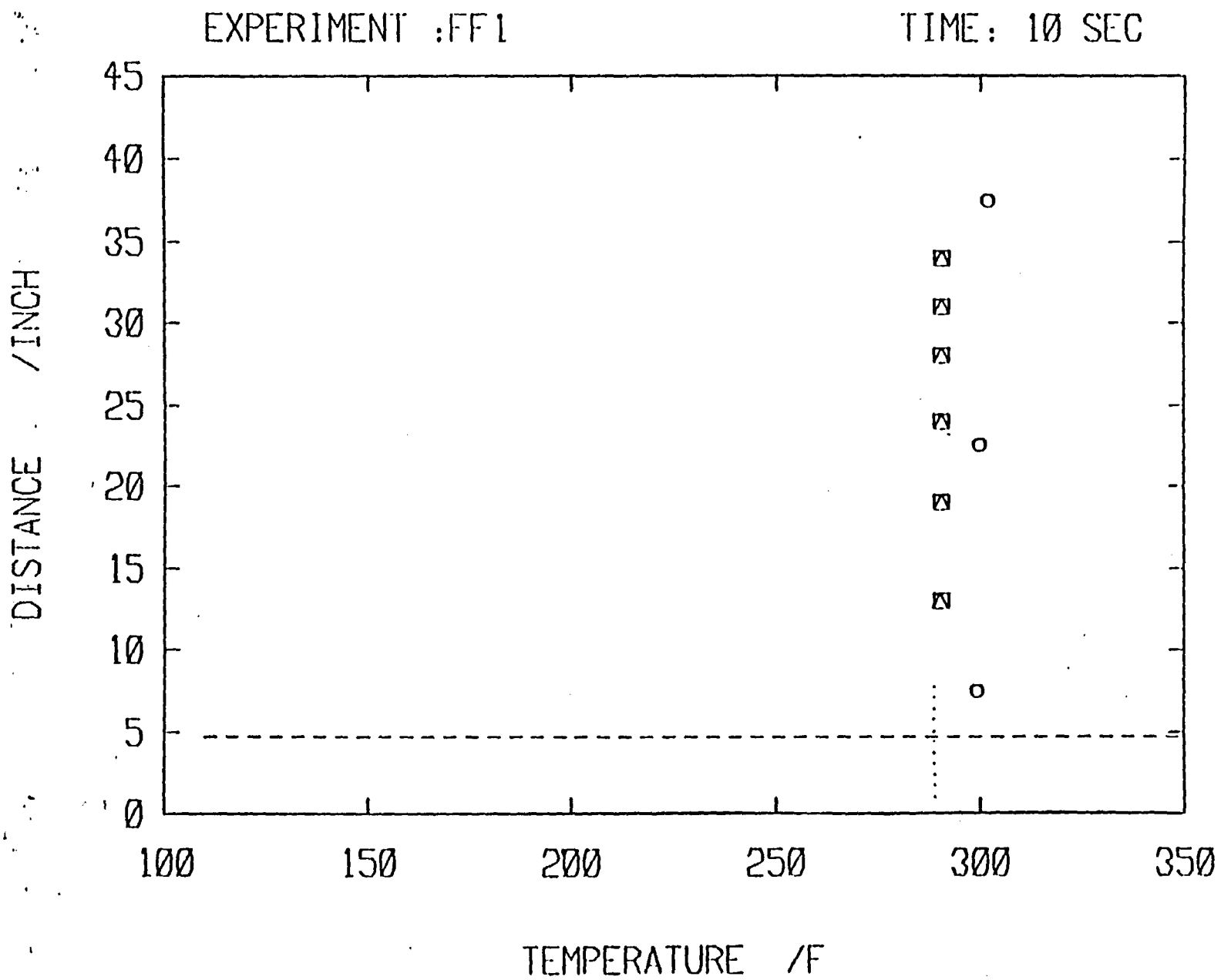
EXPERIMENT :FF1
TIME: 10 SEC
DISTANCE /INCH
45
40
35
30
25
20
15
10
5
0
100
150
200
250
300
350
TEMPERATURE /F

Fig. A.3.4

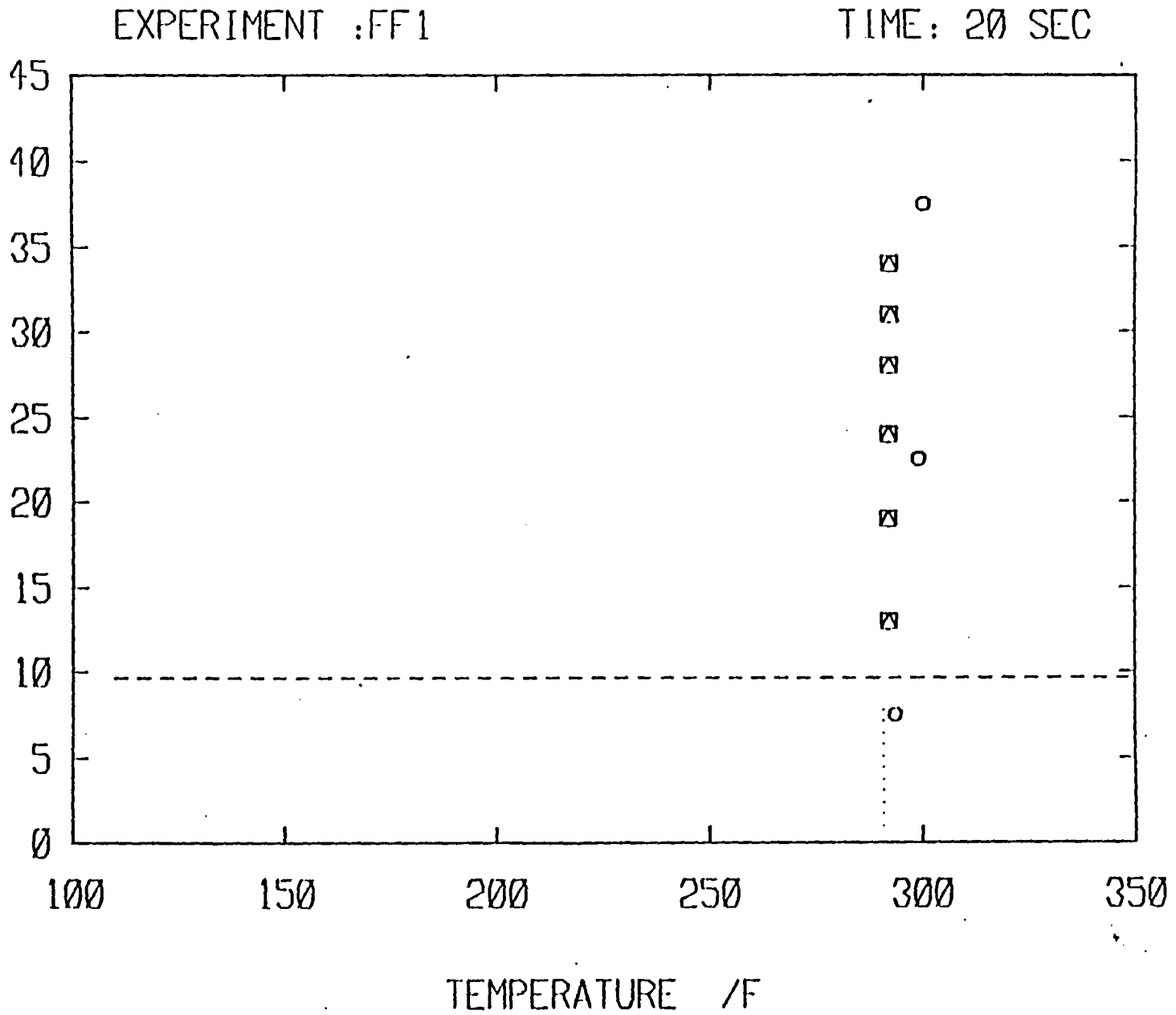
EXPERIMENT :FF1
TIME: 20 SEC
DISTANCE /INCH
45
40
35
30
25
20
15
10
5
0
100
150
200
250
300
350
TEMPERATURE /F

Fig. A.3.5

EXPERIMENT :FF1
TIME: 28 SEC
DISTANCE /INCH
45
40
35
30
25
20
15
10
5
0
100
150
200
250
300
350
TEMPERATURE /F

Fig. A.3.6

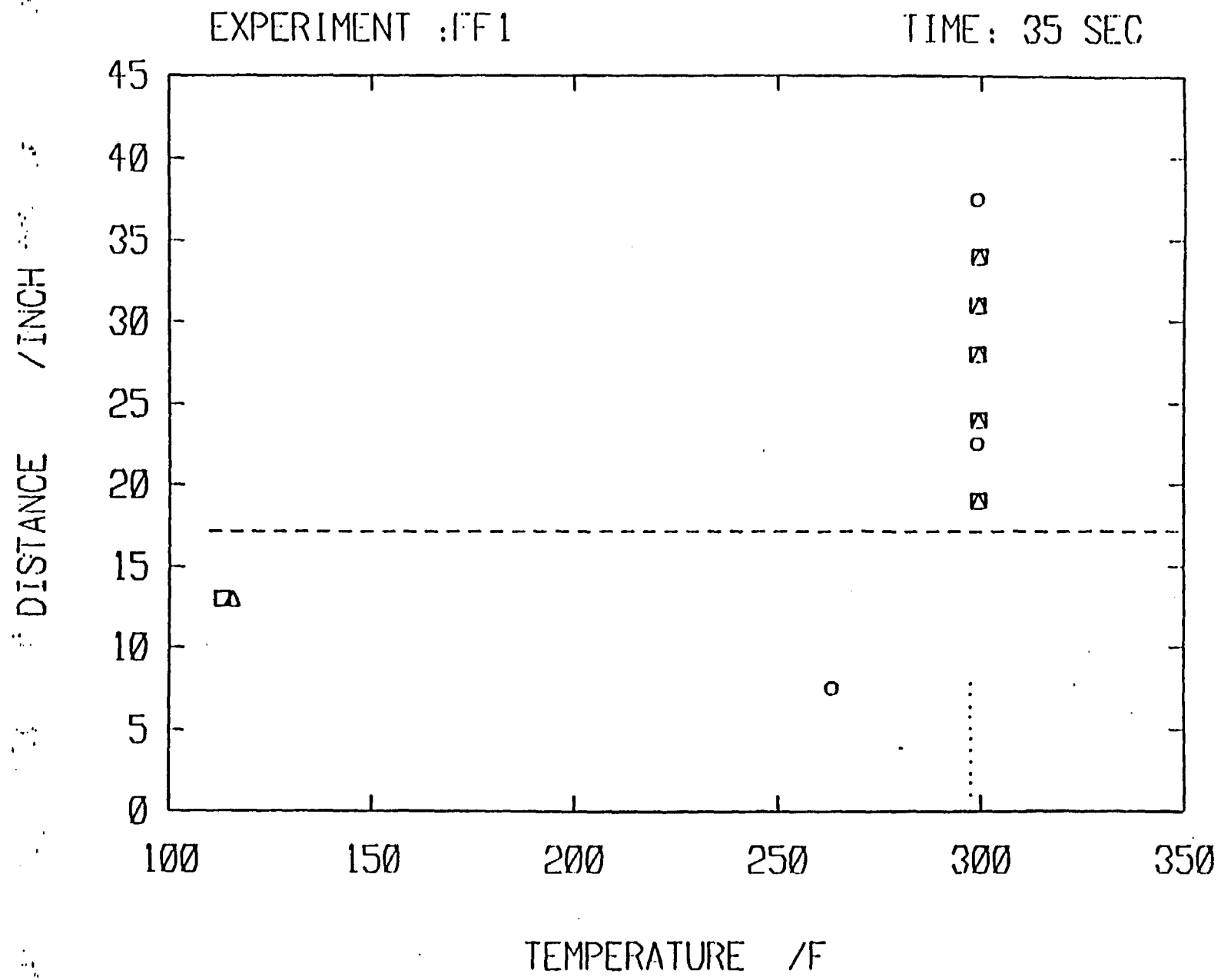
EXPERIMENT :FF1
TIME: 35 SEC
DISTANCE /INCH
45
40
35
30
25
20
15
10
5
0
100
150
200
250
300
350
TEMPERATURE /F

Fig. A.3.7

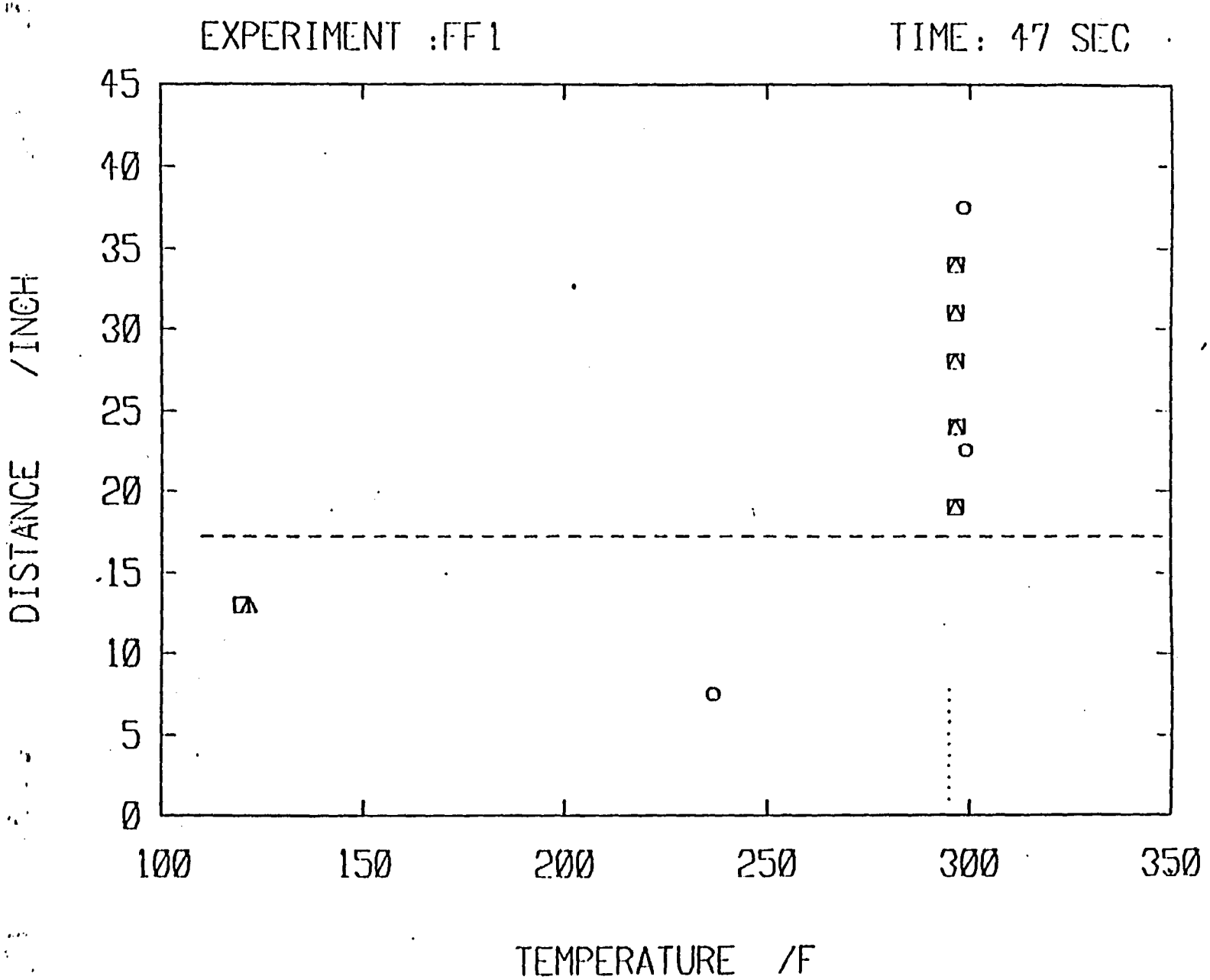
EXPERIMENT :FF1
TIME: 47 SEC
DISTANCE /INCH
45
40
35
30
25
20
15
10
5
0
100
150
200
250
300
350
TEMPERATURE /F

Fig. A.3.8

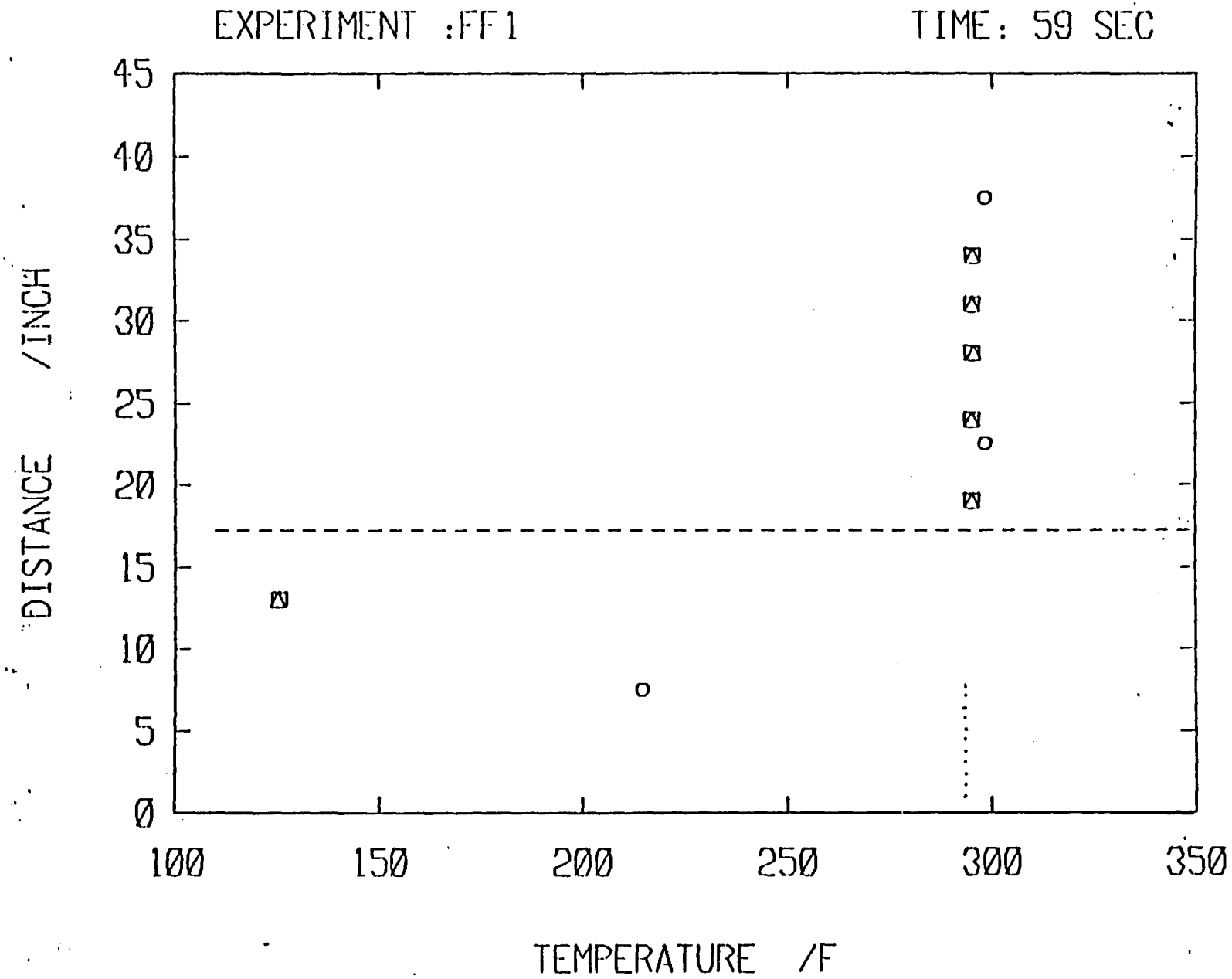
EXPERIMENT :FF1
TIME: 59 SEC
DISTANCE /INCH
45
40
35
30
25
20
15
10
5
0
100
150
200
250
300
350
TEMPERATURE /F

Fig. A.3.9

A.4 Experiment: ST4

Water level at t = 0 sec : L = 17 in.

Water level increase : ΔL = 18 in.

Insurge time : t = 41 sec.

This experiment was done using the axially located thermocouples. As it is shown in Figs. A.4.4 through A.4.11; there are two distinct liquid region: the main liquid region, which retains its initial temperature; and the subcooled liquid region which consists of few layers of stratified liquid. Liquid temperature distribution in Fig. A.4.8 was traced for a better visualization. The subcooled liquid region proved to be stable after the insurge was stopped, Figs. A.4.9 through A.4.11.

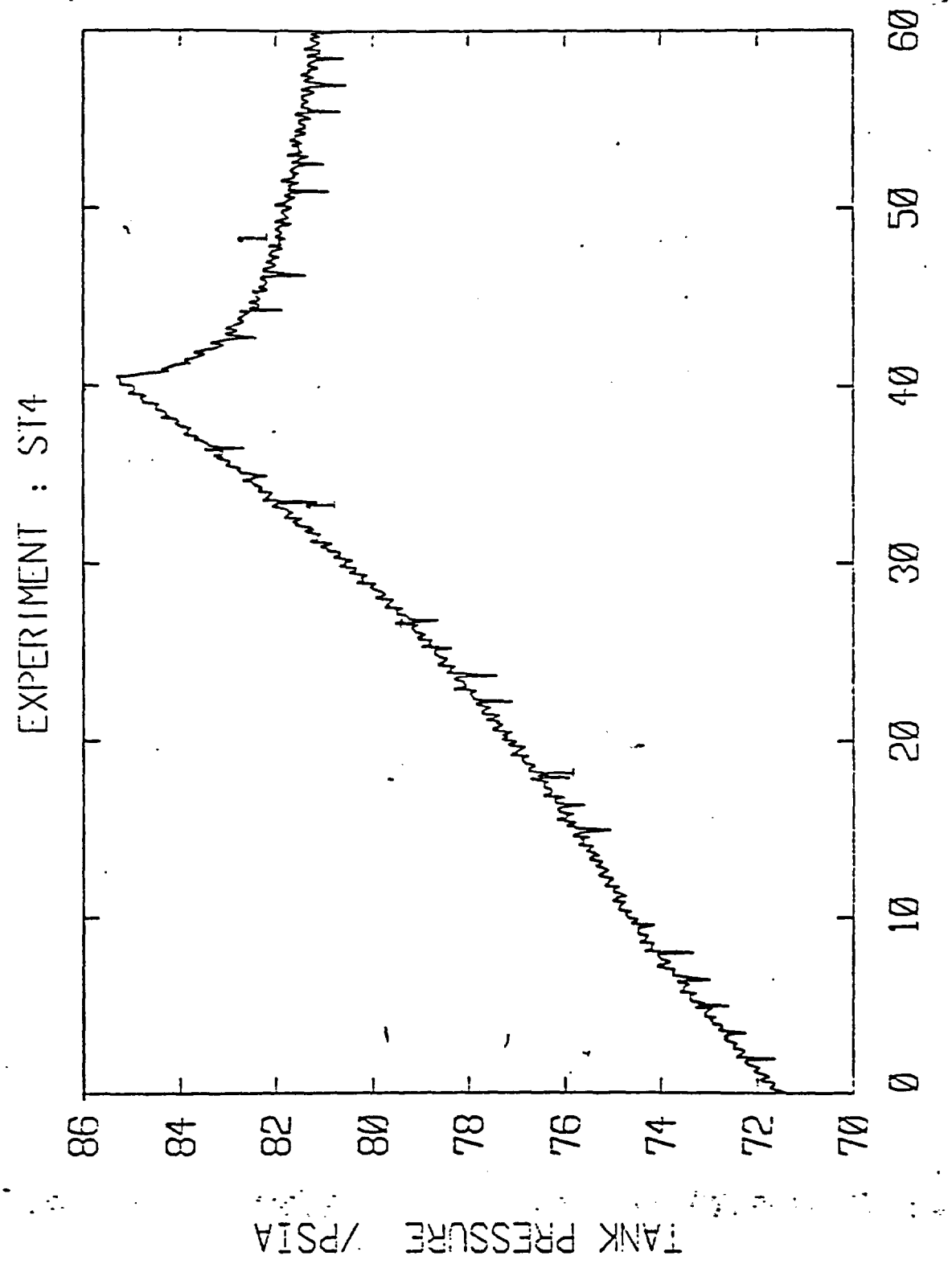
EXPERIMENT : ST4
TANK PRESSURE /PSIA
86
84
82
80
78
76
74
72
70
0
10
20
30
40
50
60
TIME /SEC

Fig. A.4.1

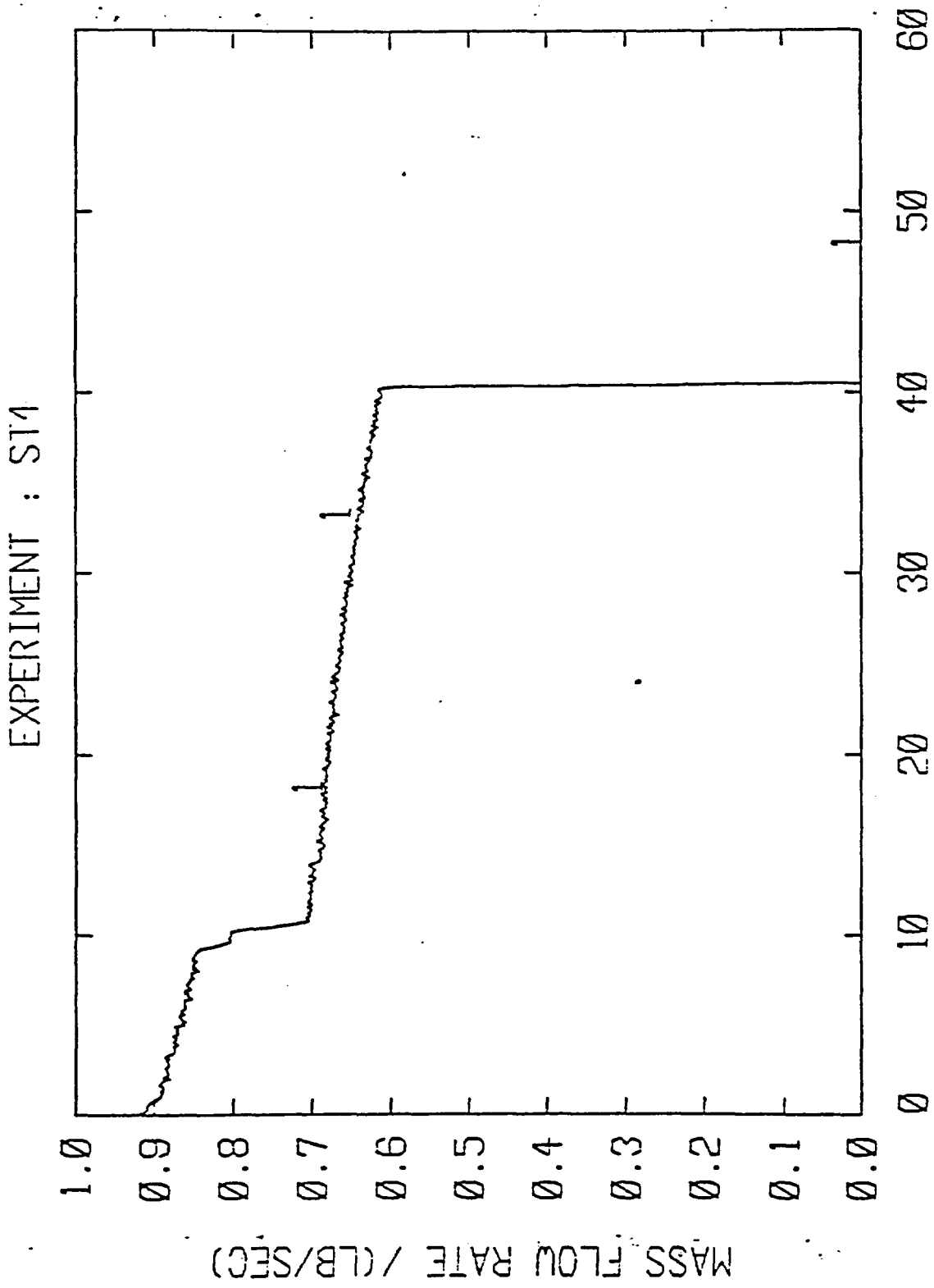
EXPERIMENT : ST1
MASS FLOW RATE /(LB/SEC)
1.0
0.9
0.8
0.7
0.6
0.5
0.4
0.3
0.2
0.1
0.0
0
10
20
30
40
50
60
TIME /SEC

Fig. A.4.2

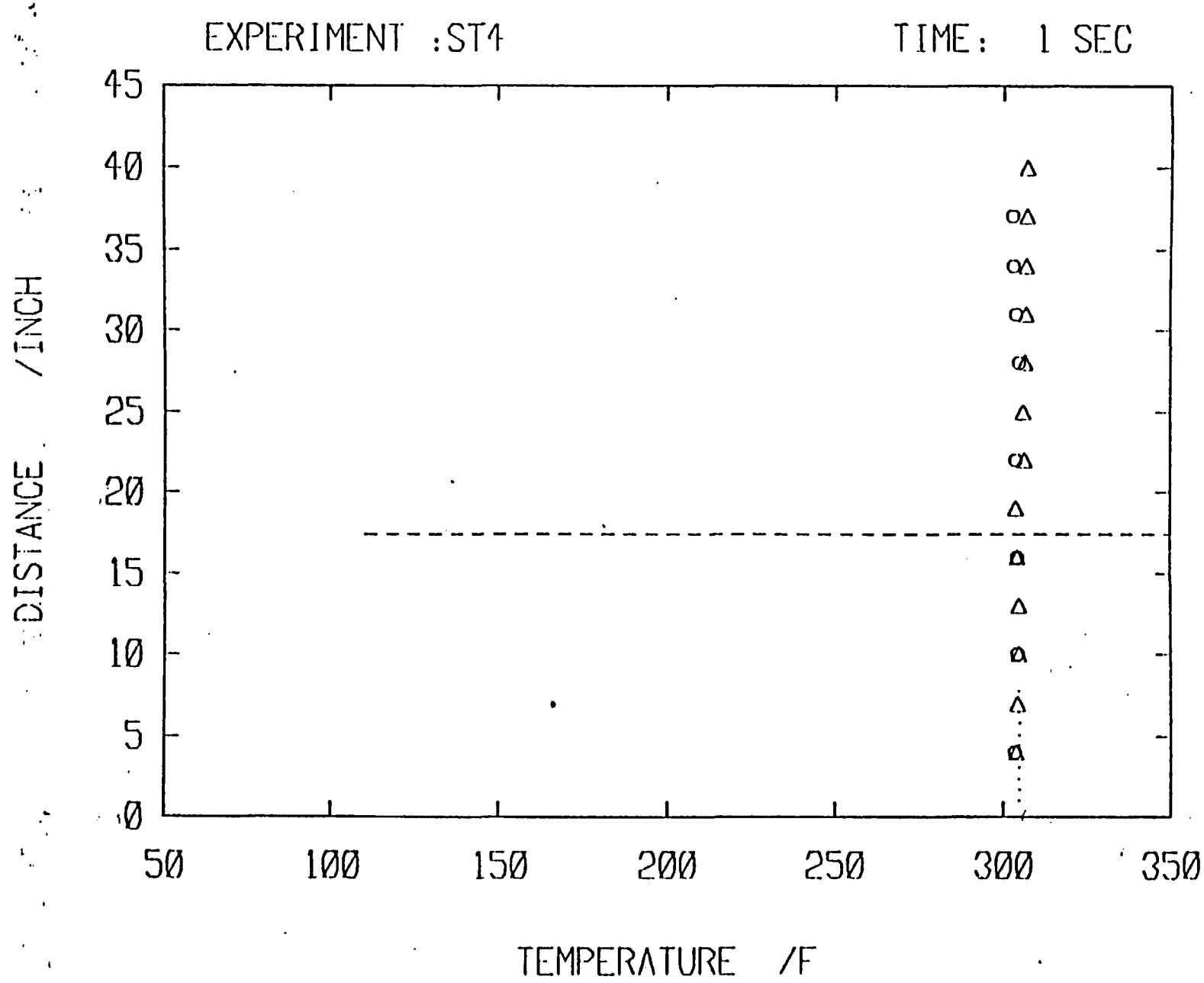
EXPERIMENT :ST4
TIME: 1 SEC
DISTANCE /INCH
45
40
35
30
25
20
15
10
5
0
50
100
150
200
250
300
350
TEMPERATURE /F

Fig. A.4.3

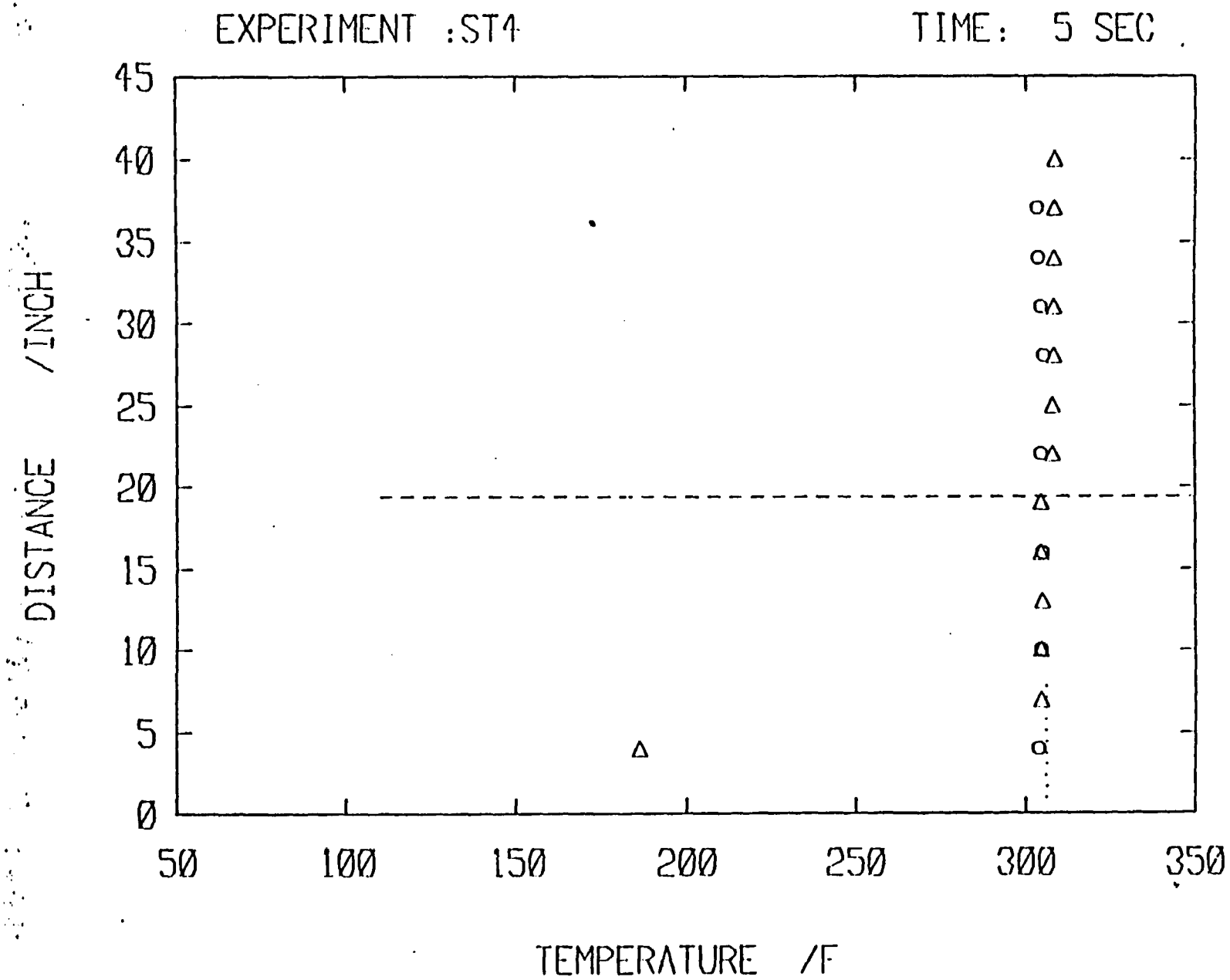
EXPERIMENT :ST4
TIME: 5 SEC
DISTANCE /INCH
45
40
35
30
25
20
15
10
5
0
50
100
150
200
250
300
350
TEMPERATURE /F

Fig. A.4.4

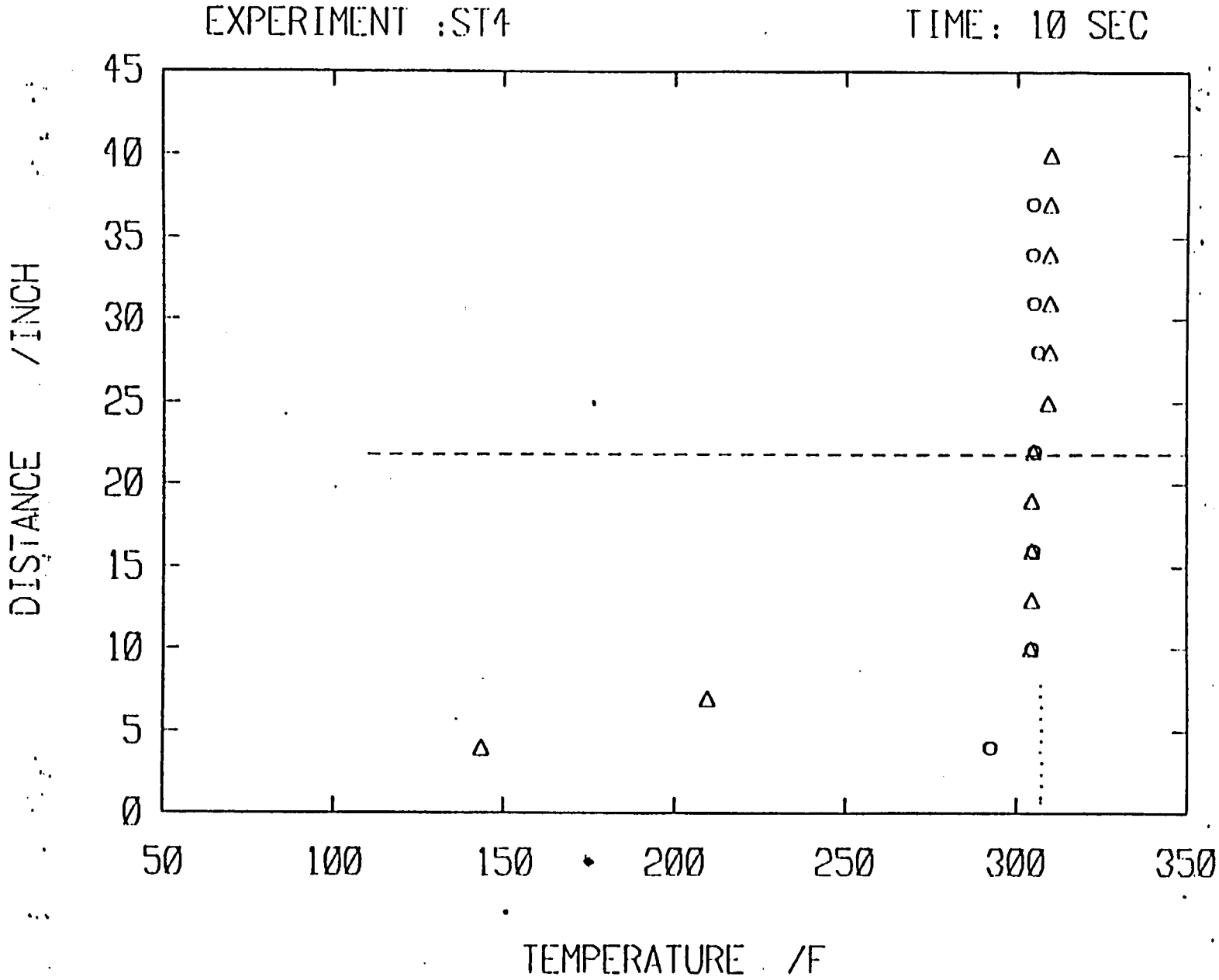
EXPERIMENT :ST4
TIME: 10 SEC
DISTANCE /INCH
45
40
35
30
25
20
15
10
5
0
50
100
150
200
250
300
350
TEMPERATURE /F

Fig. A.4.5

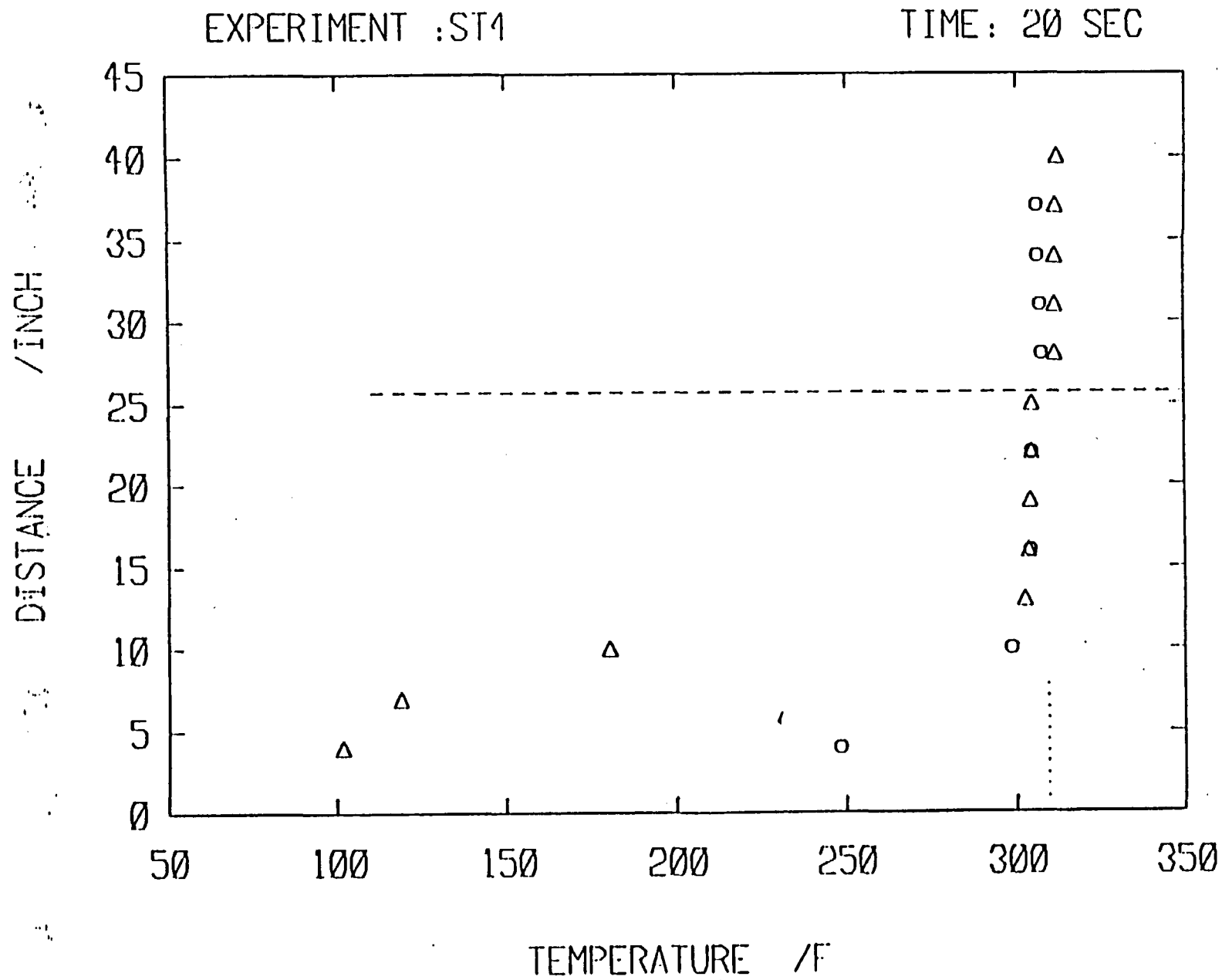
EXPERIMENT :ST1
TIME: 20 SEC
DISTANCE /INCH
45
40
35
30
25
20
15
10
5
0
50
100
150
200
250
300
350
TEMPERATURE /F

Fig. A.4.6

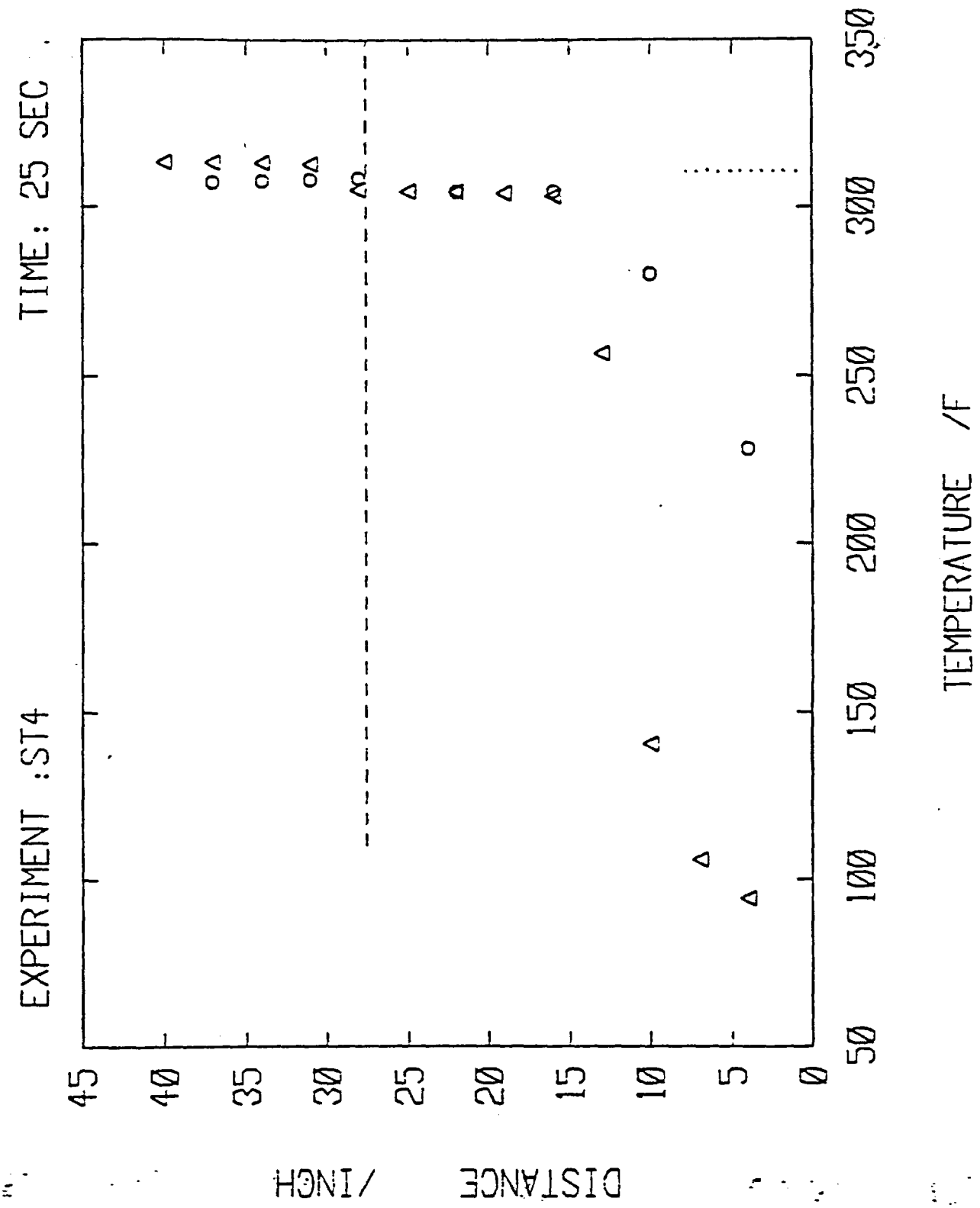
EXPERIMENT :ST4
TIME: 25 SEC
DISTANCE /INCH
TEMPERATURE /F
45
40
35
30
25
20
15
10
5
0
50
100
150
200
250
300
350

Fig. A.4.7

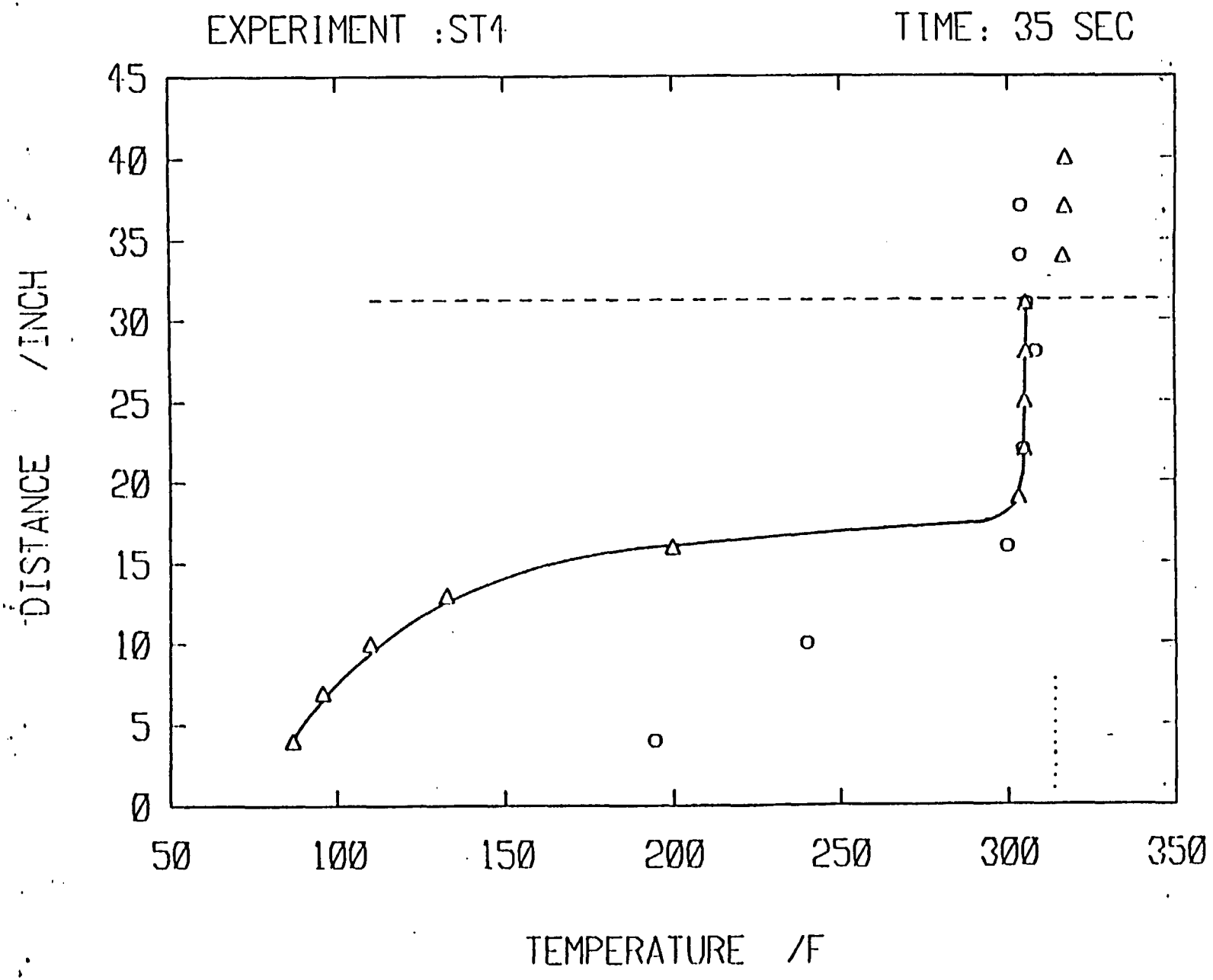
EXPERIMENT :ST1
TIME: 35 SEC
DISTANCE /INCH
45
40
35
30
25
20
15
10
5
0
50
100
150
200
250
300
350
TEMPERATURE /F

Fig. A.4.8

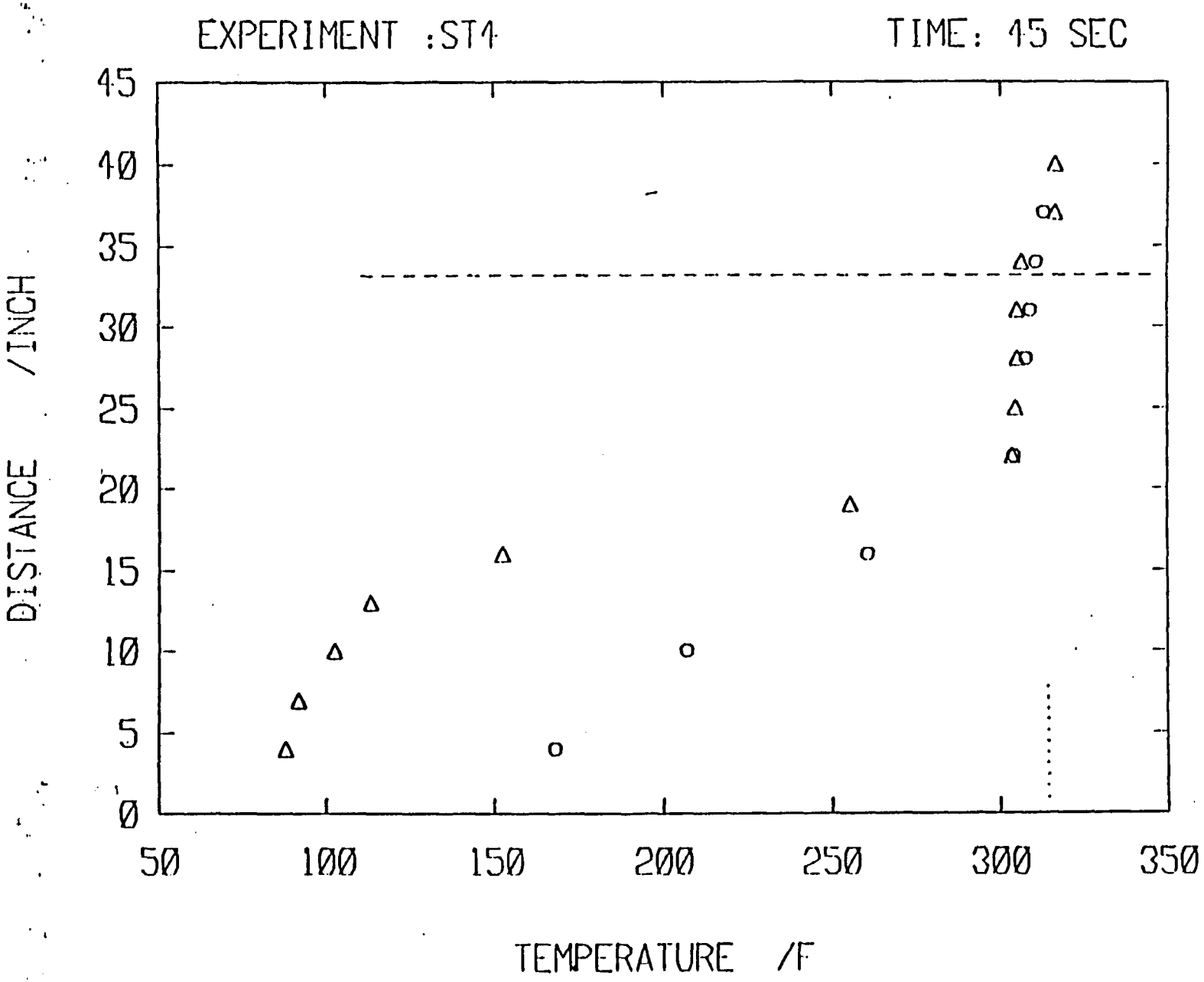
EXPERIMENT :ST4
TIME: 15 SEC
DISTANCE /INCH
45
40
35
30
25
20
15
10
5
0
50
100
150
200
250
300
350
TEMPERATURE /F

Fig. A.4.9

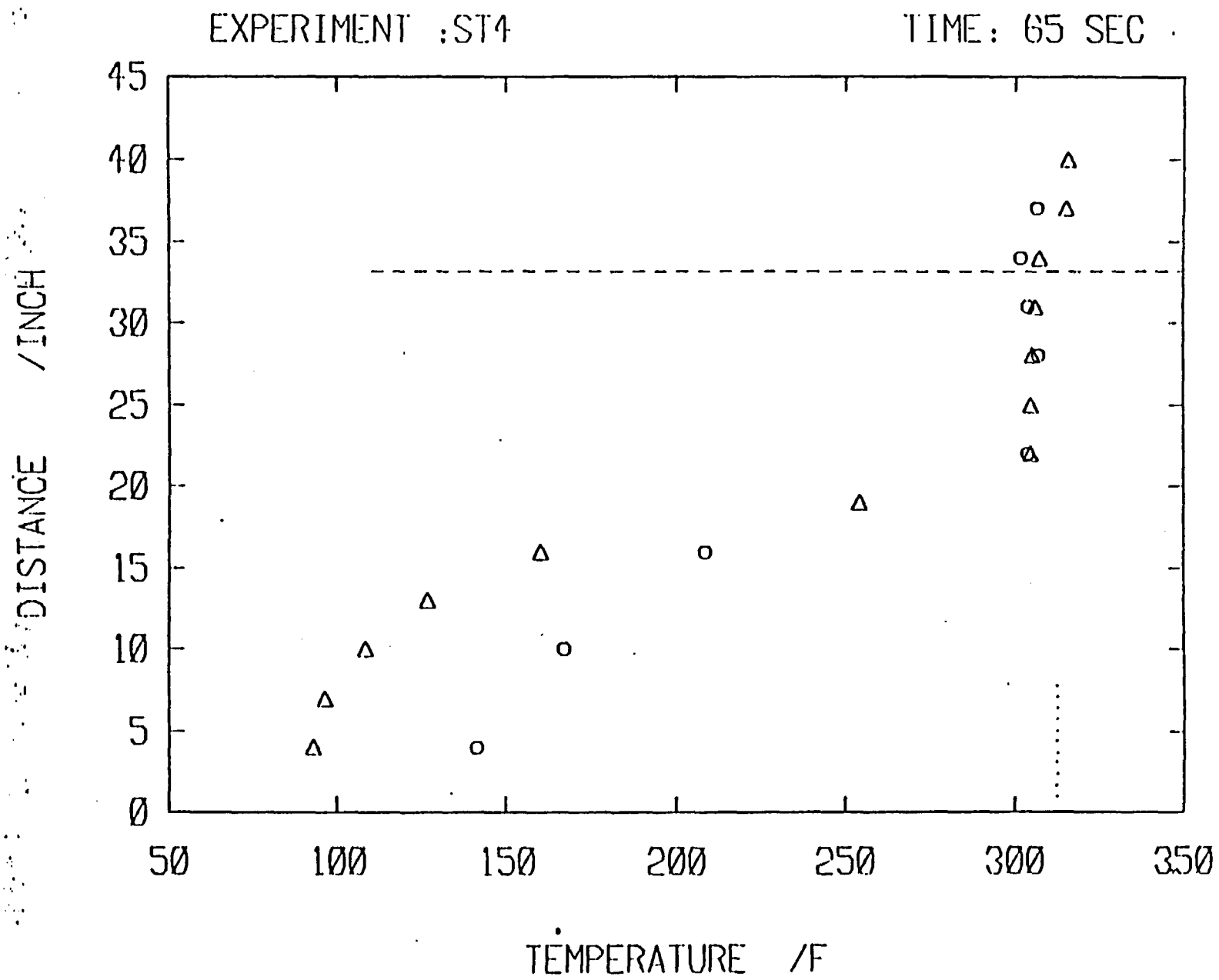
EXPERIMENT :ST4
TIME: 65 SEC
DISTANCE /INCH
45
40
35
30
25
20
15
10
5
0
50
100
150
200
250
300
350
TEMPERATURE /F

Fig. A.4.10

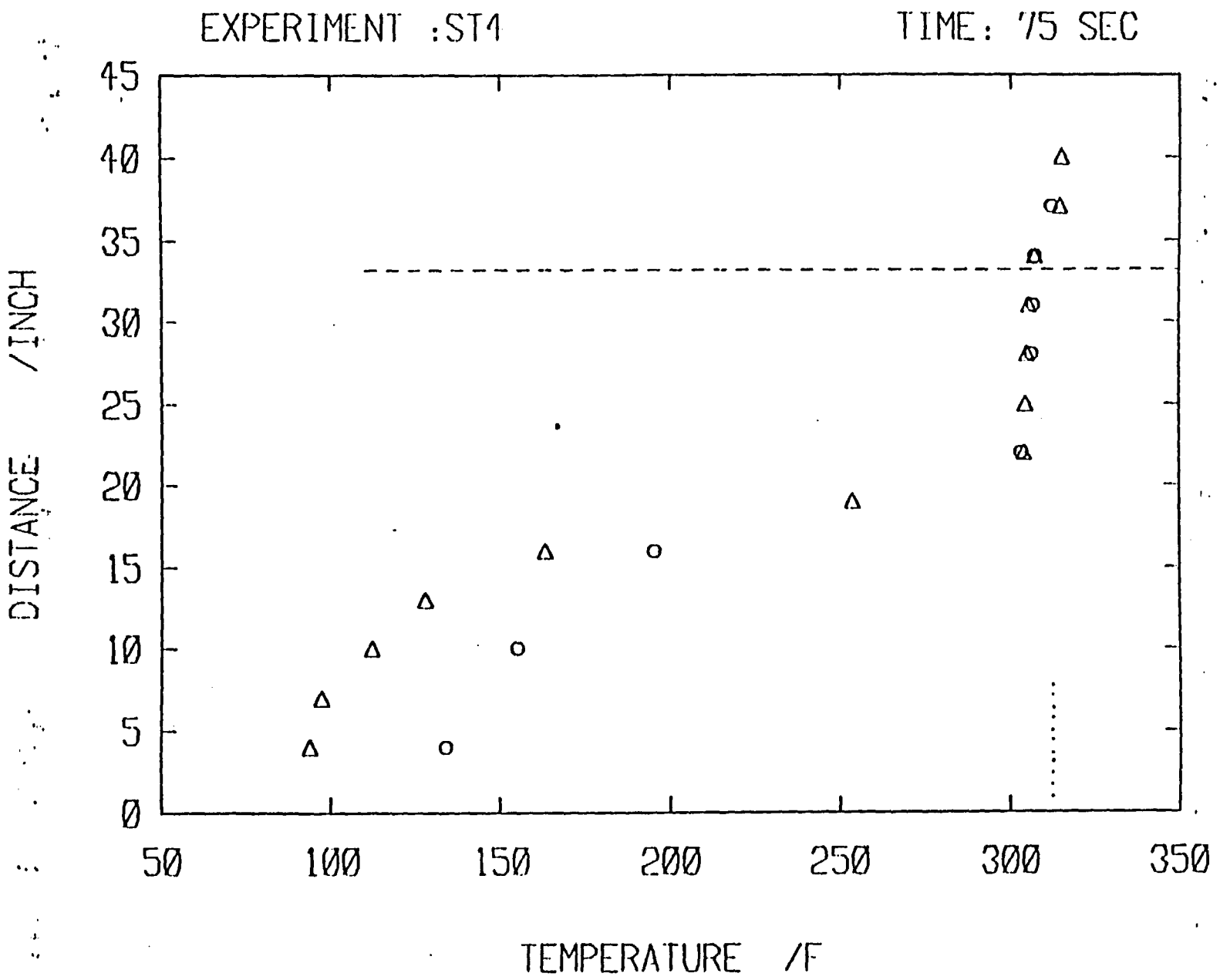
EXPERIMENT :ST4
TIME: 75 SEC
DISTANCE /INCH
45
40
35
30
25
20
15
10
5
0
50
100
150
200
250
300
350
TEMPERATURE /F

Fig. A.4.11

A.5 Experiment: EM9

Water level at t = 0 sec : L = 0 in.

Water level increase : ΔL = 18 in.

Insurge time : t = 31 sec.

This transient was initiated by insurging cold water into the tank filled with saturated vapor. The axially located thermocouples were used for determining temperature distribution inside the tank.

It should be noted that the sudden drop in pressure at time, t = 14 sec. (Fig. A.5.1), is due to the presence of the window, see Fig. 2. It is postulated that due to an area increase, a new surface is formed hence an increase in the interfacial heat transfer and a drop in pressure.

This experiment also showed that the behavior and temperature distribution of the subcooled liquid region in the case of insurge to partially filled tank, e.g. experiment: ST4, is quite similar to that of empty tank transients (see Figs. A.5.5 through A.5.14).

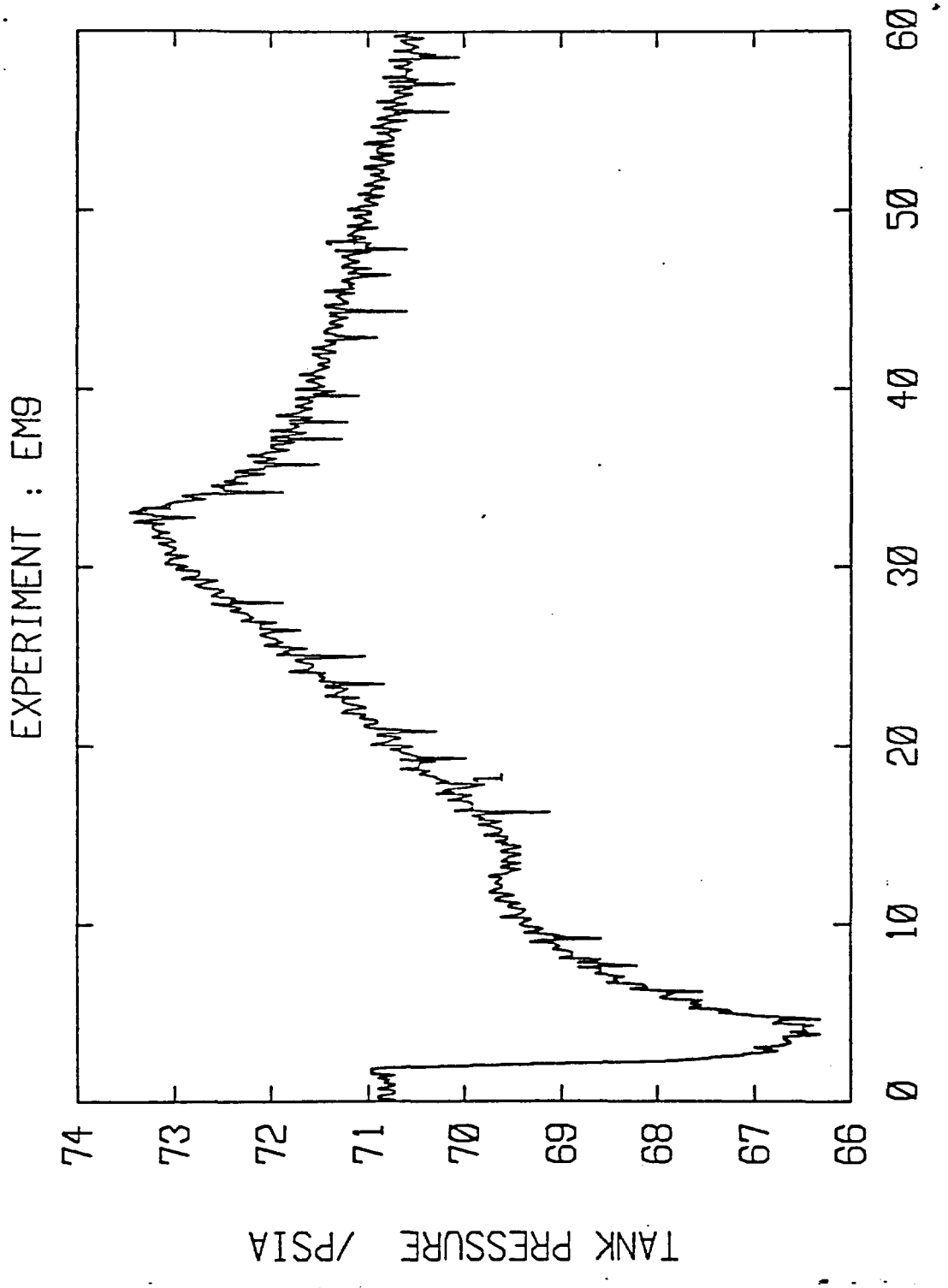
EXPERIMENT : EM9
TANK PRESSURE /PSIA
TIME /SEC
74
73
72
71
70
69
68
67
66
0
10
20
30
40
50
60

Fig. A.5.1

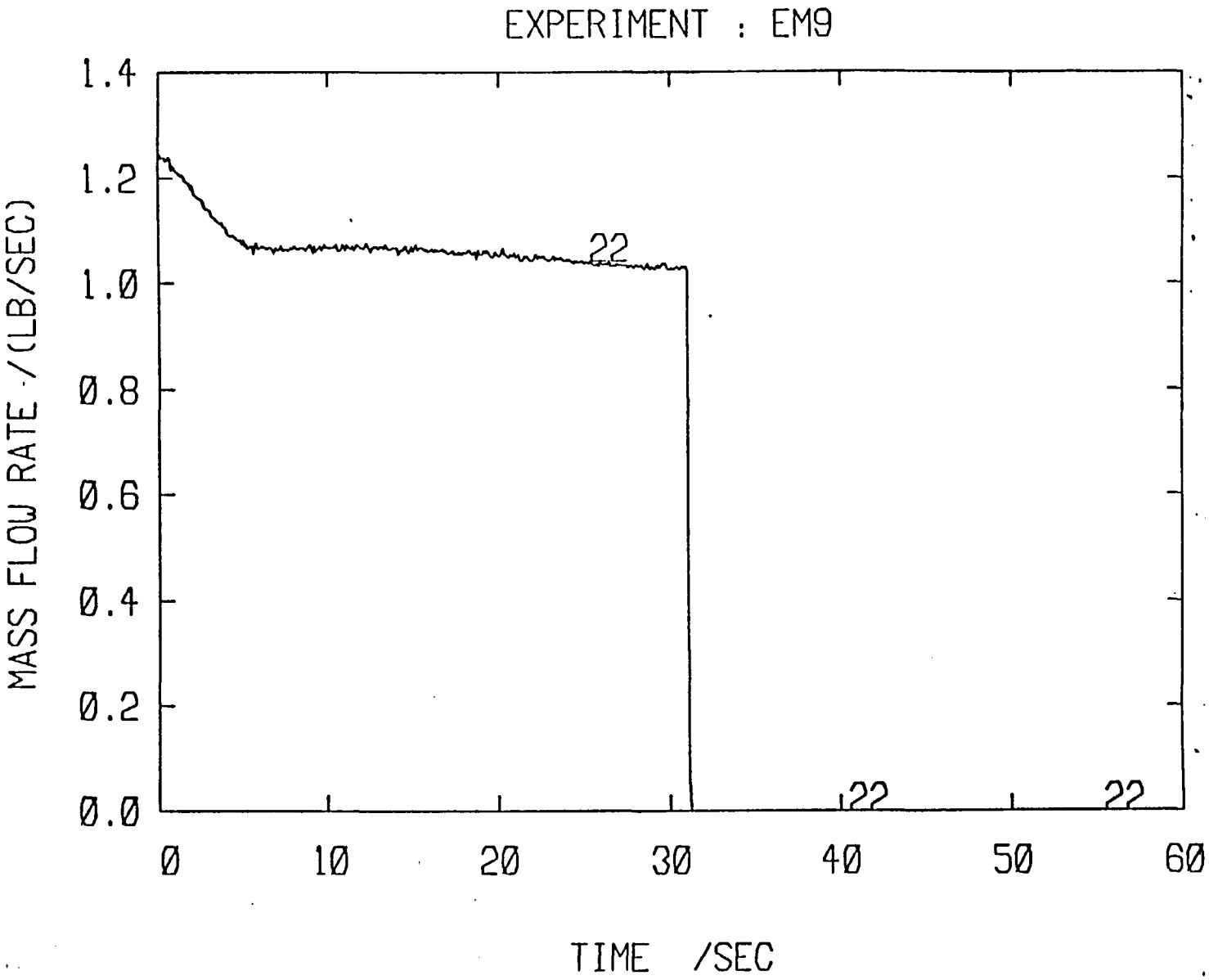
EXPERIMENT : EM9
MASS FLOW RATE /(LB/SEC)
1.4
1.2
1.0
0.8
0.6
0.4
0.2
0.0
0
10
20
30
40
50
60
TIME /SEC
22
22
22

Fig. A.5.2

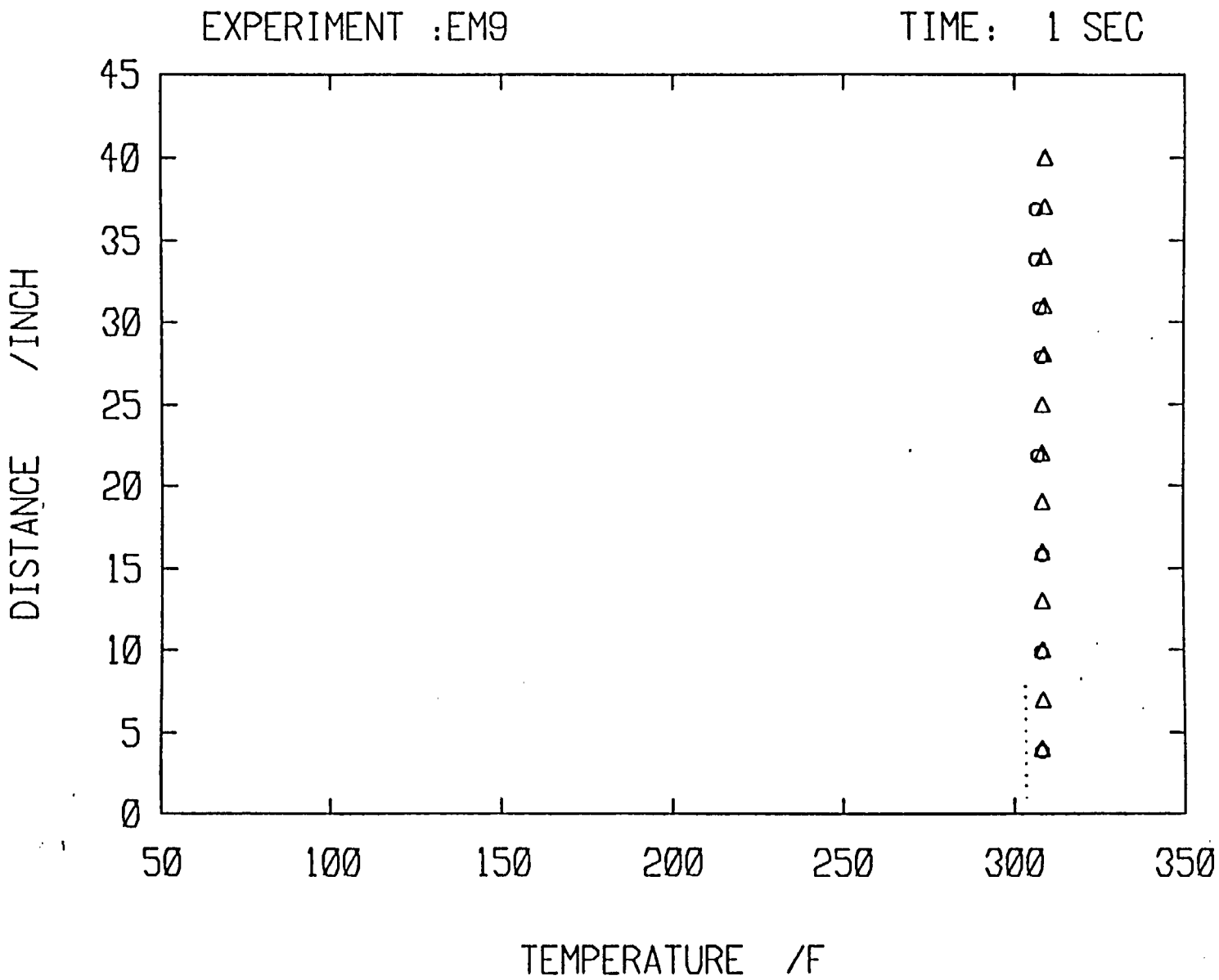
EXPERIMENT :EM9
TIME: 1 SEC
DISTANCE /INCH
45
40
35
30
25
20
15
10
5
0
50
100
150
200
250
300
350
TEMPERATURE /F

Fig. A.5.3

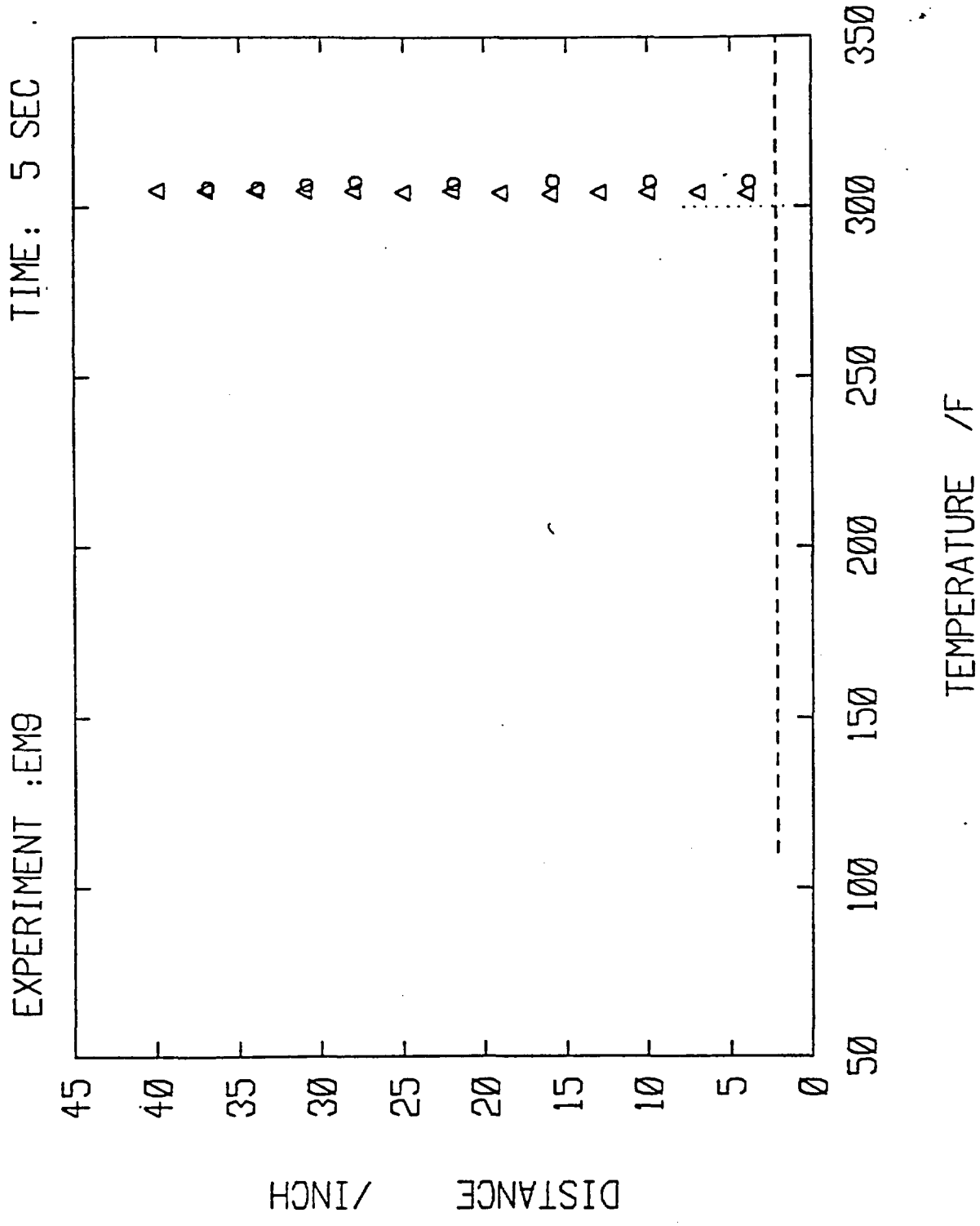
EXPERIMENT :EM9
TIME: 5 SEC
TEMPERATURE /F
50
100
150
200
250
300
350
DISTANCE /INCH
0
5
10
15
20
25
30
35
40
45

Fig. A.5.4

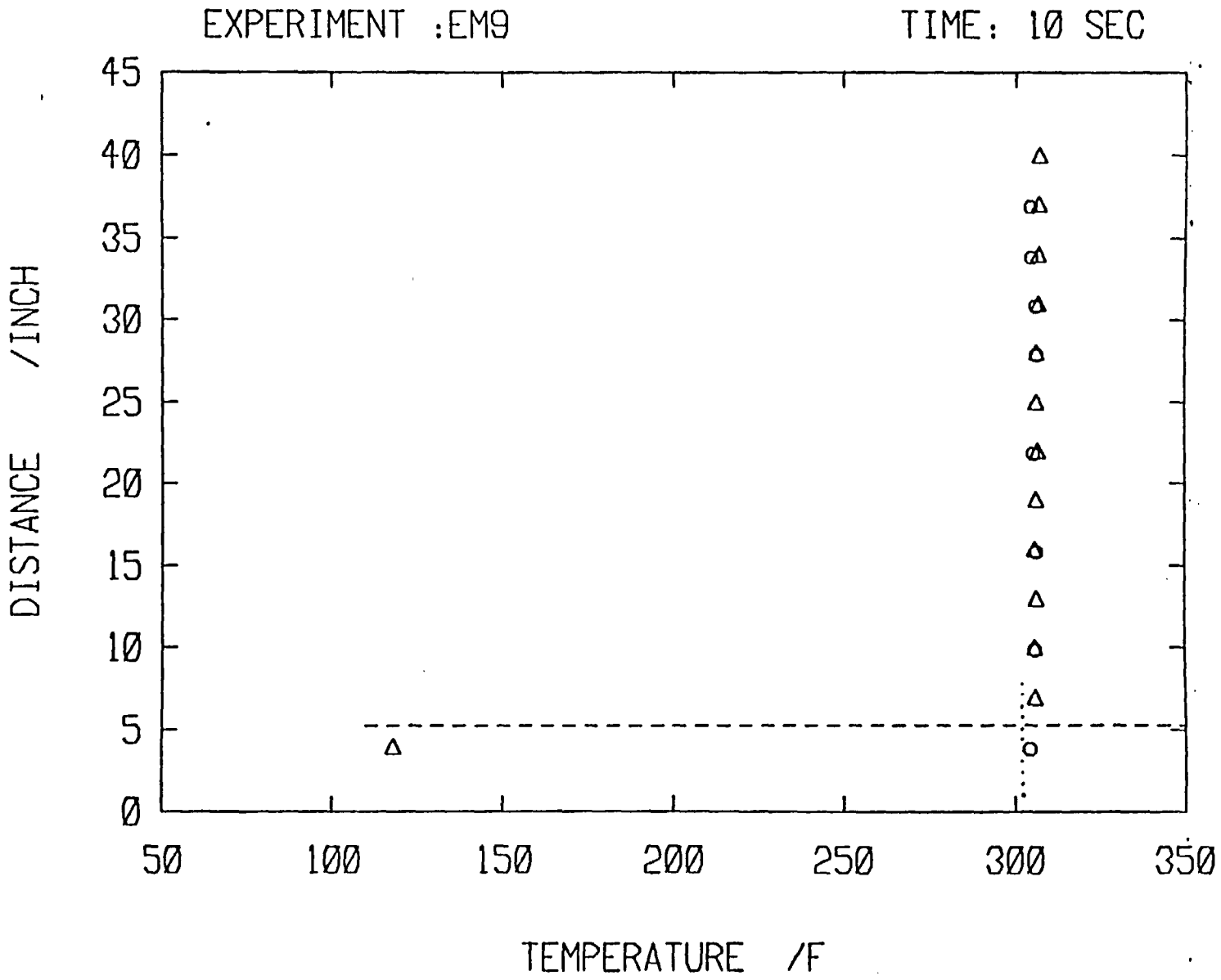
EXPERIMENT :EM9
TIME: 10 SEC
DISTANCE /INCH
45
40
35
30
25
20
15
10
5
0
50
100
150
200
250
300
350
TEMPERATURE /F

Fig. A.5.5

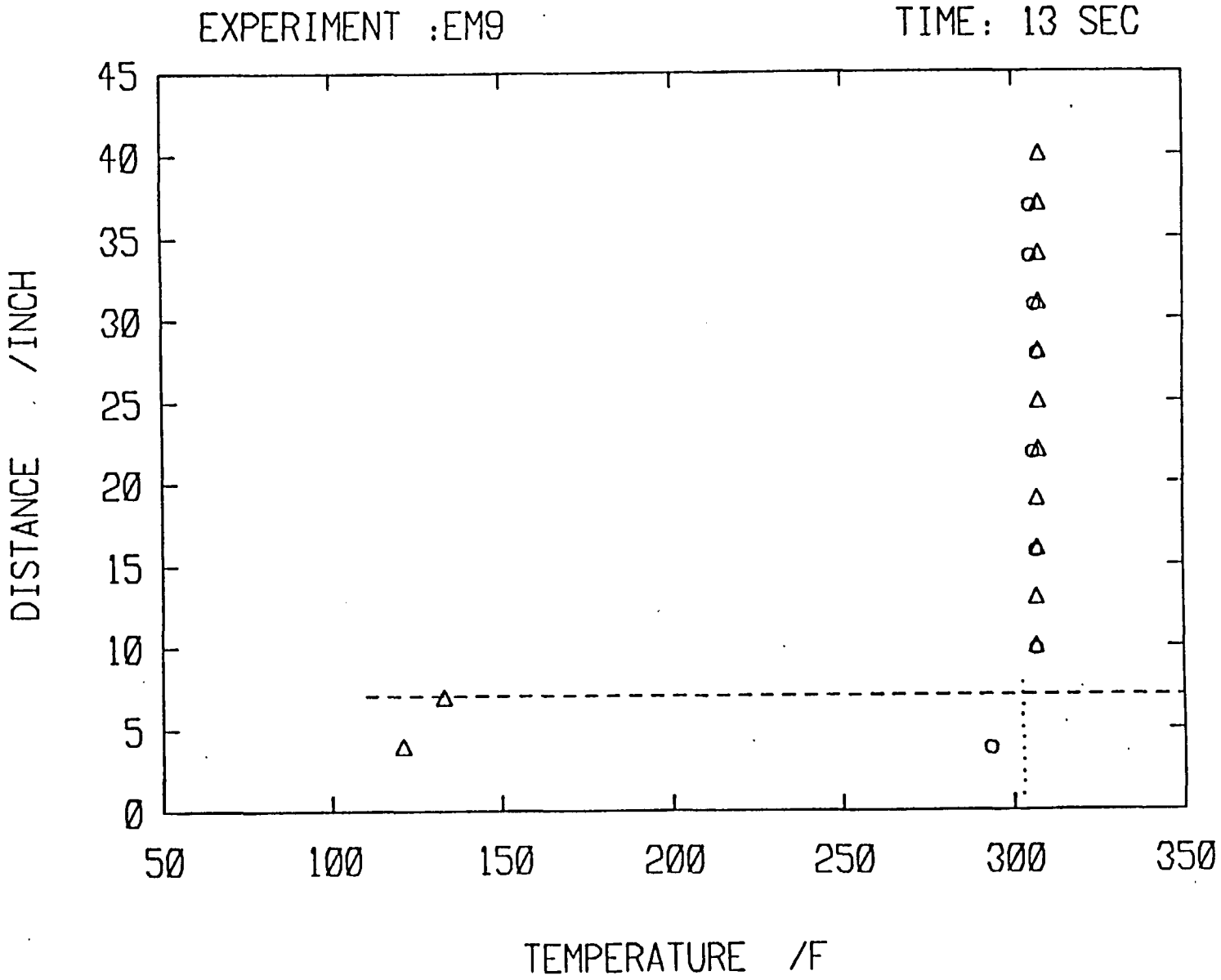
EXPERIMENT :EM9
TIME: 13 SEC
DISTANCE /INCH
45
40
35
30
25
20
15
10
5
0
50
100
150
200
250
300
350
TEMPERATURE /F

Fig. A.5.6

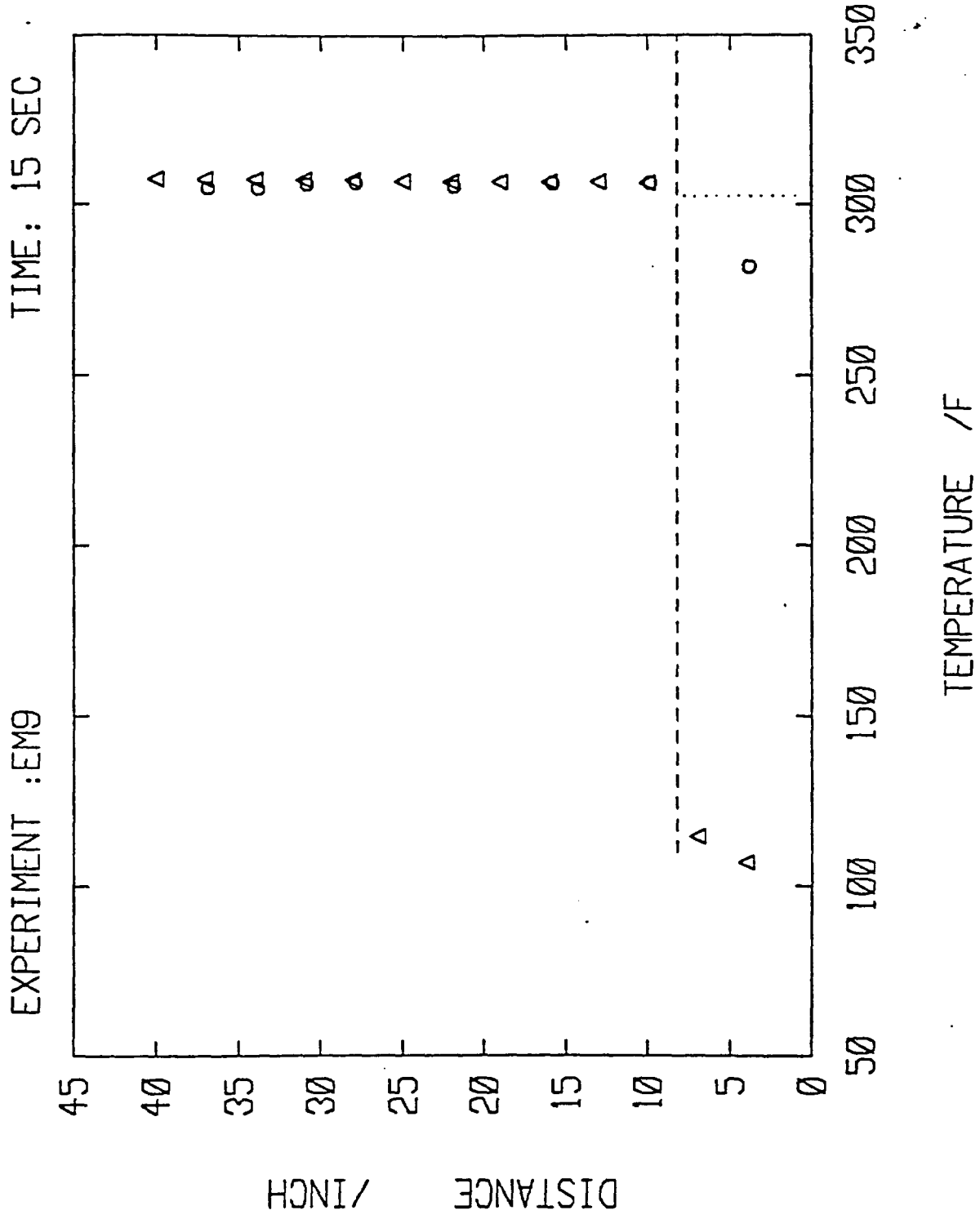
EXPERIMENT :EM9
TIME: 15 SEC
DISTANCE /INCH
TEMPERATURE /F
45
40
35
30
25
20
15
10
5
0
50
100
150
200
250
300
350

Fig. A.5.7

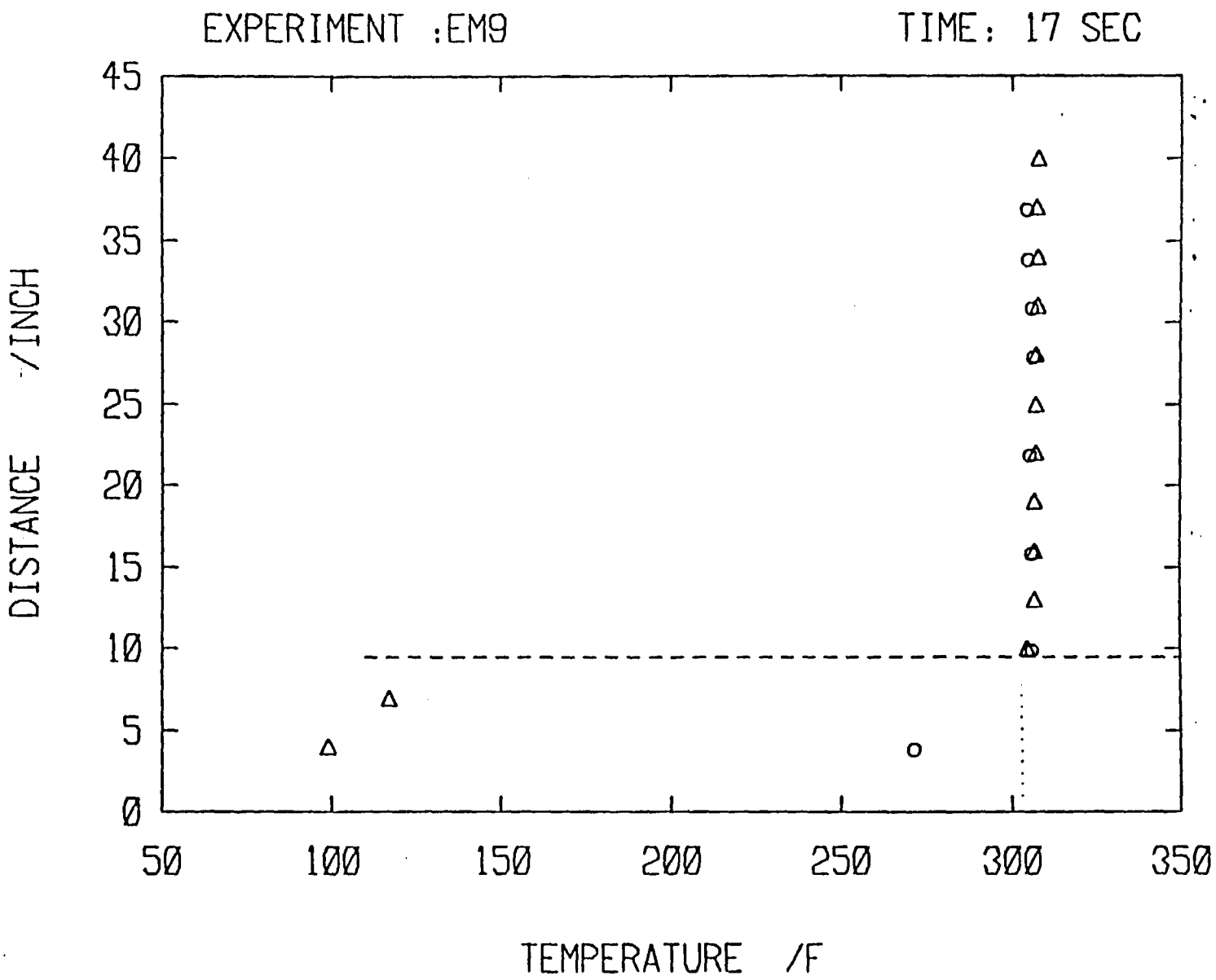
EXPERIMENT :EM9
TIME: 17 SEC
DISTANCE /INCH
45
40
35
30
25
20
15
10
5
0
50
100
150
200
250
300
350
TEMPERATURE /F

Fig. A.5.8

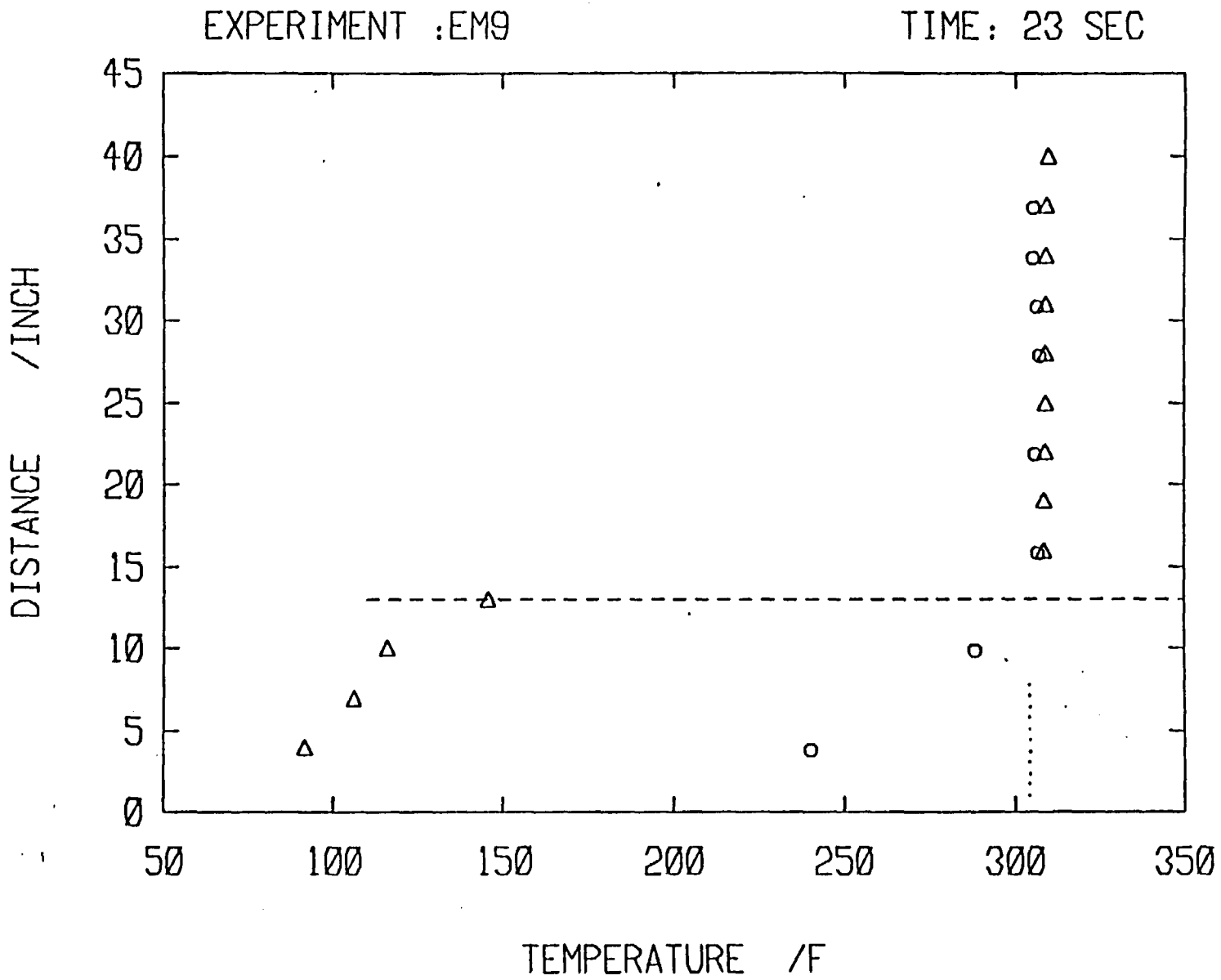
EXPERIMENT :EM9
TIME: 23 SEC
DISTANCE /INCH
45
40
35
30
25
20
15
10
5
0
50
100
150
200
250
300
350
TEMPERATURE /F

Fig. A.5.9

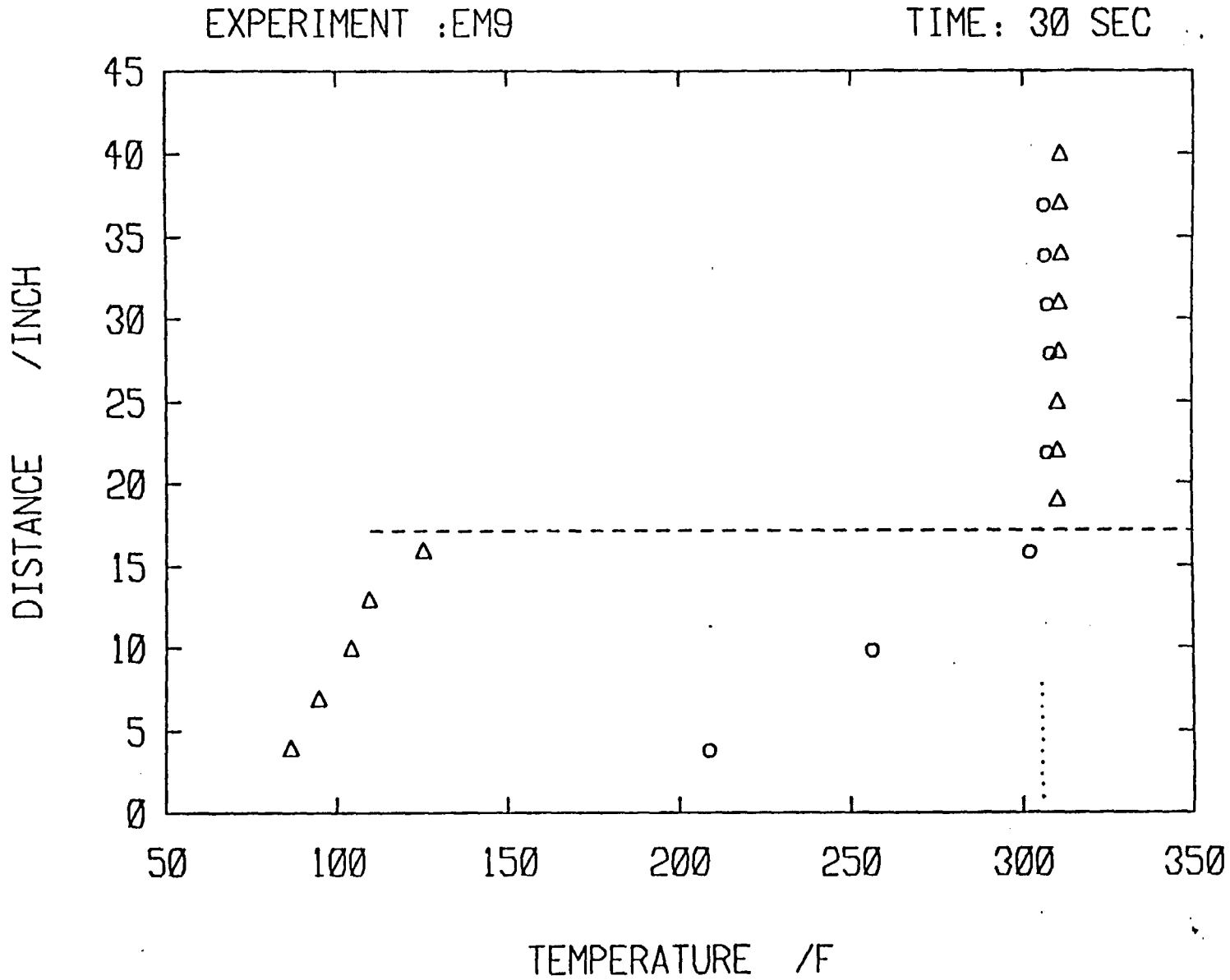
EXPERIMENT :EM9
TIME: 30 SEC
DISTANCE /INCH
45
40
35
30
25
20
15
10
5
0
50
100
150
200
250
300
350
TEMPERATURE /F

Fig. A.5.10

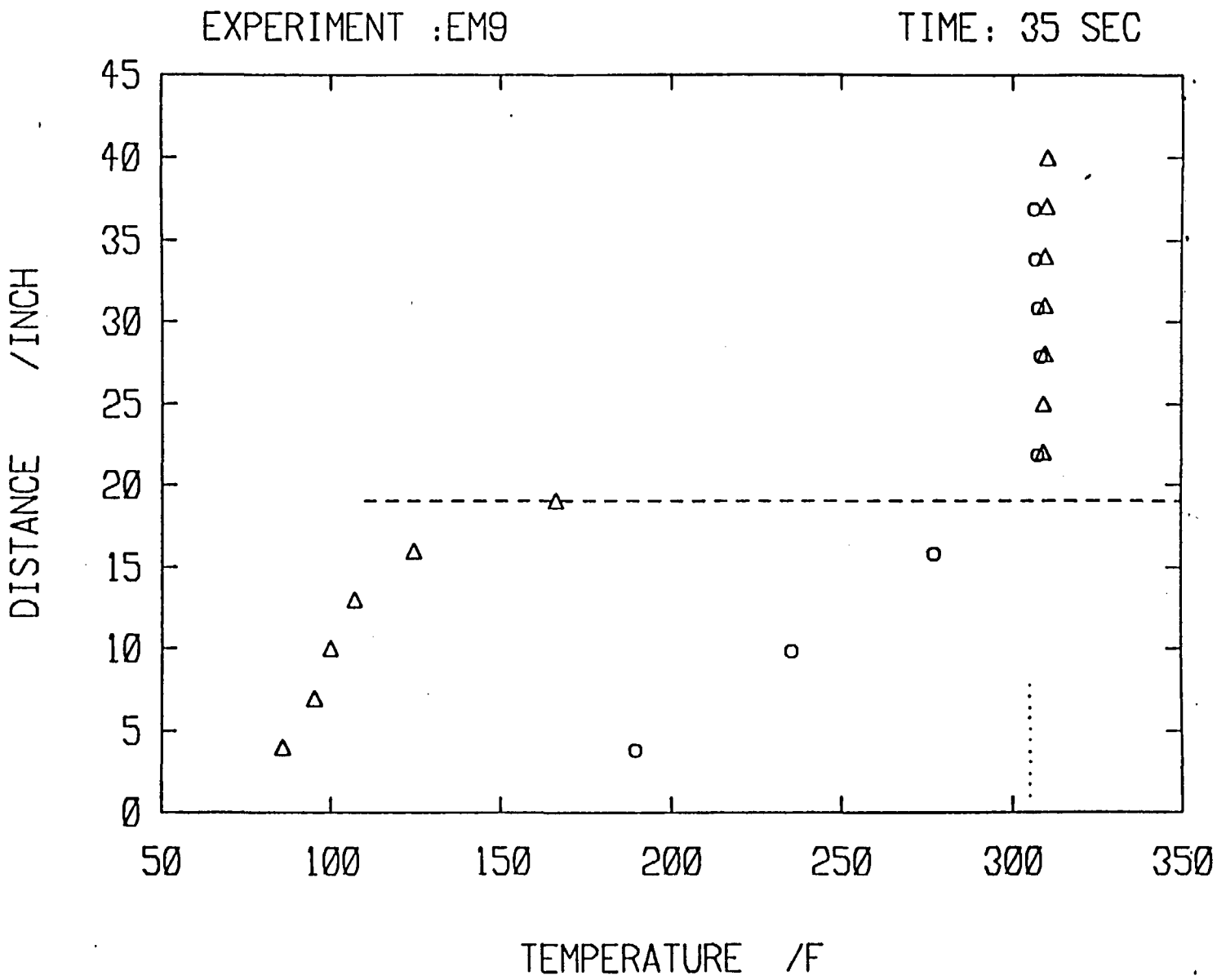
EXPERIMENT :EM9
TIME: 35 SEC
DISTANCE /INCH
45
40
35
30
25
20
15
10
5
0
50
100
150
200
250
300
350
TEMPERATURE /F

Fig. A.5.11

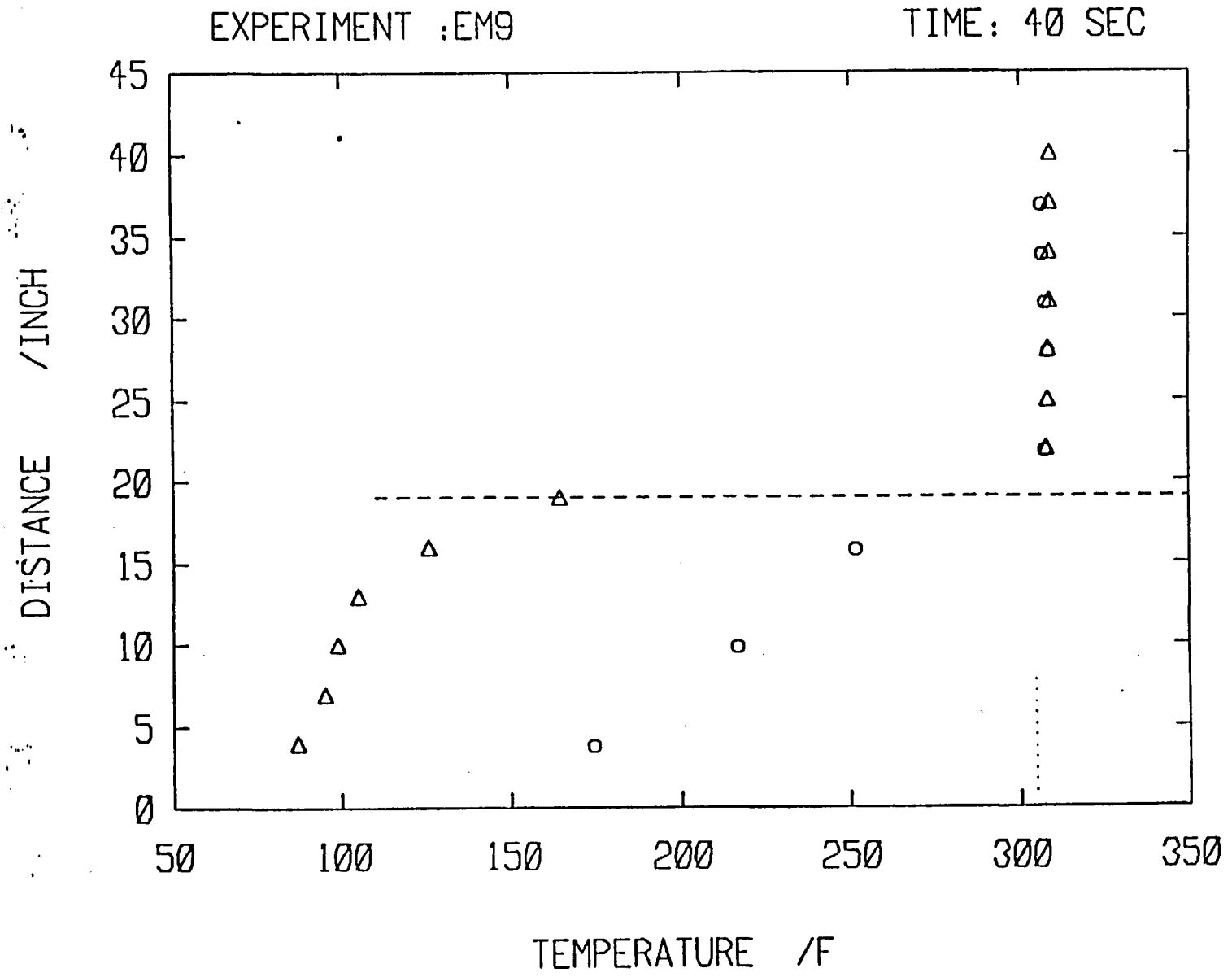
EXPERIMENT :EM9
TIME: 40 SEC
DISTANCE /INCH
45
40
35
30
25
20
15
10
5
0
50
100
150
200
250
300
350
TEMPERATURE /F

Fig. A.5.12

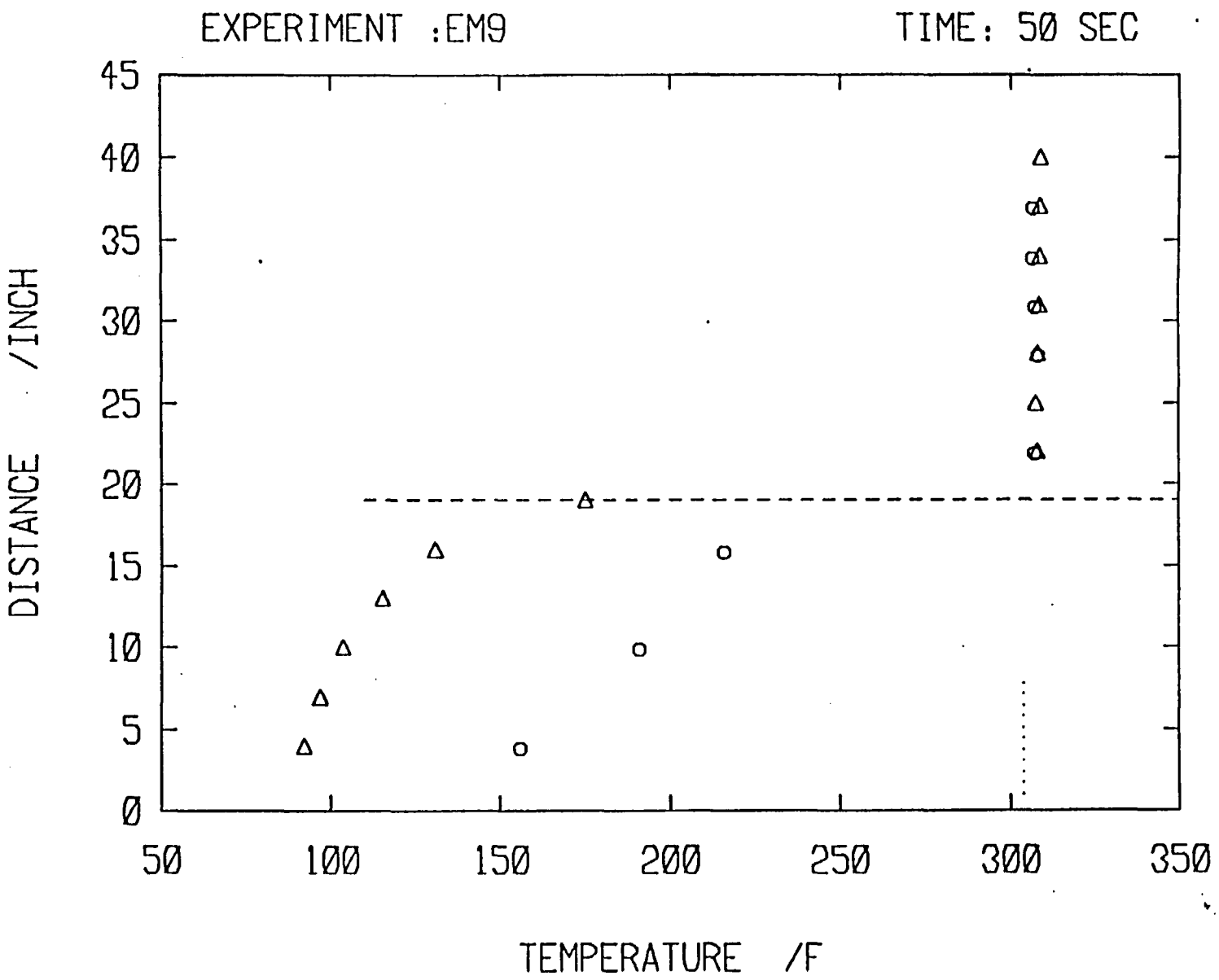
EXPERIMENT :EM9
TIME: 50 SEC
DISTANCE /INCH
45
40
35
30
25
20
15
10
5
0
50
100
150
200
250
300
350
TEMPERATURE /F

Fig. A.5.13

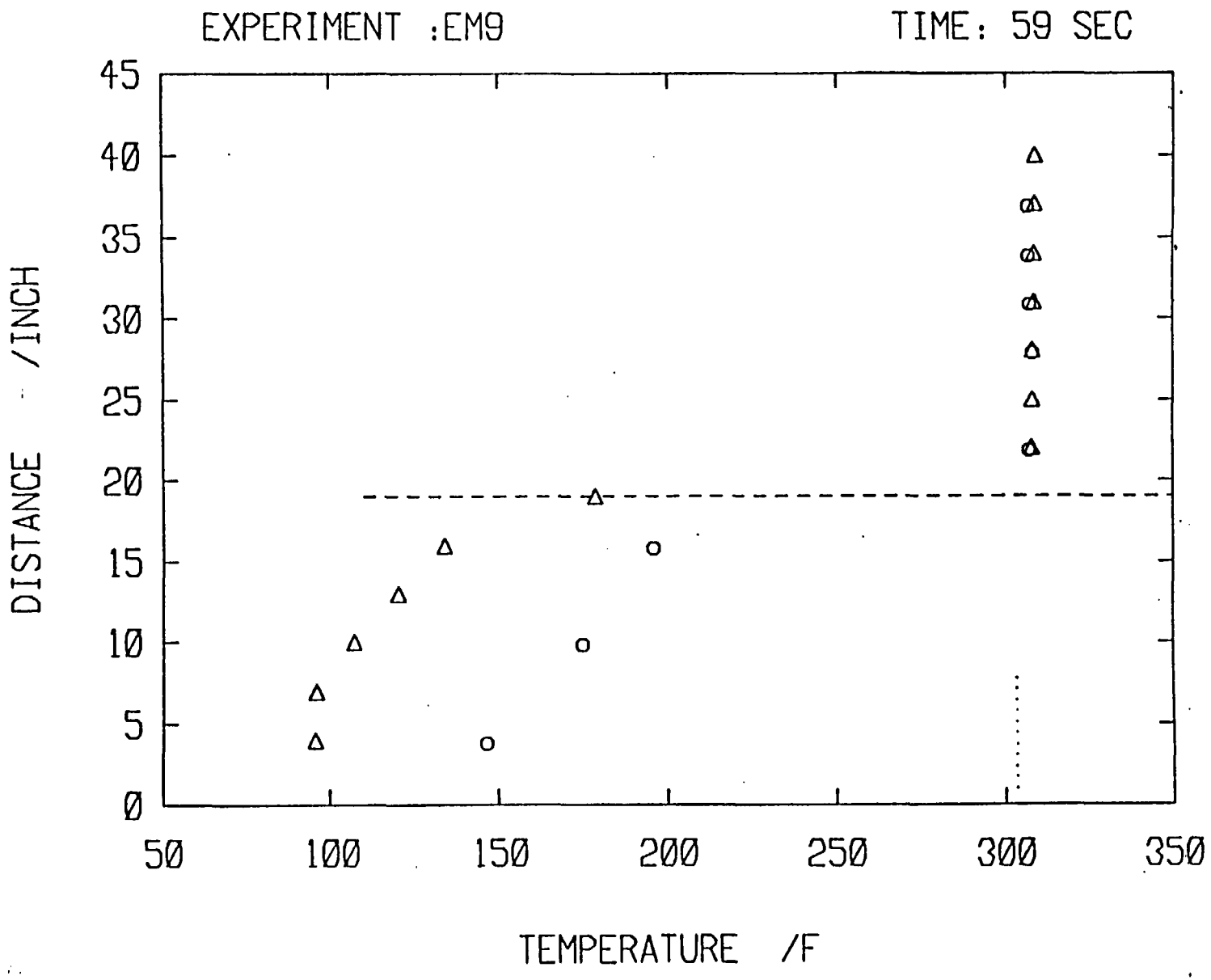
EXPERIMENT :EM9
TIME: 59 SEC
DISTANCE /INCH
45
40
35
30
25
20
15
10
5
0
50
100
150
200
250
300
350
TEMPERATURE /F

Fig. A.5.14

A.6 Miscellaneous Experiments

The following description of experiments, belong to the experiments that were referred to during the main text, but were not described in the previous sections.

Experiment : KK1

Water level at t = 0 sec : L = 17 in.

Water level increase : ΔL = 18 in.

Insurge time : t = 41 sec.

Experiment : FT5

Water level at t = 0 : L = 17 in.

Water level increase : ΔL = 18 in.

Insurge time : t = 23 sec.

Experiment : FT2

Water level at t = 0 : L = 17 in.

Water level increase : ΔL = 18 in.

Insurge time : t = 30 sec.

APPENDIX B

Conservation Equations for Deformable Control Volume

Energy Equation for a deformable control volume can be written as [14];

$$\sum\dot{Q} + \sum\dot{W} = \frac{d}{dt}\int_{c.v.} e\rho dV + \int_{c.s.} \rho(e + \frac{p}{\rho})\,\bar{V}_r\cdot\bar{\bar{dA}}$$

$$+ \int_{c.s.} \rho\bar{V}_b\cdot\overline{dA} \qquad (B.1)$$

where,

e = specific energy

$\sum\dot{W} = \dot{W}_s + \dot{W}_{inertia} + \dot{W}_{shear}$

$\bar{V}_r$ = velocity of fluid relative to control surface boundary

$\bar{V}_b$ = velocity of control surface boundary

For any region in the pressurizer, kinetic and potential energy can be neglected. Furthermore,

$$\sum\dot{W} \equiv 0 \qquad (B.2)$$

So,

$$\sum\dot{Q} = \frac{d}{dt}(mu) + \sum\dot{m}(u + pv) + p\dot{V} \qquad (B.3)$$

Conservation of mass can be written as;

$$\frac{d}{dt}\int_{c.v.}\rho dV + \int_{c.s.}\rho\,\overline{V_r}\cdot\overline{dA} = 0 \qquad (B.4)$$

Hence, for any given region

$$m = -\sum_i m_i \qquad (B.5)$$

APPENDIX C

Orifice Plate and Its Calibration

An orifice plate, made of 1/8" stainless steel plate, was used to measure the mass flow rate. The inlet opening was 0.218" in diameter and was tapered at 40° angle.

The orifice was calibrated off the test loop with water. The data were plotted (see Fig. C1) on a LOG-LOG graph of mass flow rate versus the pressure drop across the orifice. This data was approximated by

$$\log_{10}(\dot{m}) = -0.889672 + (0.482954)\ \log_{10}(\Delta p) \qquad (C.1)$$

where, $\dot{m}$ = mass flow rate of water through the orifice

Δp = pressure drop across the orifice, psi

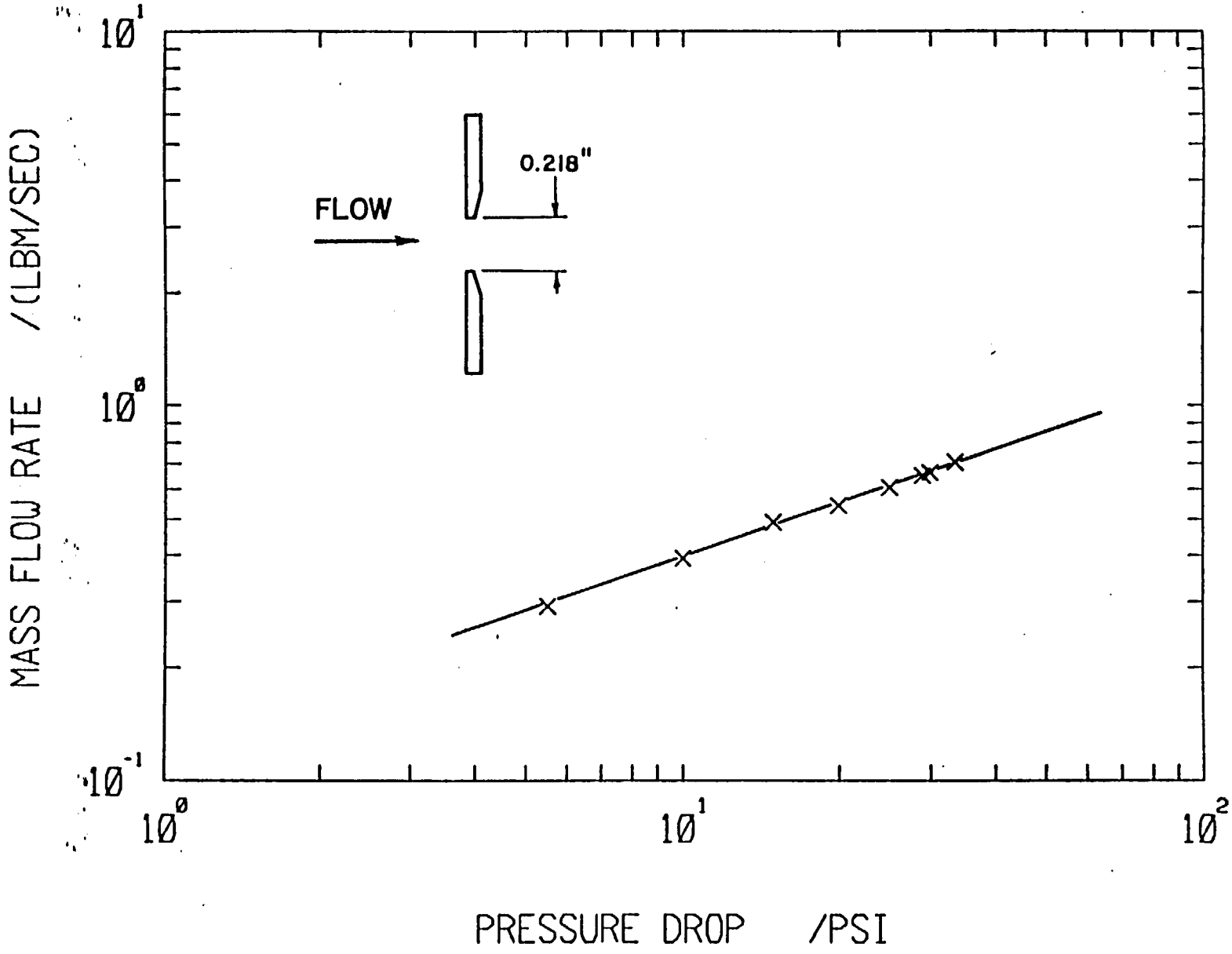
MASS FLOW RATE /(LBM/SEC)
10^{1}
10^{0}
10^{-1}
0.218"
FLOW
10^{0}
10^{1}
10^{2}
PRESSURE DROP /PSI

FIG. C I

APPENDIX D

DETAILS OF A WESTINGHOUSE PRESSURIZER

In this Appendix, the geometric and some operational routines for a Westinghouse pressurizer will be discussed [15]. Figures D.1 and D.2 shows the details of such a pressurizer. As it is shown in these diagrams, the pressurizer is equipped with immersion heaters coming in from the bottom. There are five banks of heaters. Banks A, B, D and E are backup heaters and are either fully onn or fully off. Back C is the control bank. The output of the heaters are given in Table D-1. A graph of total heater output versus system pressure for pressurizer levels between 11.5% and 52% is given in Fig. D-3.

Under normal operating conditions, i.e. system pressure at or below 2012 psia, there is a dribbling flow from the spray nozzle at an approximate rate of 1.5 gpm.

TABLE D-1: Output of the Heaters

Bank	Heat Output (KW)
A	303.5
B	260
C	173
D	303.5
E	260

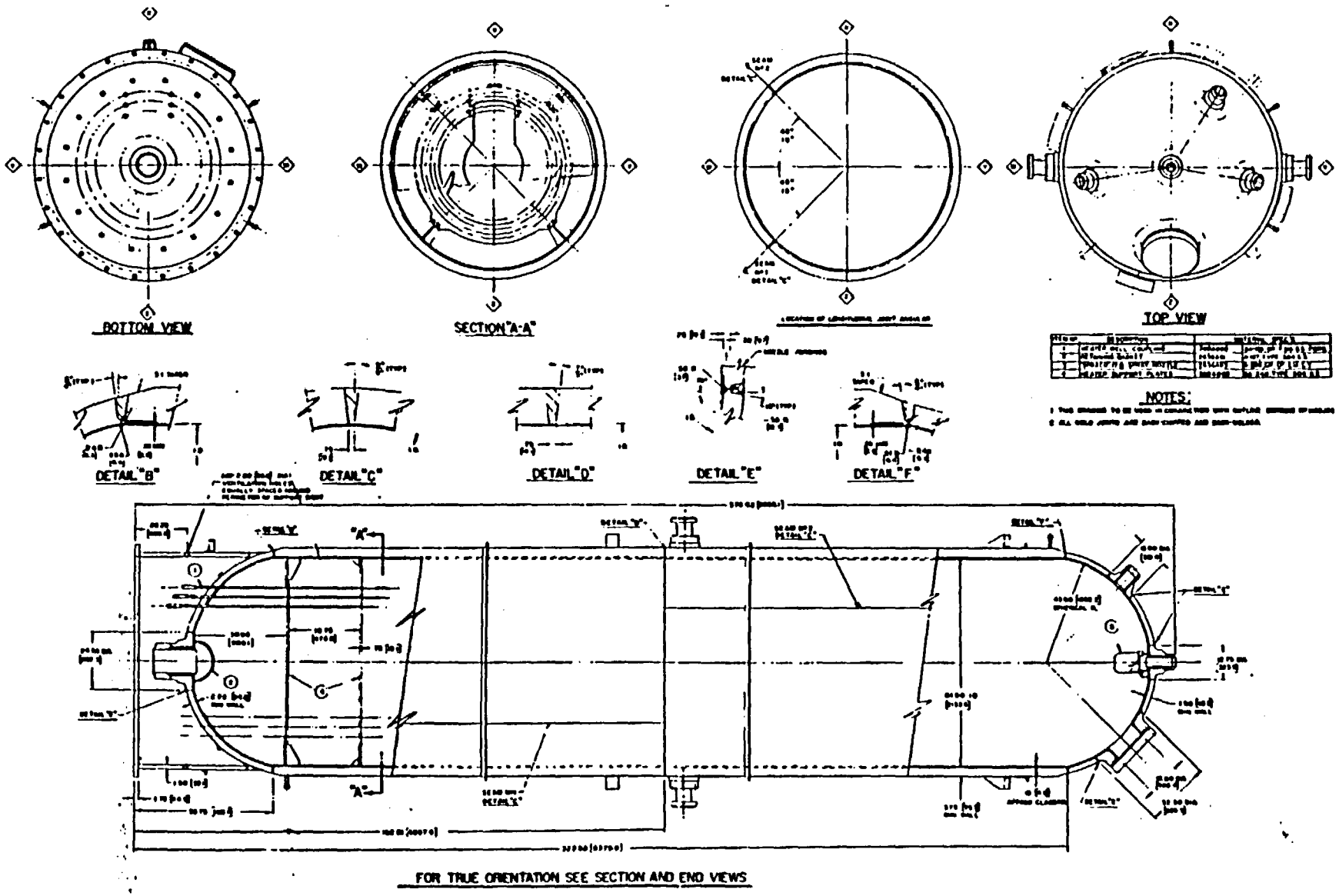

FIG. DI - GENERAL ARRANGEMENT FOR WESTINGHOUSE PRESSURIZER

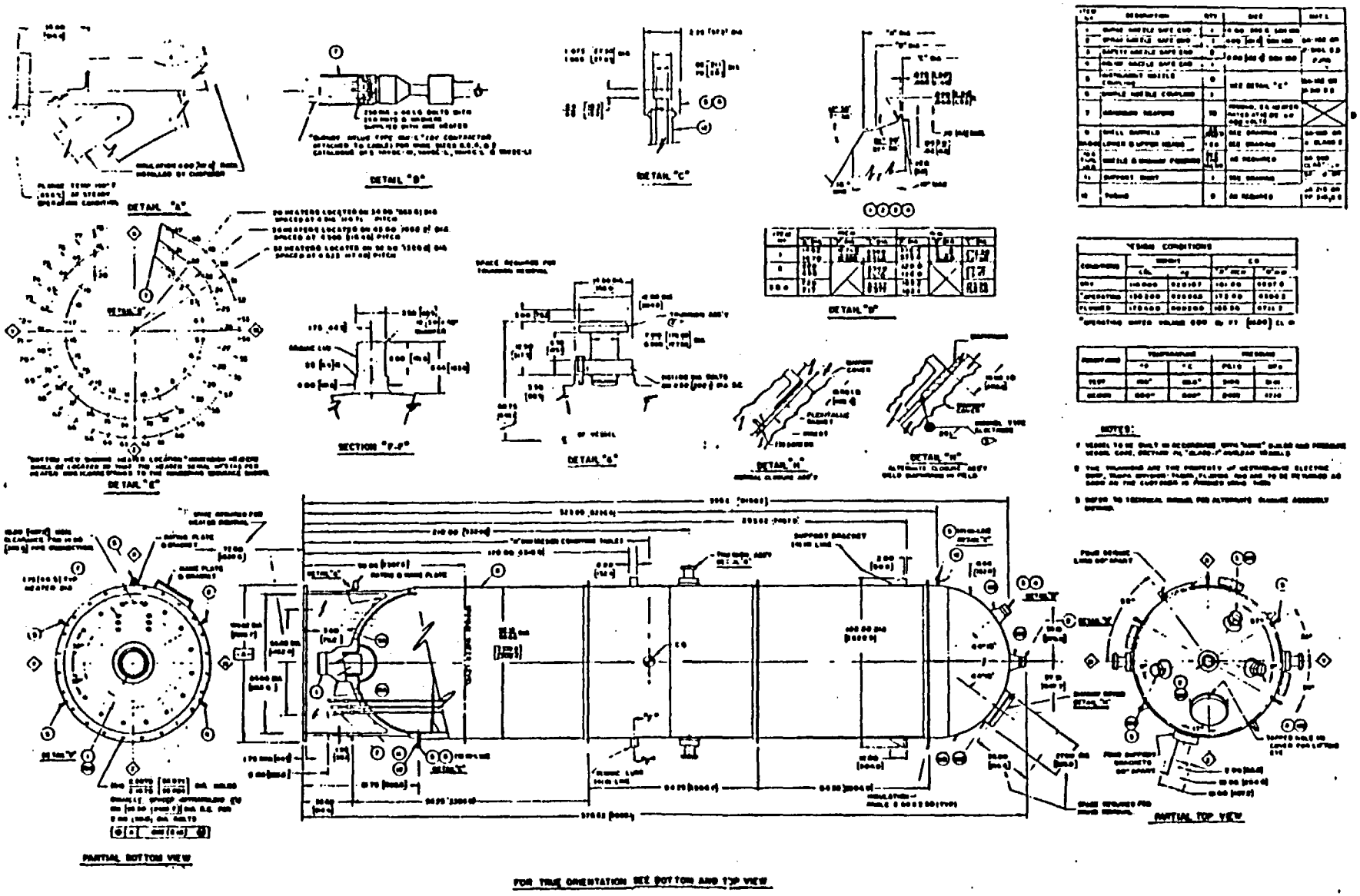

FIG. D2 - OUTLINE OF WESTINGHOUSE PRESSURIZER

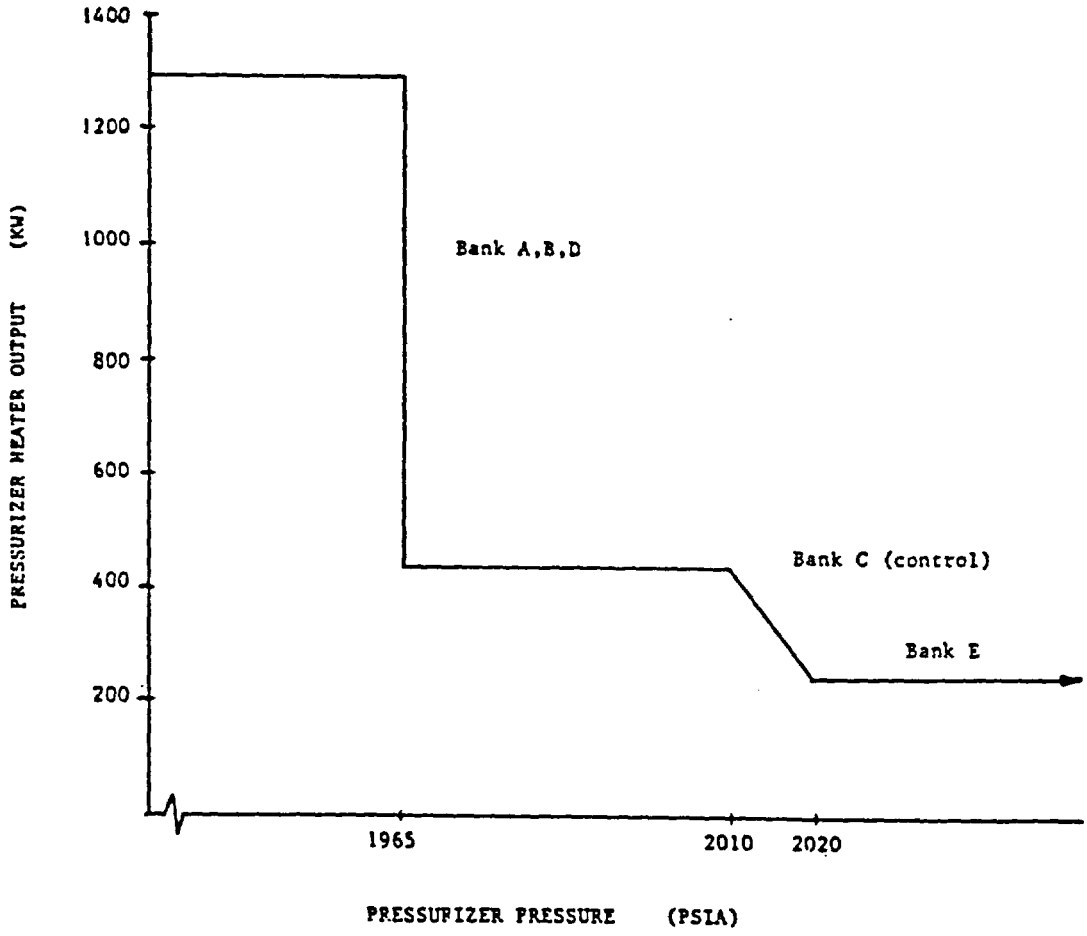

TOTAL HEATER OUTPUT

FIG. D3